Guidelines for Drone Geophysics

Near-Surface Geophysics Inter-Society Committee on UAV Geophysics Guidelines

UAV Total and Vector Field Magnetics Surveying Guidelines (Version 1)

November 2022

Near-Surface Geophysics Inter-Society Committee on UAV Geophysics Guidelines

Document Title: - UAV Total and Vector Field Magnetics Surveying Guidelines (Version 1)

Document purpose: - For global geoscience industry use as Drone Magnetics Guidelines

Intended Use and Distribution: - Downloadable from **https://www.guidelinesfordronegeophysics.com/**

Copyright: - Open-source for update to Version 2

Citation: - Near-Surface Geophysics Inter-Society Committee on UAV Geophysics Guidelines, 2022, UAV Total and Vector Field Magnetics Surveying Guidelines (Version 1). https://www.guidelinesfordronegeophysics.com/

Near-Surface Geophysics Inter-Society Committee on UAV Geophysics Guidelines

NAME	ORGANIZATION	EMAIL	SOCIETY AFFILIATION(S)
Tim Archer	Reid Geophysics	tim@reid-geophys.co.uk	EAGE, SEG, PESGB
Chase Attwood	SkySkopes, Inc.	Chase.attwood@skyskopes.com	
Elizabeth Baranyi	Seequent	elizabeth.baranyi@seequent.com	SEG, AGU
Ron Bell	IGS, LLC	rbell@igsdenver.com	SEG
Ed Cunion	Red Rocks Geophysics	ed.cunion@gmail.com	SEG, KEGS
Alexey Dobrovolskiy	SHP Engineering	ADOBROVOLSKIY@ugcs.com	EAGE
Irina Filina	Univ. of Nebraska Lincoln	ifilina2@unl.edu	SEG, AGU, AAPG
Jan Francke	Ground Radar	jfrancke@groundradar.com	APEGA
Jeff Gamey	Tetra Tech	Jeff.Gamey@tetratech.com	EEGS
Bruno Gavazzi	Enerex	bruno.gavazzi@enerex.fr	SEG, EGU
Rob Harris	Geonics	rob@geonics.com	SEG, EEGS, KEGS
James Jensen	Southern Geoscience Consultants	james.jensen@sgc.com.au	ASEG, SEG
Bob Lawson	Geophex Pty Ltd	blawson@geophex.com	
Jean Legault	Geotech Airborne	jean@geotech.ca	SEG, EEGS, EAGE, ASEG, SAGA
Leslie McChesney	Southpac Aerospace	Leslie@southpac.biz	IAGSA, ISASI, ASASI, WIA
Paul Mutton	Touchstone Geophysics	paul@touchstonegeophysics.com.au	ASEG, AIG
Geoff Pettifer	GHD / Terra Entheos Geoscience	terraentheosgeoscience@gmail.com	EEGS, SEG, EAGE, ASEG, KEGS, IAH, AEG
Johannes Stoll	Mobile Geophysical Technologies GmbH	jstoll@mgt-geo.com	SEG, EAGE, DGG
Steven van der Veeke	Medusa Radiometrics / University of Groningen	steven@medusa-online.com	EAGE
Rainer Wackerle	GeoIntrepid Namibia / Intrepid Geophysics	wackerle@afol.com.na	None
Callum A. Walter	Queens University	11caw13@queensu.ca	SEG, AGU
Dennis Woods	Discovery International	dennis.woods@discogeo.com	IAGSA

Occasional Assistance to the Committee

Alan Reid	Reid Geophysics	alan@reid-geophys.co.uk	EAGE, SEG, KEGS
Robert B. K. Shives	GamX	rob@gamx.ca	SEG, PDAC

Document Status

Rev No.	Author	Reviewer		Approved for Issue		
		Name	Signature	Name	Signature	Date
0 (Draft)	Committee	G. Pettifer		Ron Bell		9/30/2022
1 (Draft)	Committee	G. Pettifer		Ron Bell		10/25/2022
2 (Draft)	Committee	G. Pettifer		Ron Bell		11/10/2022
Version 1	Committee	G. Pettifer		Ron Bell		11/13/2022

Contents

Table index

Figure Index

1.   INTRODUCTION

1.1   Background

This document "**UAV Total and Vector Field Magnetics Surveying Guidelines (Version 1)**", November 2022, arose from the SEG Summit on Drone Geophysics, 2020 (*https://www.linkedin.com/pulse/summit-drone-geophysics-seg-annual-meeting-call-laurie-whitesell/*), and a group of concerned geophysicists that were practitioners or interested users, in the emerging field and practice of use of UAV (drone)-based geophysical sensors for acquisition of magnetics, radiometrics, electromagnetics, ground penetrating radar (GPR), remote sensing and eventually gravity data. It was recognised in the discussions at the Summit, that many drone users, not experienced in geophysics, increasingly were developing drone mounted geophysical systems and acquiring data. Many geophysicists who were new to drone geophysics, coming from a land surveying or airborne surveying background were also on a learning curve on how to best acquire quality drone geophysical data.

There was evidence that a significant proportion of the data collected on these surveys, was of a lower quality standard than the geophysical industry was accustomed to, compared to ground or conventional airborne geophysical acquired data and this sub-quality data proliferation needed to be addressed for the benefit of the reputation of the geophysics industry and for protection of clients paying for drone geophysical services.

The urgent need was recognized for a set of guidelines for the various drone geophysical sensors Accordingly, a **Near-Surface Geophysics Inter-Society Committee on UAV Geophysics Guidelines** was formed and because drone-based magnetics was the most common data being acquired, it was decided for the Committee to first develop Guidelines for Drone Magnetics as a template for subsequent guidelines on drone-based radiometrics, electromagnetics, radar, remote sensing and possibly gravity data.

Guidelines can be easily developed and readily updated, which is much suited to the rapid evolution of drone-based geophysical technologies. Standards are more difficult to develop and get agreement on, but as these guidelines and technology matures, these guidelines could be developed further into industry standards. Until that time, with industry self-regulation and clients demanding quality data, these guidelines can serve as de-facto standards.

This Version 1 document is the end-product of the above concerns and Committee work and is by no means a complete coverage of all drone magnetics operation and quality considerations. Throughout this document the terms "UAV", "sUAS" and "drone" are used inter-changeably with the same intended meaning. The document is freely available to all, being downloadable from https://www.guidelinesfordronegeophysics.com/, where comments and suggestions for improvement can also be uploaded, for incorporation into Version 2 (due for release in April 2023). Feedback and comments for improvement of Version 1 are most welcome.

The industry is urged (1) to refer to and promulgate these guidelines, (2) for UAV magnetics operators to study and follow them, (3) for clients for their own protection, to require that UAV magnetics operators follow and demonstrate adherence to these guidelines, and (4) for interpreters to educate themselves about these guidelines when ascertaining the provenance and quality of the UAV magnetics data they are interpreting.

The Committee is also working on guidelines for radiometrics, electromagnetics and GPR. During the compilation of these guidelines, the release of the AMIRA Global Project P1204 - Developing UAV – Mounted Geophysical Sensor Arrays public version report (Francke et al, 2020) was released. It contains a wealth of information on the status and developing trends in drone geophysical sensor systems, including magnetics and the Amira Global document is recommended reading as a complement to these guidelines.

1.2   Aim of this document

What is a best practice?

A best practice is a standard or set of guidelines that is known to produce good outcomes if followed. Best practices are related to how to carry out a task or configure something. Strict best practice guidelines may be set by a governing body or may be internal to an organization. Other best practices may be more informal and can be set forth in manufacturer's guidance, in published guidelines or even passed along informally.

In some industries, there may be a legal requirement to follow best practice guidelines. In many technological fields, however, a best practice usually presents the optimal way to work, how to use a product or a set of ideals to reach toward. It may not be required to follow a best practice, but an organization should consult a best practice regularly and follow it wherever possible.

Source: **https://www.techtarget.com/searchsoftwarequality/definition/best-practice**

With the objective that widespread use of these guidelines will lead to better outcomes in terms of a general high level of data quality in acquisition and processing among the UAV magnetics operator and user community, the aim of this document is to provide **best practice guidelines** (see inset box above) with a six-fold range of objectives and end-users (stakeholders) in mind: -

1. to guide UAV magnetics operators (both geophysicists that are either experienced or not experienced in ground or airborne magnetics acquisition and data processing but who may be new to UAV-based operations and those experienced UAV platform operators that are new to geophysics especially magnetics data acquisition and data processing) on how to produce high quality final magnetic data.

2. to inform potential clients as to what should be expected from correctly acquired and processed UAV-based magnetic data, supplied by their contract UAV magnetics operators.

3. to give technical guidelines to underpin development and promulgation of Terms of Reference and/or contract specifications for clients and contract UAV magnetics operators to follow.

4. to educate interpreters of drone magnetics data, about the intricacies of such data in terms of how it can be properly collected, processed and presented and what to understand in terms of data quality.

5. to provide best practice guidelines for UAV magnetics that can be regularly updated, in the rapidly evolving field of UAV geophysics and that may lead to the eventual establishment of industry-recognized formal standards; and finally

6. to provide references and a bibliography of the rapidly evolving literature resources for further reading and deeper understanding on how to properly acquire and process UAV magnetic data.

The document provides an overview of:

- the basics of the magnetic method,
- what to consider when building and operating a drone magnetics system,
- survey planning and ancillary data to assist good planning,
- acquisition procedures including drone surveying etiquette, regulations and safety,

- data reduction, noise removal and processing principles and techniques develop for airborne magnetic data with special focus on how this can be applied to magnetics acquired on UAV platforms,
- imaging and interpretation of UAV acquired data, as well as'
- references and a selection of current relevant bibliography.

The authors acknowledge that there are operators producing final processed UAV magnetics data of the highest quality and clients who understand what good data is or is not and who know who are the best contractors to provide best practice UAV magnetics services. These stakeholders may believe they do not need any advice, but they can benefit from having these independently developed guidelines for best practice, to give confidence as to the best practice bona fides of the services provided and immediate and legacy value of the final data products of their UAV magnetics surveys, much the same as the geoscience industry has benefited from the long-established airborne magnetics survey guidelines (Coyle et al, 2014).

1.3 Providing feedback to update this Version 1 Document to a Version 2

This Version 1 of the UAV Total and Vector Field Magnetics Surveying Guidelines is to be updated to a Version 2 document due for release in early April 2023. Refer to the Website for updates on the next release (https://www.guidelinesfordronegeophysics.com/).

To create the Version 2 document, the Near-Surface Geophysics Inter-Society Committee on UAV Geophysics Guidelines is seeking feedback, edits and suggested improvements of the Version 1 document from industry and users of the guidelines. Instructions on how to download from the Guidelines website and edit an editable Version 1 Word document (.docx format) and then upload the edited Version 1, again to the Website, are given in Section 14.

We are also seeking input and suggestions for Guidelines for other UAV geophysical sensor mounted systems in preparation (radiometrics, EM, GPR). Suggestions can be emailed to the contacts as listed on the website.

The Committee appreciates your assistance in improving these and upcoming guideline documents.

1.4 Acknowledgement of Contributions to the Guidelines

The guidelines were devised by the entire Committee contributing ideas. The contributing authors, for each section of the Guidelines are acknowledged in Table 1 with the main author's entry bolded in the Table. The document editing was managed by Geoff Pettifer. The Guidelines launch event was organised by Laurie Whitesell (SEG), Tim Archer and Ron Bell. Ron Bell managed creation and organisation of the Website.

The entire Committee and their Professional Society and company/organisation affiliations are listed in the Table in the Document Status Page (frontispiece) before the Table of Contents and this shows that this document is truly an Inter-Society, industry ⇔ researcher and inter-company experience and intellectual property sharing and collaborative effort.

Many of the Committee edited drafts of the Guidelines. Shawn New of SEG Standards Committee provided comments on format and structure of the Guidelines. Laurie Whitesell of SEG helped with the Guidelines launch event. Drone Geoscience has kindly sponsored initial set-up of the Drone Geophysics Guidelines Website (https://www.guidelinesfordronegeophysics.com/).

The Committee thanks all Contributors, their employee organisations and affiliated Societies for providing their experience and intellectual property to the Guidelines and therefore for the benefit of the geoscience industry, the UAV geophysics community and end-users of drone magnetics data.

Table 1 Guidelines Content Contributing Authors

Section Numbers	Section Title(s)	Author (s)
1	**INTRODUCTION**	**Geoff Pettifer**
2 to 3	**MAGNETICS BASICS** **MAGNETIC SURVEY TYPES**	**Rainer Wackerle** Bruno Gavazzi
4	**CONFIGURING A UAV MAGNETICS SYSTEM**	**Ron Bell** James Jensen Alexey Dobrovolskiy Geoff Pettifer
5	**UAV MAGNETICS SURVEYING SAFETY AND REGULATIONS**	**Leslie McChesney** **Ron Bell** Alexey Dobrovolskiy
6.1 to 6.5	**POSITIONING & MAPPING (Positioning)**	**Jeff Gamey** Alexey Dobrovolskiy
6.6 to 6.7	**POSITIONING & MAPPING (Mapping)**	**Geoff Pettifer** **Alexey Dobrovolskiy**
7.1	**SURVEY PLANNING AND PREPARATION** **(Master Survey Plan)**	**Elizabeth Baranyi** Alexey Dobrovolskiy
7.2 to 7.4	**SURVEY PLANNING AND PREPARATION** **(Altitude, Line Separation, Specifications)**	**Rainer Wackerle** Alexey Dobrovolskiy
8.1 to 8.3; 8.5 to 8.6	**MAGNETIC SURVEY NOISE SOURCES** **(Instrument, Manoeuvre, Artefacts, Total system)**	**Rainer Wackerle** **Paul Mutton**
8.4	**MAGNETIC SURVEY NOISE SOURCES** **(Drone Electromagnetic Interference)**	**Callum Walter**
9.1	**SURVEY ACQUISITION AND QA/QC (Repeatability Test)**	**Paul Mutton**
9.2	**SURVEY ACQUISITION AND QA/QC (Tendering, QA/QC)**	**James Jensen**
10.1	**COMPENSATION AND CALIBRATION** **(Total Field Magnetics)**	**Rainer Wackerle** Paul Mutton
10.2	**COMPENSATION AND CALIBRATION (Vector Magnetics)**	**Johannes Stoll**
11	**PROCESSING AIRBORNE AND UAV MAGNETICS DATA**	**Rainer Wackerle**
12	**IMAGING OF UAV MAGNETICS DATA**	**Tim Archer**
13	**INTERPRETATION OF UAV MAGNETICS DATA**	**Tim Archer** **Bruno Gavazzi**
14	**CONCLUSIONS AND RECOMMENDATIONS**	**Geoff Pettifer** All Authors
15	**REFERENCES AND BIBLIOGRAPHY**	**All Authors**

2.   MAGNETICS BASICS

> *"… it has always been and still is my impression that a magnetometer survey is just as much a means of mapping geology as are the air photograph and the surface geological traverse …"*
>
> *Norman R. Patterson [believed to be attributed to either Telford or Blakely]*

2.1   Preamble – the Magnetic method

Measuring the spatial variation of the Earth's magnetic field is one of the most successful geophysical exploration techniques, due to the facts that terrestrial magnetization related properties (susceptibility, remanent magnetization) vary over a very large range and that magnetic surveys are relatively cheap. Magnetometers vastly improved from the first 'Swedish Mining Compass' (~ 1850) with a sensitivity of probably 1000 nT to modern instruments with sensitivities of 50 pT per $\sqrt{Hz}$ (SQUID) and sampling rates of up to 1000 Hz or more. At the same time mathematical methods to calibrate and process magnetic data were developed as well as interpretation and modelling techniques. Combined with highly accurate satellite navigation/positioning, high precision magnetic surveys are possible with reliable accuracies of around 0.1 nT. Many surveys may not achieve this accuracy, however.

The first airborne magnetic measurements were done in 1910 and during WW2 airborne magnetic surveys were used to detect enemy submarines using the fluxgate magnetometer device invented by Victor Vacquier (https://www.latimes.com/science/la-me-vacquier24-2009jan24-story.html). In 1947 Canada embarked as the first country in the world on a systematic national aeromagnetic coverage closely followed by Australia and Finland in 1951 (after Nabighian et al, 2005**)**. Nowadays many countries have a complete or partial coverage with 400, m 200 m or even 100 m line spacing aeromagnetic surveys.

Mounting a magnetometer on an airborne platform has the large advantage (over ground surveys), in that the data are collected as a spatially related unbroken time line, thereby facilitating quality control and data processing. Airborne surveys generally have few access problems and can be carried out over large areas and for longer periods, compared to ground surveys, and further allow the coverage of an area in a regular acquisition pattern which further improves the quality and evenness of spatial coverage, of the final data.

It therefore comes as no surprise that people wanted to mount magnetometers on UAVs, the moment they became available to the general public. UAV based magnetic surveys are by principle, airborne magnetic surveys and should be treated as such. However, drones are used for different purposes than conventional manned airborne surveys and given that magnetic signal strength and lateral differentiation of magnetic anomalies falls of rapidly with height of the magnetic detector above the ground, drone surveys can fill the gap between low level ground surveys and higher-level surveys from conventional aircraft. Nobody would plan to achieve countrywide or map sheet area coverage with magnetic data using a drone, but drones can fly at lower ground clearances, are easily mobilised and cheaper to operate. Hence, they can be used for smaller surveys in remote areas as well as for ultra-high-resolution surveys such an UneXploded Ordnances (UXO) detection or archaeological targets. Drones can further be used in populated areas or urban environments which are not accessible to manned aircraft due to safety regulations and other operational requirements.

It is the relatively low price of (some) drones, the fact that a drone pilot license can be achieved with a few weeks training and the ever-decreasing size of geophysical instruments which makes drone based magnetic surveys so popular. However, as stated above, there is no real reason as to why drone-borne magnetic surveys should not be subjected to the same rigorous quality and processing specification as conventional airborne surveys.

The above statement means that by measuring the spatial variations of the Earth's magnetic field we are able to identify and locate structures in the subsurface which are not necessarily visible on the surface. Magnetometer surveys are traditionally employed in exploration for natural resources but are nowadays also used to identify anthropogenic objects such as UXO, pipelines, waste dump sites, detailed outlines of remnant archaeological sites etc.

Measuring the strength of the magnetic field and its direction at a single point on Earth does not yield any information except for the direction to magnetic North (Compass). In order to obtain information about the subsurface, the spatial variation of the magnetic field in the area of interest needs to be known, e.g., we need many measurements. The easiest way to obtain many observations that eventually result in a complete coverage of the survey area (grid or image) is to measure along parallel lines. This can be done on the ground, from a vessel or from air. Airborne geophysical surveys have the huge advantage that they are fast and have much less access problems than other survey types.

In order to understand what we are doing we have to take a look at some fundamentals of magnetics as used in geophysics.

2.2   History of Geomagnetism

The study of geomagnetism has a longer history than other branches of geophysics (Mitchell, 1932 and 1946; Stern, 2002; Nabighian et al, 2005), because of its use as an aid to navigation. Petrius Peregrinus (Pierre de Maricourt of France, 1269, translated in Brother Arnold, 1904) introduced the word "poles" in connection with magnets (https://en.wikipedia.org/wiki/Petrus_Peregrinus_de_Maricourt). Evidence that the Earth is a great magnet was presented (in Latin) in Gilbert's book "De Magnete", published in 1600 (Gilbert, 1600; https://en.wikipedia.org/wiki/De_Magnete). C.F. Gauss was first to apply spherical harmonics to its analysis (https://en.wikipedia.org/wiki/Carl_Friedrich_Gauss). However, the idea that it was maintained by internal electric currents arose much later. It has long been speculated that this mechanism is a convective dynamo operating in the Earth's fluid outer core, which surrounds its solid inner core, both being mainly composed of iron (Larmor, 1919; Parker, 1955).

2.3   Earth's Magnetic Field

Modern three-dimensional numerical simulation of the geodynamo reveals, that the Earth's Magnetic Field can be explained by a dynamically self-consistent model. It explains why the geomagnetic field has the intensity as it does, has a strongly dipole-dominated structure with a dipole axis nearly aligned with the Earth's rotation axis, and has non-dipolar field structure that varies on the time scale of ten to one hundred years and why the field occasionally undergoes dipole reversals. Such numerical dynamo models which qualitatively reproduce some structural characteristics of the present-day geomagnetic field, are described e.g., by Glatzmaier & Roberts (1995) and Christensen et al. (1998).

At any point on the Earth's surface, the magnetic field F has some strength and points in some direction (see Figure 1). Declination is the angle between north and the horizontal projection of F. This value is measured positive through east and varies from 0 to 360°. Inclination is the angle between the surface of the earth and

direction of the magnetic field F. Positive inclinations indicate F is pointed downward; negative inclinations indicate F is pointed upward. Inclination varies from -90 to 90 degrees. The magnetic equator is the location around the surface of the Earth where the Earth's magnetic field has an inclination of zero and the magnetic poles are the locations on the surface of the Earth where the Earth's magnetic field has an inclination of either plus or minus 90 degrees. Note, these locations do not necessarily correspond to the Earth's rotational equator/ poles and because of the properties of the dynamo of the earth causing the earth's magnetic field the magnetic pole and equator locations can change over time.

The magnetic field (magnetic flux density) in SI units is measured in Tesla (T) which is defined as: A particle, carrying a charge of one Coulomb and moving perpendicularly through a magnetic field of one Tesla, at a speed of one metre per second, experiences a force with magnitude one Newton. $T = N/A \cdot m = V\ s/m^2$. In geophysics we usually talk about 10^{-9} Tesla or nano-Tesla (nT) with the strength of the Earth's magnetic field varying roughly from 20 000 to 70 000 nT.
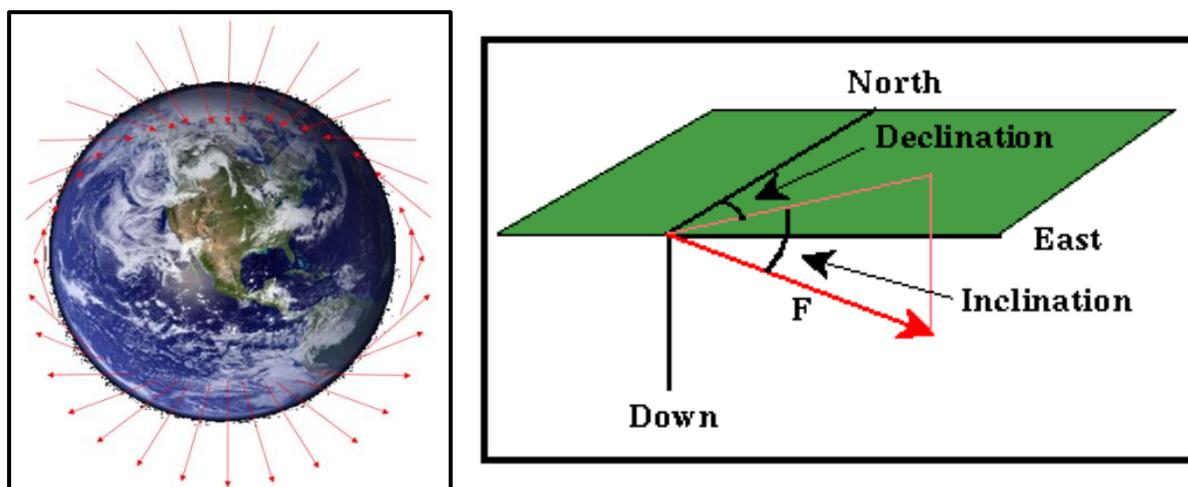
Figure 1   The Earth's magnetic field - definitions.

The present-day Earth's magnetic field is best described by the International Geomagnetic Reference Field (IGRF). It is a standard mathematical description of the large-scale structure of the Earth's magnetic main field and its secular variation. It is created by fitting parameters of a mathematical model of the magnetic field to measured magnetic data from surveys, observatories and satellites across the globe. The IGRF has been produced and updated under the direction of the International Association of Geomagnetism and Aeronomy (IAGA) since 1965. The current 13th edition of the IGRF model was released in December 2019 and is valid from 1900 until 2025 (https://earth-planets-space.springeropen.com/articles/10.1186/s40623-020-01288-x). Figure 2 shows a global map of the magnitude of the IGRF (the field in the map is dated 28 March 2000).

2.4   Local magnetic anomalies

At local scales however, the magnetic field over a homogeneous earth is (almost) constant. The field is distorted when there is a magnetic contrast in the Earth's crust. From the shape of the distortion (anomaly) of the normal field, we can deduce some attributes of the source body as shown in Figure 3.
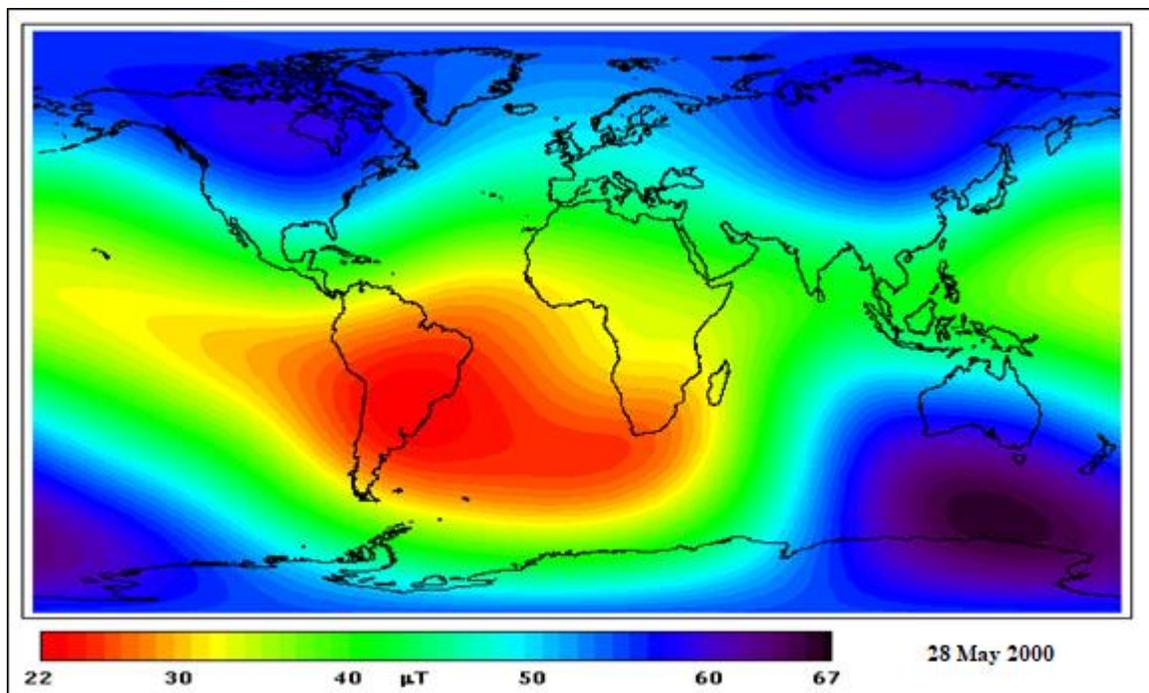
Figure 2   Magnitude of the International Geomagnetic Reference Field (IGRF)
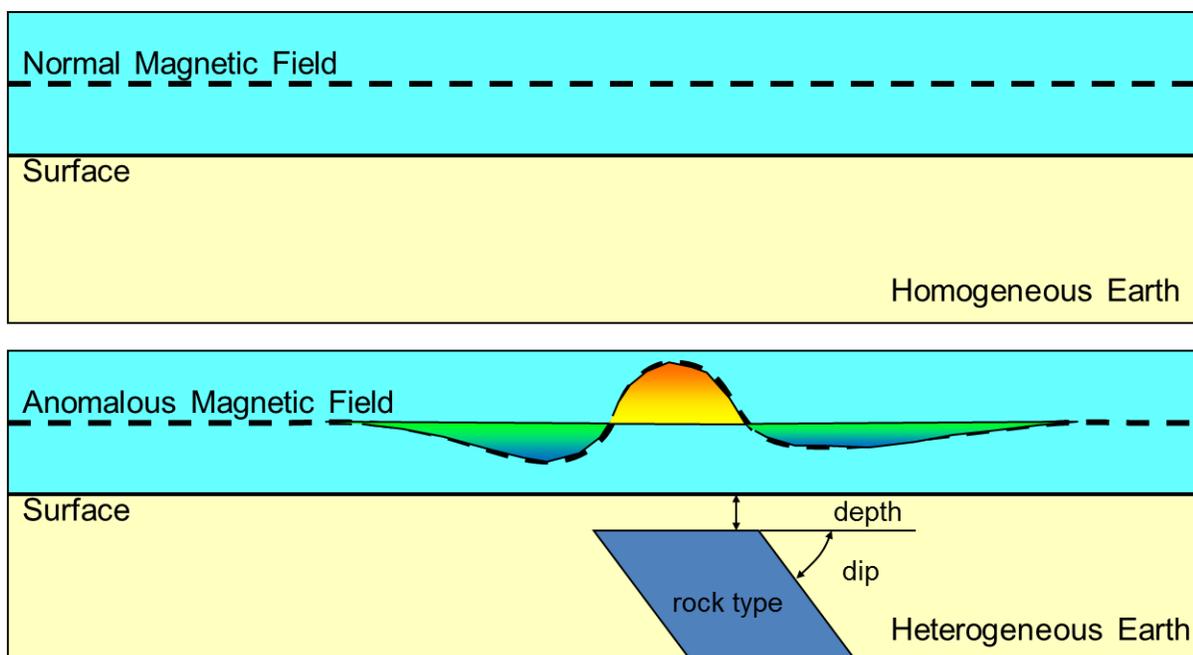
Figure 3   Principle of the anomalous magnetic field

When computing the anomalous magnetic field over a large area we get a magnetic anomaly map. Figure 4 compares the anomalous magnetic field over Namibia with the simplified geological map demonstrating the wealth of information added by the magnetic data to the surface geology.
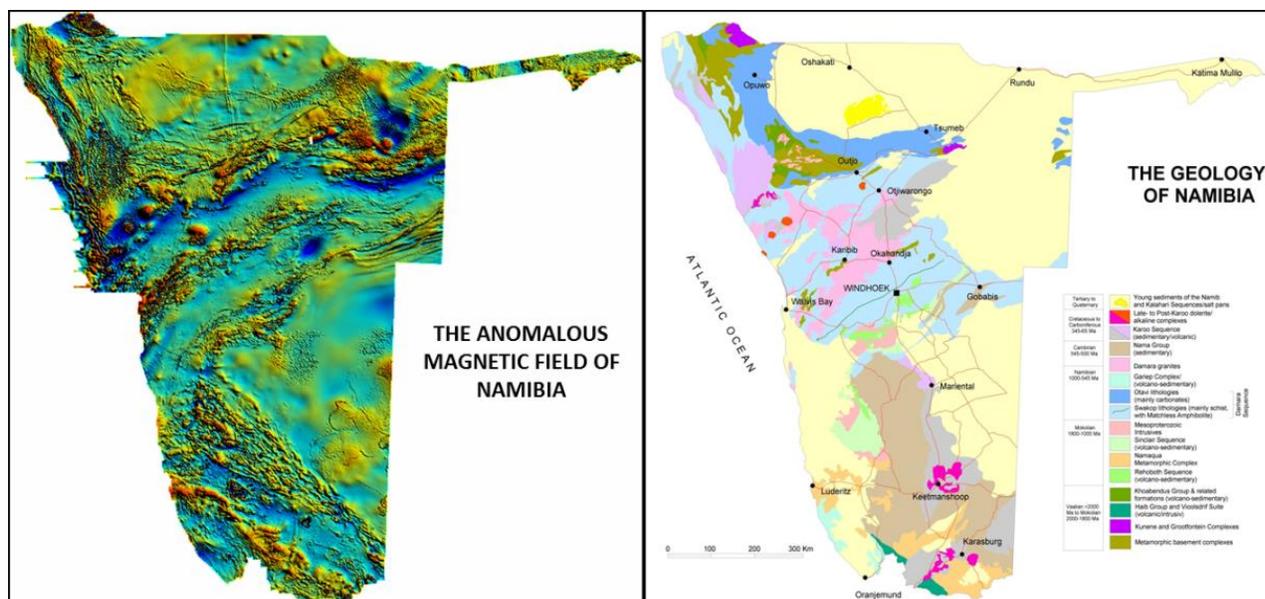
Figure 4   Anomalous magnetic field of Namibia juxtaposed to the simplified geology.

(Source: "Earth Data Namibia Information System of the Geological Survey of Namibia" https://www.mme.gov.na/edn/)

2.5   Magnetic Susceptibility of Rocks and Minerals

In magnetic prospecting, the magnetic susceptibility is the fundamental material property; its spatial distribution as a proxy for lithology is what we are attempting to determine. Most common rock-forming minerals exhibit a very low magnetic susceptibility. Rocks owe their magnetic character to the small proportion of magnetic minerals that they contain. There are only two geochemical groups which provide such minerals (Dentith and Mudge, 2014). The first of these groups is the iron-titanium-oxygen group from magnetite to ulvöspinel. The other common iron oxide, haematite, is antiferromagnetic and thus does not give rise to magnetic anomalies unless a parasitic anti-ferromagnetism is developed. The second of these groups is the iron sulphur group which provides the magnetic mineral pyrrhotite whose magnetic susceptibility is dependent upon the actual composition. By far, the most common magnetic mineral is magnetite. For a list of the more common minerals that demonstrate magnetic properties, refer to *http://www.galleries.com/minerals/property/magnetis.htm*.

Nevertheless, the magnetic susceptibilities of common rocks and sediments, e.g., the proportion of magnetic minerals they contain, vary over a large range as shown in Figure 5. This variation is the main reason for the success of magnetic surveys in geo-exploration.

Any rock containing magnetic minerals may possess both induced **and** remanent magnetizations. Induced magnetisation is proportional to both the ambient field and the magnetic susceptibility, whereas remanent magnetization is related to the past induced magnetisation and is defined by the strength and direction of the earth's magnetic field at the time of the rock formation (*https://en.wikipedia.org/wiki/Remanence).* These may be in different directions and may differ significantly in magnitude. The magnetic effect of such a rock arises from the resultant magnetization vector of the two vectors. Its magnitude controls the amplitude of the magnetic anomaly and the orientation its shape. The relative intensities of induced and remanent magnetizations are commonly expressed in terms of the *Königsberger Ratio* (*https://wiki.seg.org/wiki/Dictionary:Koenigsberger_ratio_(Q)*; Hood, 1964)

All magnetic anomalies caused by rocks are superimposed on the main geomagnetic field. Magnetic anomalies are complex, however, as the geomagnetic field varies not only in amplitude, but also in direction.
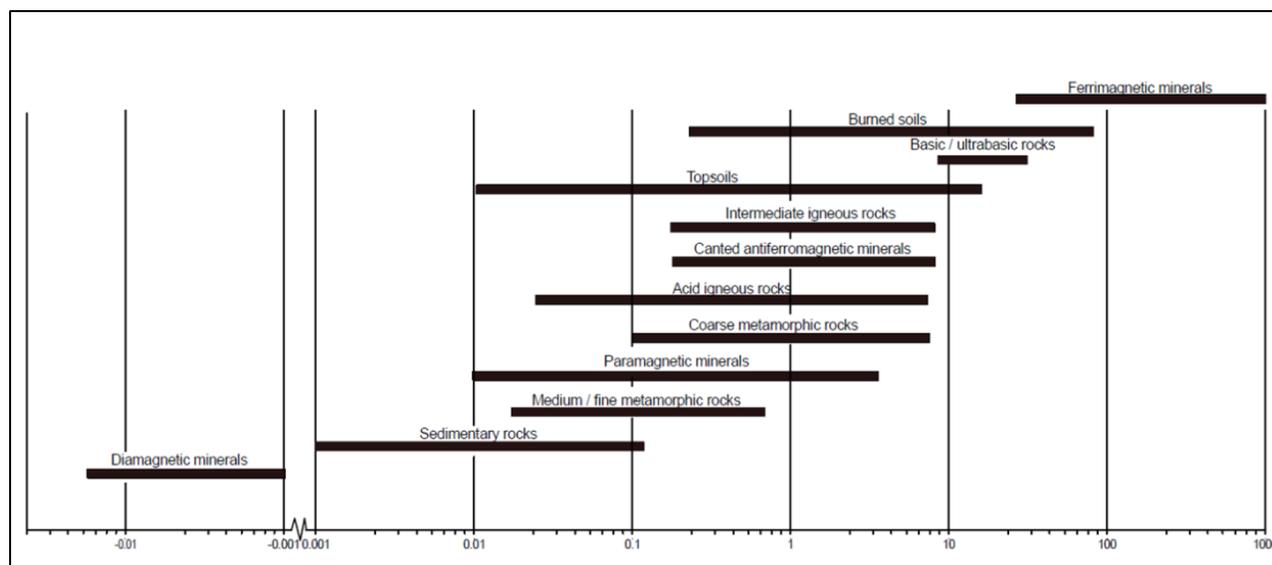
Figure 5   Magnetic susceptibilities of common rocks and sediments

2.6   Components of the Earth's magnetic field

As previously mentioned, the spatial distribution of magnetic susceptibility is what we are attempting to determine in magnetic prospecting. In order to do this successfully and to be able to compare/merge magnetic data from neighbouring surveys, we need to separate the geological (or anthropogenic) part of the magnetic field. As observed on the surface of the earth, the magnetic field can be broken into three separate components:

2.6.1   Main Field (IGRF)

This is the largest component of the magnetic field and is outlined by the International Geomagnetic Reference Field (IGRF) as described in Section 2.3. This field, which is also known as the ambient field, acts as the inducing magnetic field and is slowly changing with time (secular variations). It is common practice to remove the IGRF from the observed magnetic data.

2.6.2   External Magnetic Field

This is a relatively small portion of the observed magnetic field that is generated from magnetic sources external to Earth (Ionosphere, sun spot, solar wind, solar cycle); it changes quickly with time.

Since Earth is revolving within the external magnetic field these variations are called **Diurnal Variations**. Diurnal variations are usually in the range of 20 to 50 nT per day, but may reach up to several 100s of nT in case of solar storms. Figure 6 compares a normal diurnal variation (top) with the variations cause by a magnetic storm (bottom).
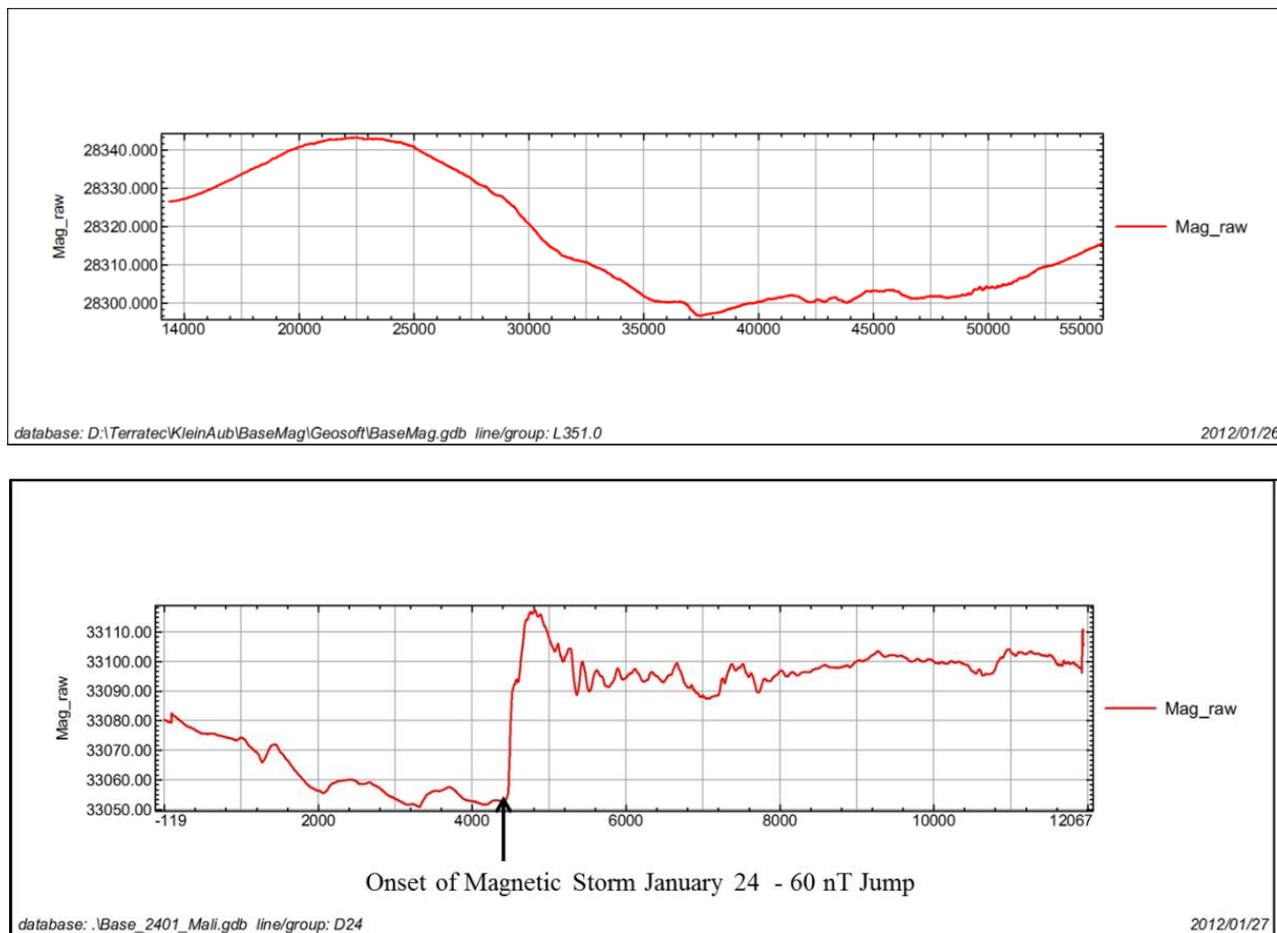
Figure 6   Examples of diurnal variations.

(Top: Typical variation. Bottom: Variation caused by a solar storm)

Diurnal variations have to be measured by a static magnetometer (base station) and removed from the measured data. Best practice is to leave a base station in the same secure, magnetic noise-free location (xyz) for the duration of a magnetic survey. Usually, all magnetic measurements undertaken during a magnetic storm are scrapped and have to be repeated, because the high frequency variations during such a solar event are prone to rapid phase changes and can therefore not be removed correctly.

2.6.3   Subsurface Rocks Field

This is the part of the magnetic field associated with the magnetism of subsurface rocks (and anthropogenic materials). It contains both, magnetism caused by induction from the Earth's main magnetic field and from remanent magnetisation. This field is the target of geomagnetic prospecting. This field measured by two surveys carried out at different times, may vary and differ, due to secular variations on a longer time scale than diurnal variations (Courtillet and Le Mouël, 1988).

2.7 Magnetic Sensors

Available magnetic sensors to measure the earth's magnetic field and their magnetic reading accuracy (instrument noise) capabilities are listed in Table 2. Instrument noise should not be mistaken as sensor noise (or sensitivity) as given by instrument manufacturers.

It is most important to understand that it is the total system noise during surveying, which is more important than instrument or sensor noise. Total system noise includes manoeuvre noise which is the real-world noise in collected drone magnetic surveys, which has to be removed by configuration of the sensor on the drone, or by removal of the system noise in processing. This is discussed in more detail in Sections 8 to 11.

Table 2 Sensor types and characteristics

Type	Dead Zone	Temperature Drift	Maximum Sampling rate (Hz)	Sensitivity
Caesium OP	$\pm15^0$ Po/$\pm15^0$Eq	nil	10-4000	High
Potassium OP	$\pm10^0$ Po/$\pm10^0$Eq	nil	20	High
Rubidium OP	$\pm7^0$ Eq	nil	400	High
Caesium (1xMFAM)	$\pm35^0$ Po	nil	1000	Variable
Caesium (2xMFAM)	0	nil	1000	Variable
Fluxgate	nil	±300-1000pT/K	10000	Moderate

2.8 The necessity for geophysical data processing

During the age-old debates between geologists and geophysicists, geophysicists often state that "… we at least get the same result when surveying an area twice…" But is this statement true, do we really produce identical results when taking measurements several times at the same location? And the simple answer is no, we don't. Only after adding a series of 'ifs' this statement becomes somewhat true.

Active geophysical measurements are where a geophysical signal is transmitted and a ground response is received, such as in electromagnetics (EM) surveying. Active geophysical measurements heavily rely on the transmitter/receiver specifications as well as their spatial geometry to such an extent that data from two different EM systems for instance can only be compared after inversion or modelling. But even data from passive methods, where only an earth's natural geophysical field or signature is measured, such as potential field measurements (for example magnetics), only yield similar or identical results when data reduction and corrections are applied correctly, as everybody who ever tried to merge data from many potential field surveys can confirm. And commonly drone surveys tend to cover larger areas by collecting a series of different (slightly overlapping) surveys, referred to as tiles, which are flown at different times.

The reason for differences in data from adjacent magnetic surveys can be found in the time varying nature of the ambient magnetic field and the disturbing influence any platform inevitably produces. Hence, we need to correct for time variations and platform influences. However, it is the magnitude of the magnetic strength of the target - in contrast to the host material - which defines the number of reductions and corrections to be applied and the required accuracies.

Figure 7 compares raw and final magnetic data from an area with very high magnetic response (top) to data from an area with rather low magnetic contrasts (bottom). Both areas span 75 flight lines with the top area flown in east–west direction and the bottom survey north-south. Whereas the difference between the raw and the final data in the high dynamic area are visible but not excessive, the raw magnetic data over the low
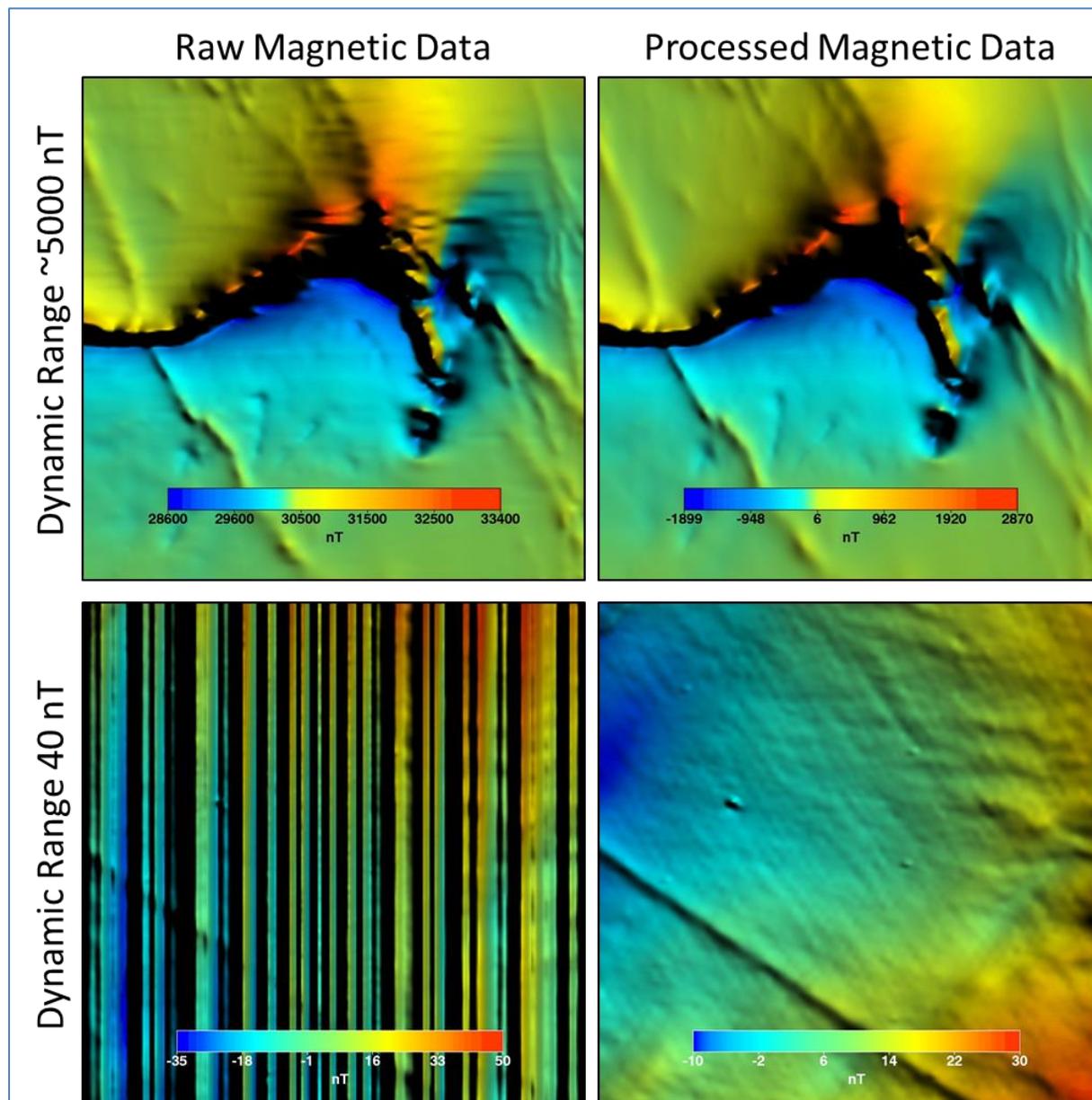
Figure 7   Comparison of raw and processed magnetic data.

(Left: Raw data. Right: Processed data. Top: Data over an iron ore deposit with a dynamic range of close to 5000 nT. Bottom: Data over a sediment basin with a dynamic range of 40 nT. Both areas cover 75 flight lines.)

dynamic area. hardly show any structure at all. Obviously, processing does improve data consistency in the high range area as well, but one can clearly identify the main structure even in the un-processed data. In the low dynamic range area on the other hand, data reductions, corrections and adequate processing are absolutely essential to produce a consistent image.

2.9 Commons reductions and corrections to magnetic data

The common reductions and corrections applied to scalar magnetic data are listed below together with their approximate magnitudes. It should be noted here that fluxgate vector magnetometers are different to scalar magnetometers in that they have to be calibrated before calculating the scalar strength of the magnetic field (see Section 10.2.2 for more details).

- Compensation / Calibration / Manoeuvre Noise < 10 nT

- Diurnal correction 10s of nT, but can reach > 100 nT

- IGRF removal (ambient magnetic field). 10s of nT

- Heading correction < 10 nT

The reason for applying the above corrections and reductions is that they are based on the principles of physics, as opposed to the rather 'cosmetic' nature of levelling processes such as tie line and micro-levelling. The corrective measures are obtained either by observing the variations directly, such as the diurnal variation or, more indirectly, the IGRF, or they do result from calibration procedures or test flights.

A rough guideline as for which anomaly strength what data reduction or correction is required is given in Figure 8. The target anomaly strength, plotted at a logarithmic scale, is compared to the magnitude of the various corrections. Please note that the boundaries are rather vague and are provided as guidelines. It
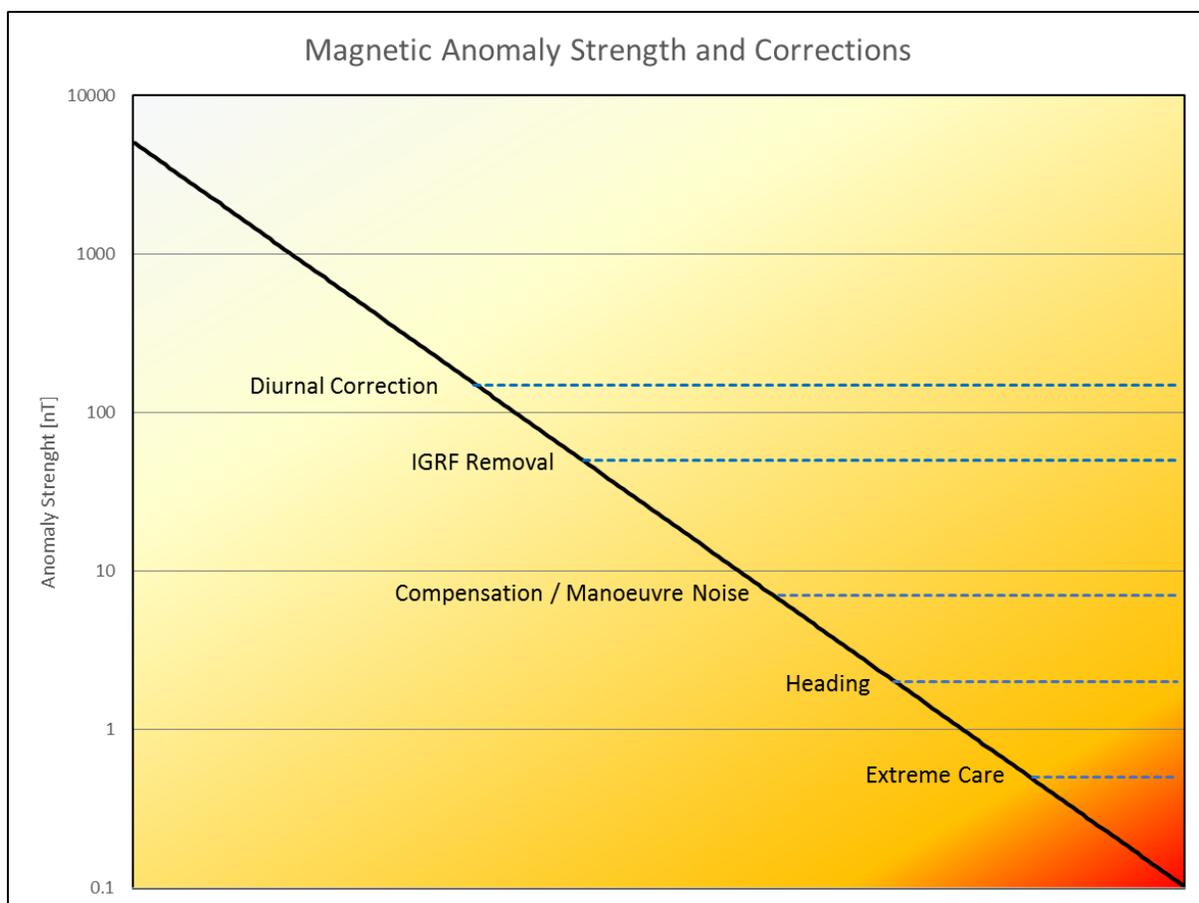
Figure 8   Magnetic anomaly strength vs the magnitude of standard corrections

(Note: The boundaries as to when a correction is required are rather fluid and the displayed values are guidelines only.)

should further be noted that applying all corrections will always improve the quality of the final data, which eventually becomes important when producing secondary products from the final data, such as derivatives, edge detection or modelling. However, applying a heading correction of 1.5 nT to the high range data shown in the top of Figure 7 is very likely not to improve the data and could therefore be omitted.

Performing all data corrections is also advised when the contrast between the target anomaly and the host material is low, regardless of the absolute strength of the anomalies, in order to avoid the identification of false targets. And it should go without saying that when the target strength reaches the sub-nT region, extreme care has to be taken not only with data corrections and processing but also with simple survey parameters such as line and height keeping.

One further has to distinguish between 'mapping' and 'target' surveys. Mapping surveys are mostly employed for the exploration of natural resources at moderate ground clearance (>5 – 40 metres depending on vegetation height), and also for geological mapping, Detailed surveys are flown for archaeological sites and for UXO with both of these surveys flown at the lowest ground clearance, safely possible and with the highest precision, meaning that the susceptibility distribution within the survey area needs to be identified as accurately as possible to allow geological or target interpretation of the magnetic data. Therefore, proper correcting and processing of the raw data, are crucial for both conventional or UAV based mapping surveys.

Drone surveys on the other hand are often flown as 'target' surveys with the sole objective of locating objects of a predefined sized and magnetisation, generally with magnetic anomaly amplitude well above noise of magnetic correction levels. InIftarget has a high susceptibility contrast to the host environment and is of a larger size compared to the line spacing, correction and processing requirements can be relaxed.

2.10   UAV Manoeuvre Noise

Whereas diurnal corrections, IGRF removal and heading corrections are fairly simple processes which are implemented in most geophysical processing packages, platform-compensation/manoeuvre-noise removal is more complicated and is **not** available as a standard tool. These corrections are therefore often neglected by drone operators. **Manoeuvre noise however, is currently the main reason for drone based aeromagnetic surveys not achieving the high-quality standards of conventional airborne data.** Manoeuvre noise is discussed in more detail in Section 8.3.

3.   MAGNETIC SURVEY TYPES

Airborne magnetic surveys for the detection and/or delineation of sub-surface structures have been used for more than half a century. With the advances in sensor technology and processing capabilities, but especially since the advent of accurate satellite navigation, nominal specifications for airborne magnetic surveys have become stricter and the quality and resolution of airborne magnetic data has increased significantly with entire regional datasets achieving sub nT accuracy at a spatial resolution of 50 metres. Drone operators should strive to reach the data quality of conventional manned airborne surveys and process their data to the full extent of the corrections available

However, drone based aeromagnetic surveys are flown for a variety of reasons, whereas conventional airborne surveys are mainly conducted for geological mapping on a much larger scale often targeting multiple users/uses. Depending on the survey objective not all drone surveys may therefore require the highest quality standards. For instance, when the location of old borehole collars is required or the extension of a shallow quarried basalt layer needs to be mapped, the requirements for data quality can be relaxed. Other drone surveys may only be flown as a replacement of wide spaced ground data due to the better production rate of airborne surveys or to bypass access problems.

Table 3 is a recommended categorization showing that there are three types of drone magnetic surveys (Levels 1 to 3) differentiated by:

- the survey objective,

- survey altitude (terrain clearance) and consequent line spacing,

- the magnetic signal of the target geology or object being mapped against the background magnetic noise (signal / noise),

- the required processed data accuracy and

- the required degree of processing to achieve the required survey accuracy and meet the survey objective.

There are many more possible applications for drone based aeromagnetic surveys especially when low ground clearance is required which in conventional (manned) airborne surveys can only be achieved by expensive rotary wing platforms. It is the ultimate responsibility of the contractor to know the final resolution of the employed sensor-platform system, for the Level of survey employed and to communicate this clearly to the client.

Table 3 Survey types and objectives

Survey Level	Survey Objective	Ground Clearance	Traverse Line spacing	Tie line spacing	Sensor Noise	Positioning / altitude accuracy	Real world system noise	Remarks
1	UXO detection and similar environmental applications including archaeological site surveys	0.2 to 5 m, typically <1 m	1 m	N/A	<0.5 nT	<10 cm	0.1 – 0,5 nT	Multi-sensor systems – Gradient / Tensor systems. High sampling rates/
2	Geological mapping in general at prospect scale or for detailed mineral exploration with the capability of detecting weakly magnetic targets (e.g., mineral sands strand lines) or distinguishing deeper targets beneath shallow sources of geological noise (e.g., maghemite, rich regolith, laterites or shallow surficial volcanics)	5 to 30 m	1 x the terrain clearance	5 x to 10 x the flight line spacing	< 1 nT	<1 to <5 m depending on the flight line spacing and the narrowness of the target.	0.1 – 0,5 nT	Sampling rate may need to be higher for higher resolution of narrow targets or to different sources of surface noise
3	Abandoned cased wells, pipelines, buried services and waste dump site detection	>5 m	1 x the terrain clearance	N/A	< 1 nT	<1 m	<5 nT	Generally high to moderate signal / noise targets

4. CONFIGURING A UAV MAGNETICS SYSTEM

The following checklists pertain to the technical, logistical, and regulatory factors relevant to optimally configuring a new UAV magnetics system or improving the performance of an existing system. Readers are encouraged to add to this checklist when making suggestions for improvements to Version 1 of these guidelines – upload updates to these Version 1 guidelines at https://www.guidelinesfordronegeophysics.com/.

A useful reference to review the literature of the variety of drone magnetic systems is Zheng et al (2021). The bibliography in these guidelines is a selection of references taken from Zheng et al (2021).

4.1   Checklists

4.1.1   Setting up a Drone Magnetics system from scratch

Some of these items will be obvious but are included for completeness. The list may not be all that may be needed to consider.

- Read and digest these guidelines first, understand what you are letting yourself in for from a budgetary, technology, safety/Regulatory and data quality perspective. Know what you need to learn and know, Consult with subject matter experts experienced in the collection of UAV enabled magnetic data,

- Refer ahead to the Surveying objectives checklist (Section 4.1.2) for likely technical and operational requirements, relevant to how you set up your drone magnetics system capability.

- What is your intended purpose for getting into the drone magnetics business? Will you be contracting out services or just working your own in-house projects? What targets and type of surveys will you be undertaking (Levels 1 to 3; Section 3; Section 4.1.2), as this determines your path through this checklist and relative relevance of some items on the checklist?

- Will beyond visual line of sight (BVLOS) operations be initially or eventually contemplated?

- Drone suitability – endurance, payload, technical specifications fit-for-purpose, security considerations on the drone manufacturer or not (e.g., US DoD Blue UAS list - https://www.diu.mil/blue-uas)

- Is a second smaller drone for survey area photography, pre-flight planning needed as well?

- Pilot certification and their understanding of drone magnetics specifics of flying a magnetics system

- Getting a safety system in place and understanding the Regulations (Section 5).

- Vector or total field magnetics system? Magnetics base station to be used? Best commercial units to buy? Refer to Table 2.

- Sling load design – distance of the magnetometer from the drone and rigidity of the suspension system and implications for the need for platform compensation or not? Either suspend the magnetometer outside the zone of noise influence of the drone and make compensation for platform noise largely irrelevant, or suspend the magnetometer closer to the drone and plan for compensation to get best quality data (Section 8.4; Figure 21). Will there be a quick release mechanism on the sensor tow cable in case of entanglement?

- Navigation technology in/on the magnetics sensor and in/on the drone and understanding of options and precision for your intended survey purposes.

- Terrain clearance requirements and technology used to measure and/or maintain UAV clearance above ground level?

- Terrain / vegetation top elevation models to be used – available or to be acquired?

- If LiDAR or photogrammetry – pre-survey is required, will it be contracted in or be acquired by you?

- Obstacle sensors if contemplating low level flying? On the drone or sensor or both?

- Flight planning and flight control software and integration with the acquisition software?

- Acquisition software and ability to integrate all data – off the shelf or your own programming?
- Maintaining radio communication (RC) with the drone during flights and provision for loss of communication scenarios?
- Will you be processing your own magnetics data or contracting it out to a geophysicist? Software to be used?
- Final system refining, integration, testing – getting the total workflows in place and working.
- Set up your technical specifications (following the guidelines).

4.1.2   Tailoring technical and safety requirements for survey objectives.

Section 3 and Table 3 discusses three types of surveys (with their own objectives, altitude, location and magnetics data precision and processing requirements). Sections 5.2.1 to 5.2.3 differentiate surveys from an altitude and safety perspective. Definitions of the acronyms are later in the document and it is best to revisit this survey objective list once a better understanding is achieved from reading the full guidelines document.

Ultra Low Altitude (Sensor is 0.5 to 5 meters AGL)

Applications include UXO Detection, archaeology, etc.

- RTK/PPK GNSS receiver is **required**.
- Terrain following system with rangefinder/altimeter is **required**.
- Obstacle avoidance sensors are **recommended**.
- Depending on targets of interest, hard mounting of magnetometer under the drone may be recommended to increase manoeuvrability and wind resistance of the UAV system.
- Flight planning software should allow to use hi-resolution orthophoto maps as background to avoid obstacles (bushes, trees, fences, etc.) on flight planning stage.
- Sampling rate should be to deliver ~10 samples per survey line meter.

Low Altitude (5 m to 30 m - height of trees)

Geological and prospect mapping, mapping of abandoned wells etc (ground clearance >5-30m, positioning accuracy <1 to <5m)

- More or less the same requirements as for Ultra Low Altitude surveys.
- Obstacle avoidance sensors not needed provided the sensor is flying well above vegetation tops.
- Vegetation tops elevation model (DSM) as well as DTM recommended for flight planning.
- Drape or constant elevation flying could be employed.

Standard Altitude (30 m to regulatory limit).

Geological and prospect mapping, etc (ground clearance >30m, positioning accuracy <1 to <5m)

- More or less the same requirements as for Low Altitude surveys.

Survey Generic considerations

- Flight planning software should support route planning according to the digital elevation models:
    i. High definition DEM/DTM should be used to assure required ground clearance,
    ii. DSM may be used to check flight's safety.
- Obstacle sensor and avoidance technology is recommended when area of investigation contains vertical structures (e.g., trees, building, towers, etc.).

- Keeping the magnetic survey base station in the same secure, xyz, noise free location for the survey duration is the best approach.

4.1.3   Planning an actual survey

- Obtain necessary permits to fly and landowner access permissions.
- Check the space weather to confirm no expected magnetic storms during acquisition (for an example refer to *https://www.sws.bom.gov.au/Geophysical*).
- Prepare the client agreed survey specifications and communicate these clearly to drone operator / pilot.
- Survey specification should be consistent with depth to and size of the target.
- Ensure that the UAV positioning system/accuracy is appropriate.
- Confirm vertical datum / projection (geoidal vs ellipsoidal heights) is set properly.
- Ideally plan for a secure, noise free area, fixed location for the magnetic base station.

4.1.4   Mobilisation - Items for daily field work operations

- UAV Pilot Certificate and other identification required by law enforcement.
- UAV and liability insurances.
- Permits to fly, client and landowner and local authorities contact information.
- Survey specification approved by client.
- Health and Safety Plan (HASP).
- UAV airspace app.
- Weather app.
- Anemometer to monitor wind speed.
- Tablet / laptop loaded with mission planning and control software.
- Photogrammetry and DEM/DSM as required.
- UAV   properly marked with reg ID UAV batteries with adequate number of spares.
- Altimeter for terrain clearance, as applicable.
- WiFi hotspot for flight control application.
- GNSS RTK for UAV with GNSS RTK base station GNSS data processing software.
- UAV Magnetometer.
- Base station magnetometer.
- Motor generator for charging batteries.
- Walkie-talkies for ground crew communication with pilot in command (PIC).
- Terminal strip(s) and extension cord(s).
- Tables, chairs and canopy for shade.
- Laptop PC equipped with data processing & mapping software.
- Camera drone.
- Photogrammetry software or processing service.

5. UAV MAGNETICS SURVEYING SAFETY AND REGULATIONS

Section 5 of these guidelines:

- looks first at practical aspects of safe flying of a drone with a magnetic sensor payload based on three different survey altitude categories: obstacle avoidance risks, navigation risks, drone communication risks (Sections 5.1 to 5.4)

- and then addresses regulatory aspects (Sections 5.5 to 5.10) and safety planning within a risk assessment safety approach, not dissimilar to other geophysical and general job safety operational health and safety planning approaches (Sections 5.11 to 5.13). The regulatory aspects and safety planning information is based on ICAO and industry standards such as Flight Safety Foundation Basic Aviation Safety (BARS) program (https://flightsafety.org/basic-aviation-risk-standard/). As such these standards are recognized by most international member states and form a framework for operations. These guidelines do not replace the country of operations Regulatory requirements.

5.1 Obstacle Avoidance

The main reason for UAV crashes during magnetic surveys is collision with obstacles.

For surveys with extremely low clearance (Survey Level 1 and possibly 3 in Table 3) obstacles are vegetation, bushes, fences, etc.

To avoid such obstacles, a drone and may be the sensor, may be equipped with obstacles sensors (radar, optical/camera-based/, laser). But these sensors should be treated in the same light as a "parachute for a manned aircraft pilot", that is they should never be relied on them in regular magnetic surveying workflows. The flight planning software should allow for import of high-resolution imagery (orthophoto map), which may be gathered as a preliminary photogrammetry survey of the AOI. Resolution of the imagery/map should be high enough to see typical obstacles (fences, etc.). That will allow planning of routes that are avoiding visible obstacles.

Obstacle avoidance strategies and technologies employed are related to survey terrain clearances of the drone and sensor and the variability of the terrain.

Note, that typical built-in obstacles sensors of commercially available drones are designed to detect something at the level of the drone. They are not suitable for drones with mag sensor on suspension system beneath the drone.

As flights are usually planned according to a DEM/DTM, precision of elevation data becomes vital. Unfortunately, free and even commercially available DEM/DTM satellite-derived data is often not precise enough, especially in rough/hilly/mountain areas.

In general, it is recommended to use LIDAR-derived data. In the US almost all territory is covered with publicly available USGS data. If LIDAR-derived data is not available before a job, it is recommended to conduct a LiDAR scanning of the survey area to gather precise Digital Elevation Model of the ground surface DEM and a Digital Surface Model (DSM) data of the tallest surfaces (typically vegetation and structure tops) across the survey area (Figure 9). Ideally, the route should be planned according to the DEM, and checked for the flight safety using the DSM.

In the case of the suspended sensor still colliding and entangling with an obstacle, a quick release mechanism on the sensor tow cable may be a good strategy to ensure at least immediate drone recovery and return to base.

Figure 9   Distinction between a DTM and DSM

(Source: https://www.neonscience.org/resources/learning-hub/tutorials/chm-dsm-dtm-gridded-lidar-data).

5.2   Airspace altitude considerations for Drone Magnetics Survey Safety

The flight operation safety guidelines need to be placed within the context of the airspace to be occupied.

The sUAS flight operational air space (FOAS) can be divided into three categories:

- Standard Altitude (SA)

- Low Altitude (LA)

- Ultra-Low Altitude (ULA)

5.2.1   Standard Altitude (top of trees (~ 30m) to regulatory limit)

Many, if not most, magnetic surveys are accomplished in the SA airspace. Aircraft navigation and flight speed are key considerations. Vertical structures are less of a concern.

Nonetheless, the UAV Pilot should always review the Area of Interest (AOI) conditions (i.e., topography, cover, etc) and adjust the flight plan to take into consideration the presence or potential presence of vertical structures. For example, high power transmission lines, trees, etc.

Forward looking sensors mounted on the UAV are generally useless for slung payload configurations. Standard GNSS for navigation is adequate. RTK positioning is not needed. The flight line spacing for magnetic surveys is in part a function of the height of the sensor above ground level. There is no benefit to measuring the magnetic field at a 5m line spacing for survey altitudes of 30+ m AGL.

A 10m x 10m DEM \ DTM is more than adequate to maintain the UAV height above ground level. A coarser DEM\DTM such as a SRTM 30m x 30m DEM can be less than adequate and a 90m DEM absolutely useless.

Flight speed needs to be as fast as possible to cost effectively acquire that data. So often data can be collected at speeds of 10 m/s and up to 17 m/s because there is little chance of colliding with a vertical structure.

5.2.2   Low Altitude (5m to top of trees (i.e., 30 m AGL)

Vertical structures are a major safety concern. The UAV Pilot needs to inspect the site and factor in the vertical structures into the flight plan. For the surveys with clearance > 10m typical obstacles are trees, poles,

powerlines, buildings, etc. These obstacles should be avoided during the route planning but obstacle sensors are also recommended.

The DEM should be as precise as possible. The photogrammetric or LiDAR survey will often provide a much better DEM/DTM than can be obtained from d publicly available datasets. The USGS has 10 m x 10 m DEM coverage for all of the US, but only a 1 m x 1 m DEM for parts of it.

Aircraft speed should be selected accordingly. The use of multiple visual observers (VO) strategically located and in constant radio communication with the pilot are highly recommended.

The use of a GNSS RTK navigation can be helpful.   However, it will require setting up a broadcast base station and ensuring constant radio communication with the UAV. This can be problematic when acquiring data over larger flight blocks within areas where the terrain variation is significant and may affect communication with the drone.

5.2.3   Ultra-Low Altitude (0.4 m to 5 m AGL)

The areas of investigation (AOI) are typically smaller due, in part, to the need to adjust the flight plan for the near surface vertical structures (i.e., fences, trees, buildings, rock formations, etc.) and, in part, due to the need to maintain good radio connection for the RTK corrections.

A pre-survey UAV photogrammetric survey is recommended but not always required. A precise DEM is required. The use of an active altimeter (laser, radar, or sonar) to maintain the UAV at a consistent altitude is essential, as the height accuracy of the standard barometric altimeters of commercially available drones, can be more than 5m during a ULA flight. This makes ULA flying with the barometric altimeter according to a designed clearance over the DEM unsafe.

An RTK GNSS navigation system might be adequate to the task. UAV survey speeds need to be significantly slower compared to operating speeds within SA and LA air space.

5.3   Communication with the Drone

In most countries it is prohibited to fly a UAV without a constant radio link with the ground station/UAV controller. As magnetic surveys often cover large areas at low altitudes, usually it is necessary to divide large areas into subareas with take-off/landing points at points where it will be possible to have a radio link with the UAV during the entire flight. The UAV should be programmed to interrupt the flight in case of lost communication with the ground station.

The above is true for most countries/territories. In some places drone operators/contractors can take a risk to conduct permitted Beyond Visual Line of Sight (BVLOS) flights without a persistent communication link. Technically it is possible, but it requires very serious planning, obstacles sensors on board of the UAV, which will be programmed to return the drone to the home position (survey base) in case of the drone and sensor encountering obstacles. Important with BVLOS as well, is planning with reduced flight times to have guaranteed endurance and return of the drone for the planned route. Note: that the factory settings in the drone may make the home base the original factory location, so after reset to factory defaults, ensuring the home base is properly set in the drone to the local magnetic survey base is absolutely crucial!

5.4   Risk of using RTK navigation for large area surveys

Nowadays modern drones are often equipped with a RTK GNSS receiver, which can be used for navigation purposes. RTK requires a persistent radio link with a base station to transmit corrections to the drone. If the radio link is interrupted, the drone's GNSS receiver will lose precision. In a best-case scenario, that transition will be smooth reduction to 3 to 5m locational accuracy instead of dozens of centimetres in RTK mode. In a worst-case

scenario, the drone's trajectory may differ from the planned trajectory by a few dozens of metres, for example if the RTK base station was not properly configured.

The largest possible locational error between RTK versus non RTK mode will be in the Z (altitude) values. So, it is recommended not to use RTK mode for navigation at all if there is a risk of the drone losing connectivity with base station during the flight.

5.5   Regulatory Framework Definitions and References

Table 4 defines commonly used acronyms within global aviation regulatory frameworks.

Table 4 Regulatory framework acronyms and definitions

TERM/ACRONYM	DEFINITION
Aerial work	An aircraft operation in which an aircraft is used for specialized services such as agriculture, construction, photography, surveying, observation and patrol, search and rescue, aerial advertisement.
ALA	Aircraft Landing Area
BARS	Basic Aviation Risk Standard – Flight Safety Foundation
BVLOS	Beyond Visual Line of Sight
CAA	Civil Aviation Authority
HLS	Helicopter Landing Site
ICAO	International Civil Aviation Organization
NOTAM	Notice to Airmen - is a notice containing information concerning the establishment, condition or change in any aeronautical facility, service, procedure or hazard, the timely knowledge of which is essential to personnel concerned with flight operations.
Part 101	Regulatory reference often used for UAV operations (ICAO and other regulators)
Populous area	An area is a populous area in relation to the operation of an unmanned aircraft if the area has a sufficient density of population for some aspect of the operation, or some event that might happen during the operation (in particular, a fault in, or failure of, the aircraft) to pose an unreasonable risk to the life, safety or property of somebody who is in the area but is not connected with the operation.
Regulator	In Section 5 this refers to the country of operation Civil Aviation Authority
UAV	Unmanned Aerial Vehicle - are also referred to as RPA (Remotely Piloted Aircraft), UA (Unmanned Aircraft), and RPAS (Remotely Piloted Aircraft Systems) or drone
UAV or UA Observer	A trained and competent person designated by the operator who, by visual observation of the unmanned aircraft, assists the remote pilot in the safe conduct of the flight.
Visual line-of-sight (VLOS)	An operation in which the pilot or observer maintains direct unaided visual contact with the unmanned aircraft
VMC	Visual Meteorological Conditions

5.6   Regulatory Framework – UAV types

UAVs are classified within the Regulatory framework into types based on weight which dictates regulatory, licencing and reporting requirements (Table 5). Most of the UAV's currently used in magnetic surveying are currently Small and Medium.

Table 5 Regulatory framework - UAV types

UAV (WEIGHT)	DEFINED WEIGHT RANGE
Micro	a gross weight of not more than 250 g
Very Small	a gross weight of more than 250 g, but not more than 2 kg
Small	a gross weight of more than 2 kg, but not more than 25 kg.
Medium	a gross weight of more than 25 kg, but not more than 150 kg
Large	a gross weight of more than 150 kg;

5.7   Basic Framework Regulatory Application

As with all aviation or specialised operations, it cannot be expected that the client knows all laws and regulatory requirements in regard to the operation.

It is the responsibility of the UAV operators contracted to know and convey to the client the relevant laws and regulatory requirements. Below are some regulatory requirements applied to the industry which may impact your drone operation. They are based on the ICAO framework, civil aviation regulations and Flight Safety Foundation BARS program.

It should be noted that much of the regulatory framework is often "excepted" with regulatory approvals and permissions. This is by an application by the operator with the UAV's operators experience, type of exception and risk assessment considered. This is the responsibility of the UAV operator, and they will receive a documented set of requirements if approved. A copy can be requested if managing an operation to assure your UAV team of the conditions.

As there are not unified regulations for UAV internationally, there is inconsistency. For example, some countries may not require pilot licencing, however due diligence may deem it a good idea for evidence of training and operator approval as a risk mitigator.

5.8   Regulatory Framework – typical Regulations and Requirements

The below Regulations and requirements in Table 6 are not inclusive. Regulatory requirements of the state should always be used for accurate requirements. The below is for reference only.

Table 6 Regulatory framework - List of Regulations and requirements

Common Requirements
Not operated within 30m of persons (measured horizontally) who is not directly associated with the operation of the UAV.
Not operated over a person unless that person is: (a) Directly participating in the operation; or (b) Located under a covered structure or inside a stationary vehicle that can provide reasonable protection;
UAV Pilots are licensed for the UAV category (i.e. Weight classification) and hold an aeronautical radio operator certificate (back up radio recommended).
UAV organization's require certification by the regulator
All UAVs should be registered with the regulator
UAV Organizations have a documented Operations Manual

A person who is operating a UA shall give way to and remain clear of all manned aircraft on the ground and in flight
Operated within Visual Line of site (VLOS) – BVLOS with permit
Must not operate over 400' AGL by day
Not operated over an area where a fire, police or other public safety or emergency operation is being conducted without the approval of a person in charge of the operation
No person shall act as a remote pilot, flight crew member or an UAV observer: (1) within [8 hours] after consuming an alcoholic beverage; (2) while under the influence of alcohol; or (3) while using any drug that impairs the person's faculties to the extent that aviation safety or the safety of any person is endangered or likely to be endangered.
Require regulator or designated authority approvals/permissions
Operations meet required conditions as per regulatory Approval, Permission, or Exemption
Operations be conducted greater than 400 ft AGL meet legislative requirements or have approval by the regulator
Operations conducted at night, in cloud, or in conditions other than Day VMC need approvals or permissions with pilots trained and approved
Operations conducted in controlled airspace or restricted airspace have required approvals
Operations conducted within 3 NM of any aerodrome (including any HLS or ALA) have been approved by the regulator
Operations conducted within the approach or departure path of a runway or over a movement area are not permitted without the approval or the regulator or designated authority
Operations conducted over a populous area must meet legislative requirements or have approval by the regulator
Operations conducted beyond VLOS are BVLOS require approvals
Considerations and Some Flight Safety Foundation Requirements (BARS)
Safety Management System
Operational Risk Assessment
Drug and Alcohol Program
Fatigue Management
Human Factors to be considered
Battery Management – with documented procedure – serial numbers or id of each battery
Battery overheating mechanism
Power status indicators (fuel or battery power)
Maintenance / inspection regime – documented
Release to service process
Fuel storage and shipping (batteries or fuel - bunded) – both DG
Fuel Quality Controls
Performance – consideration to weather, conditions, landing areas
Ground Crew
Emergency Response Plan
Engine Failure
Public Relations
Return To Base Procedures
Loss of Signal – RF Signal Analysis
All mod approved where required or proven through test procedures
Ensuring timely alerting and location identification to provide awareness of system status.

5.9   Pilot Experience and Recency (Flight Safety Foundation BARS Program)

Regulatory framework UAV pilot experience and recency requirements are outlined in Table 7. It is noted that many drone pilots may not have slung load experience and this experience and certification is necessary to obtain for drone geophysics operations.

Table 7 Regulatory framework – UAV pilot experience and recency requirements

RPA	Operating Conditions	Licence	Total Hours	Missions on Type	Recency	Simulator
Very Small Small	1. Standard Operating Conditions	RPL	5	5		
Very Small	1. Non-standard Operating conditions	RPL	20	10		As required
Small	2. BVLOS/Night Operations				Three take-off and landing (launch / capture) cycles in previous 90 days	
Medium	1. Standard Operating conditions					
Large	2. Non-standard Operating Conditions	RPL and Instrument Rating (theory)	100	20		Annual
All	3. BVLOS/Night Operations					

5.10   Planning to meet Regulatory requirements

In any operation, there are always many items to be considered from both a technical and safety perspective. Many items have already been looked at through regulatory requirements, however a Job Safety and Environment Analysis (JSEA), risk assessment or risk evaluation tool is the most effective methodology in systematically documenting the operational risk and mitigations.

Table 8 outline some risks to consider (may be managed by the UAV company, however, may impact your start time or operation):

Table 8 Regulatory framework – Other Safety Risks

Other Safety Risks for Consideration
Drug and Alcohol Management Plans or Policy and application
Liability Insurance
Battery Transport –international or remote jobs could be impacted due to restrictions – Lithium batteries are dangerous goods
Weather / climate – winds or rain may impact the operation of the UAV
UAV duration – number or landing areas / access to areas
Community awareness – disturbance – notification
Crew Composition defined – Single pilot / observer(s) / technician
Crew Responsibilities – i.e. Additional crew for crowd control / bird capture as needed, etc.
Crowd Control – Persons / animal / activity in landing area
Fatigue of crew (hours of operation and conditions)
Aircraft traffic in area – agricultural / mining / helicopter
Emergency Plans including client and emergency contacts
Weak link near UAV to prevent rotor or propeller entanglement for bird loss
Other UAV operations (mining)

5.11   Risk Management

This Risk Management section is based on the principle of identification and assessment of all potential risks associated with UAV operations and the implementation of suitable risk reduction and control mechanisms to mitigate or reduce these risks to **As Low As Reasonably Practicable (ALARP).** This process is in alignment with the principles and guidelines of **Australian Standard AS/NZS ISO 31000:2009 Risk Management.**

5.11.1   Risk and Hazard Identification

The risk and hazard identification process comprises the following action items:

- A system is in place to identify hazards and assess the consequences of health, safety and environmental incidents by providing essential information for decision making.
- Qualified personnel, including third party expertise as appropriate.
- Risks are documented and updated at specific intervals and as changes occur.
- Includes a follow up process to ensure that decisions have been implemented.
- Utilise questions such as -What can happen, where and when? Why and how it can happen?

5.11.2   Risk Analysis and Evaluation

Risks are analysed to provide an understanding of their causes and consequences and to provide input on whether risks need to be treated. Factors that affect likelihood and consequence need to be identified. Risk is then analysed by combining the consequences and their likelihood, taking into account existing controls.
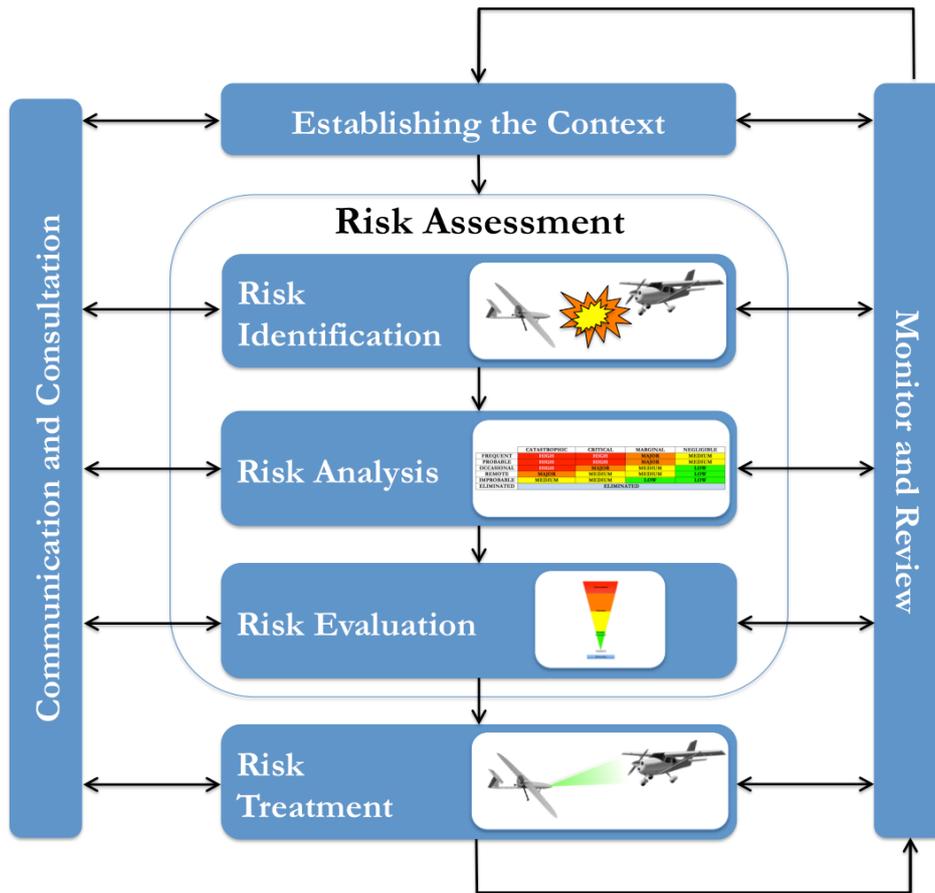
Figure 10   Risk Management Process schematic.

A risk matrix uses words to describe the magnitude of potential consequences and likelihood. The risk levels are assessed by experienced personnel using the risk ranking matrix shown below. Judgements are made about the consequence and likelihood and these are coupled to determine the risk level.

Risk evaluation involves comparing the level of risk found during the risk analysis, to risk acceptance criteria. This will identify the need for mitigation or treatment of risks or acceptance.

A sample Operational Risk Assessment (ORA) from Flight Safety Foundation - BARS Program is shown in Table 9.

The necessary Risk Assessment process component tools are provided in:

- Figure 10 Risk Management Process schematic,

- Table 10 Sample Operational Risk Assessment (ORA) from Flight Safety Foundation - BARS Program,

- Table 11 Consequence Assessment Matrix, and

- Table 12 Risk Assessment Matrix.

Table 9 Sample ORA from Flight Safety Foundation - BARS Program

Control	Query			Additional Mitigations
Planning	Is the operation being conducted in accordance with the Standard Operating Conditions? · Operation of one RPA per Remote Pilot at any one time; · Maintaining Visual Line of Sight (VLOS) during day operations and below 400 feet Above Ground Level (AGL); · Not to be operated closer than 30 meters to personnel who are not associated with the flight; · Not to be flown over populous areas and/or personnel in the area of operation; and · Not to be flown within 3 nautical miles (nm) of any aerodrome, and to remain outside all active prohibited and restricted areas.	Y	N	If no, the operations should not take place until the Standard Operating Conditions are satisfied OR the activity is undertaken using an operator with a valid ReOC.
Remote Pilot	Is the Remote Pilot properly qualified and experienced in accordance with Appendix 2?	Y	N	If no, either complete additional training or currency flying outside the tasking environment to meet the required standards.
	Is the Remote Pilot or any member of the ground affected by fatigue?	Y	N	If yes, postpone operation until fatigue status is suitable for the intended operation.
	Is the Remote Pilot or any member of the ground affected by D&A?	Y	N	If yes, postpone operation until D&A status is suitable for the intended operation.
RPA	Has the RPA been inspected and considered airworthy for the intended operation?	Y	N	Complete inspection and verify airworthiness.
	Is any outstanding maintenance due?	Y	N	If yes, complete required maintenance prior to flight.
	Are all elements of the RPA and RPAS Control System functioning correctly?	Y	N	If no, rectify defects or verify that the defective system is not required for the intended flight.
	Has a performance assessment been completed for the RPA to verify that it is suitable for the intended task in the forecast operating environment?	Y	N	If no, complete assessment. If the assessment results confirm that the operating environment is not suitable, postpone the flight or modify the intended task so that it meets performance criteria.
	Is a Certificate of Airworthiness required?	Y	N	If the C of A has not been validated or not issued, cancel the intended flight.
	Has a Release to Service certification been completed?	Y	N	If no, complete a Release to Service certification prior to flight.
Power Source	Are all batteries fully charged or fuel load sufficient for planned sortie?	Y	N	If no, source replacement batteries or additional fuel.
	Is the power source indicator functioning correctly and is it indicating the expected figure?	Y	N	If no, do not commence flight until the defect is rectified.
	Have all batteries or fuel been stored and transported appropriately?	Y	N	If no, complete testing of fuel source to confirm it is suitable for use.
	Is the method of fuel and battery management, testing, sampling, connection/delivery understood by the operator and/or ground crew?	Y	N	If no, postpone the operation and completed training of staff to confirm that the appropriate power source management procedures are in place.

Table 9 (Continued) Sample ORA from Flight Safety Foundation - BARS Program

Control	Query			Additional Mitigations
Weather	Has a forecast of the daily weather conditions been received?	Y	N	If no, source a weather forecast to verify that conditions are suitable.
	Are any localized weather phenomenon likely to impact operations?	Y	N	If yes, postpone flight until conditions are suitable.
	Have the following weather limits been established? · Cloud; · Turbulence; · Visibility; · Icing; and · Wind; · Temperature Limits.	Y	N	If no, establish the required limits and comply with them in operations.
	Have the weather limits been briefed and understood by all?	Y	N	If no, provide training to confirm that the weather limits are understood.
Operations	Does the operation require regulatory approval?	Y	N	If yes, confirm that regulatory approval has been provided.
	Has an airspace assessment been completed?	Y	N	If no, complete an airspace assessment to confirm that the intended operation can be undertaken without penetrating unapproved airspace.
	Does the operation require NOTAMs to be issued?	Y	N	If yes, confirm that the applicable NOTAMs have been released.
	Has a radio check been completed to verify radio serviceability?	Y	N	If no, conduct radio check. If radio check confirms radio is not serviceable, have defect rectified before flight.
	Have the necessary radio broadcasts been completed?	Y	N	If no, conduct the required radio broadcasts.
	Is the RF spectrum analysis complete?	Y	N	If no, complete an RF spectrum analysis to confirm that the operation can be effectively conducted with no impact to operations.
	Are the launch and recovery areas suitable?	Y	N	If no, relocate to a more suitable area.
	Are the lost link procedures understood?	Y	N	If no, conduct training to confirm that all staff involved with the operation understand the procedures and actions required should a lost link event occur.
	Verify that the correct RTB position has been established?	Y	N	If the incorrect RTB position is programmed, amend the position to the correct location.
	Is the appropriate emergency equipment on hand?	Y	N	If no, postpone the flight until the required equipment is on hand.
	Are all team members briefed and ready for the intended operation?	Y	N	If no, postpone the operation until the necessary briefings have been completed and every team member is ready.
	Is the launch and recovery site clearly demarcated?	Y	N	If no, postpone operations until launch and recovery site is clearly identified to safeguard unauthorized entry of persons.
	Is the launch and recovery site protected from an unauthorized/accidental entry?	Y	N	If no, postpone operations until launch and recovery site is effectively protected from entry of personnel.
	Has effective dust suppression mitigations been implemented for under ground or for surface operations?	Y	N	If no, postpone operations until such time as an effective dust suppression practice has been applied to the launch and recovery site that will be effective for the duration of the RPAS operation.

Table 10 Consequence Asssessment Matrix

	Consequence					
	0	**1**	**2**	**3**	**4**	**5**
People	No injury	Minor injury that does not require medical treatment	Minor injury that requires first aid treatment	Serious injury causing hospitalisation or multiple medical treatment cases	Permanent injury or disability (including blinding) that may result in hospitalisation of at least one person	One or more deaths, multiple severe injuries or permanent total disability
RPAS	Any element of the RPAS is degraded but task unaffected	A failure not serious enough to cause RPAS damage but which will result in unscheduled maintenance or repair or incomplete task	Minor RPAS damage resulting in damage to components, incomplete task and future unserviceability of RPAS	Significant RPAS damage but repairable	Complete loss of or destruction of a RPAS component (RPA, camera transmitter, sensor, etc.)	Loss of all RPAS elements
Reputation	Small delay, internal inconvenience only	May threaten an element of the service resulting in the task or objective being delayed	Risk does not violate any law and can be easily remedied. It has some effect on reputation and/or external stakeholders	Risk does not violate any law and can be easily remedied. It has some residual effect on reputation and/or external stakeholders and while reputation is damaged it is recoverable	Risk violates a law but can be remedied. It has a residual effect on reputation and/or external stakeholders and may result in damage to reputation	Risk violates a law and is unable to be remedied. It has a significant impact on reputation and/or external stakeholders and will result in loss of reputation
Cost / Property Damage	Negligible	Less than $1,000	More than $1,000 less than $10,000	More than $10,000 less than $100,000	More than $100,000 less than $1,000,000	Loss or damage exceeding $M1
Airspace	No aviation airspace safety implication	Minor breach of aviation safety regulations or RPA Area Approval	Serious issues of compliance with aviation safety regulations, RPA Area Approval or operations resulting in potential avoiding action by a manned aircraft but no collision	Serious issue of compliance with aviation safety regulations or operations or the loss of separation resulting in the potential for a collision with a manned aircraft but the manned aircraft is able to land with no serious injuries or fatalities	Potential for aviation safety incident/s involving multiple life-threatening injuries, or fatalities, to less than 10 people	Potential for multiple fatal aviation safety incidents causing multiple fatalities, to 10 or more people
Equitable access of airspace	No effect on access to airspace users	Some users of the airspace may perceive or experience airspace inequality resulting in between 5 to 10 minute delay or minor detour	Some users of the airspace may perceive or experience airspace inequality resulting in more than 10 minute delay or major detours	Most users of the airspace will experience airspace inequality resulting in long delay (>30 minutes) or major detours	All users of the airspace will experience airspace inequality resulting in long delay (>30 minutes) or major detours	Airspace users are prohibited from operating in the airspace causing significant disruptions to operations and financial cost

Table 11 Likelihood Assessment Matrix

LIKELIHOOD	Almost Certain	5	>1 in 10	**Is expected to occur in most circumstances**
	Likely	4	1 in 10 – 100	**Will probably occur**
	Possible	3	1 in 100 – 1000	**Might occur at some time in the future**
	Unlikely	2	1 in 1000 – 10000	**Could occur but considered unlikely or doubtful**
	Rare	1	1 in 10000 - 100000	**May occur in exceptional circumstances**
	Extremely Rare	0	< 1 in 100000	**Could only occur under specific conditions and extraordinary circumstances**

Table 12 Risk Rating Assessment Matrix

			CONSEQUENCE					
			0	**1**	**2**	**3**	**4**	**5**
LIKELIHOOD	Almost Certain	5	5	6	7	8	9	10
	Likely	4	4	5	6	7	8	9
	Possible	3	3	4	5	6	7	8
	Unlikely	2	2	3	4	5	6	7
	Rare	1	1	2	3	4	5	6
	Extremely Rare	0	0	1	2	3	4	5

Untreated Risk Scores

8,9,10 (Extreme risk) - Task is not permitted. Risk controls are required to ensure residual risk is acceptable.

6,7 (High risk) - Task is not permitted. Risk controls are required to ensure residual risk is acceptable.

4,5 (Medium risk) - Task may proceed, however, risk must be reduced to 'as low as reasonably practicable' (ALARP).

1,2,3 (Low risk) - Task may proceed.

Table 13 Risk Control Worksheet

Risk ID #	Category or Risk Type	Risk	Consequence	Existing Controls Description and Adequacy	Risk Rating			Additional Risk Mitigations	Risk Rating after mitigation		
					L	C	R		L	C	R

5.11.3   Risk Treatment

Risk mitigation involves identifying the range of options for mitigating risks, assessing these options and the preparation and implementation of treatment plans. Selecting the most appropriate option involves consideration of the costs of implementing each option against the benefits derived from it.

5.11.4   Hierarchy of Risk Controls

In many cases there will be a number of safeguards that are available to manage a particular hazard and risk. In most cases it will be necessary to use a number of safeguards.
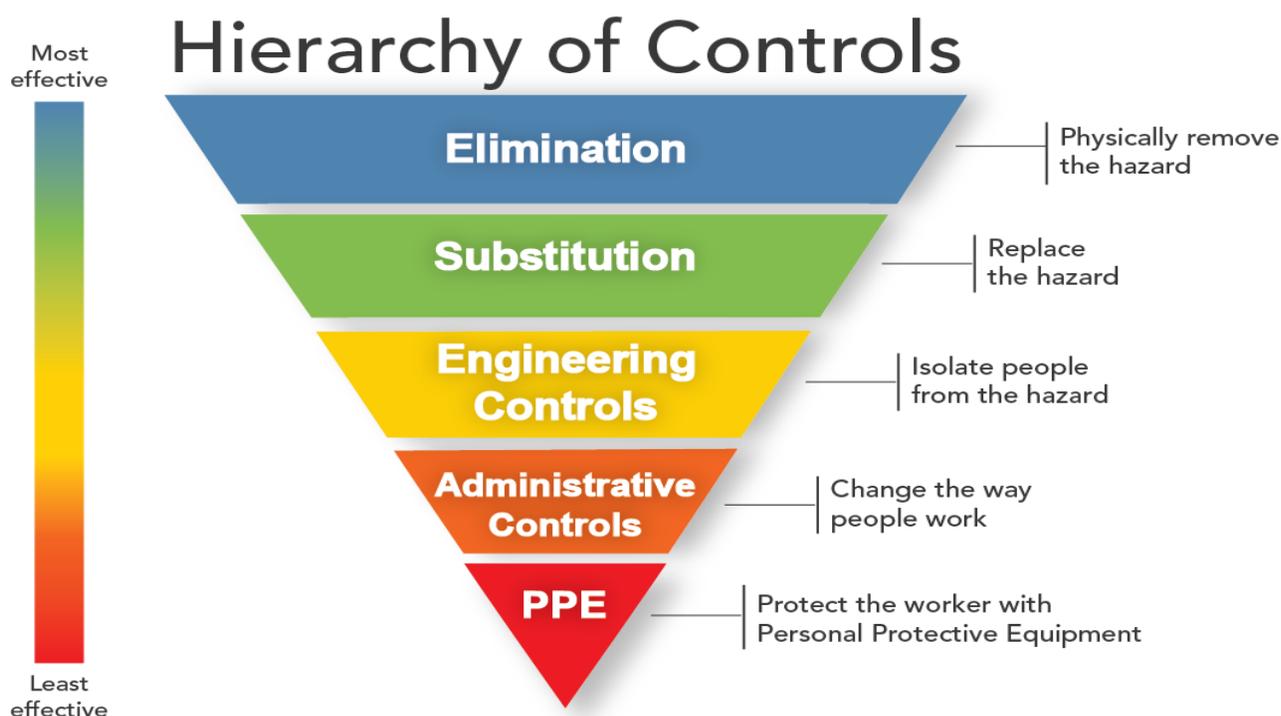
Figure 11   Hierarchy of Controls.

5.11.5   Monitor and Review

Ongoing review is essential in the risk management process since factors that may affect the likelihood and consequence of an outcome may change or the factors that affect the suitability or cost of treatment options. It is therefore necessary to repeat the risk management process regularly.

Monitoring and review involve learning lessons from the risk management process by reviewing the outcomes of audits, safety reports (incident, accident and hazards reports) and reviews.

5.12 Accident or Incident Reporting

The reporting procedures and body to report incidents to vary globally

5.12.1 Based on ICAO – international standards

No later than [48 hours] after an operation that meets the criteria of either paragraph, a remote pilot shall report to the regulator - Serious injury to any person

5.12.2 Australia – ATSB (Australian Transport Safety Bureau)

Type 1 UAVs are those which are type certified, large (over 150 kg) or medium (25 kg to 150 kg).

Type 1 operators will be required to immediately report to the ATSB UAV occurrences involving:

- death or serious injury;
- accidents;
- loss of a separation standard with aircraft; and,
- serious damage to property.
- Less serious incidents and occurrences are required to be reported within 72 hours

Type 2 UAVs are those that are not Type 1, and are not an excluded or micro (under 250 g).

Occurrences involving Type 2 RPAs will generally only need to be immediately report to the ATSB if they involve death or serious injury, while less serious incidents and damage to the RPA will need to be reported within 72 hours.

5.13 Further Details and Reference

5.13.1 Fitness for Duty

The operator is committed to providing an environment that ensures the optimal performance of any person working under the authority of this UAV.

Remote Pilots or any other person involved in the operations of RPAS are required to consider their fitness for duty prior to undertaking any duty under the authority of this UAV, including but not limited to the following:

- general well being
- adequately rested
- alcohol consumption
- drugs and medication use
- adversely affected by stress
- mental fitness.

Alcohol consumption

Remote Pilots or any other person involved in the operations shall not perform their duties whilst under the influence of alcohol. Alcohol must not be consumed less than 8 hours prior to UAV operations or during any period of an operation.

Drugs and medication use

Remote Pilots or any other person involved in the operations shall not perform their duties whilst having consumed, used, or absorbed any drug, pharmaceutical or medicinal preparation or other substance in any quantity that will impair their ability to perform their duties under the authority.

No person working is permitted to perform any tasks whilst under the influence of illegal drugs.

Fatigue management

Fatigue is to be considered in all UAV operations. This includes travel time to a location, the complexity and duration of an operation, the time of day, and other environmental conditions that can impact on the performance of a person.

5.13.2   Transportation of Dangerous Goods

Parts of the UAV may be classified as dangerous goods and may present a significant risk during transportation.

Depending on the type, role or configuration of an UAV, the following goods could be considered as dangerous:

- LiPo batteries and fuel cells
- internal combustion engines
- fuel, chemicals, poisons and their containers and dispensers
- magnetising materials
- pyrotechnics, flares and firearms.

Full disclosure must be made to the carrier prior to the consignment or carriage of dangerous goods.

5.13.3   UAV Serviceability Pre-Flight

Pre-flight and post flight checks are mandated for all operations. The Remote Pilot must record the completion of these checks on the Flight Log. All defects found in the UAV must be recorded on the Defect/ Maintenance Log.

The Remote Pilot must ensure that all defects or outstanding maintenance actions detailed in the Defect/Maintenance Log have been addressed prior to operation of the UAV.

5.13.4   Recording Hours in Service and Defects

Each Remote Pilot is responsible for ensuring that 'time in service' is recorded in the UAV Aircraft Flight Log and all defects and maintenance is recorded in the UAV Maintenance and Defect Log.

6.   POSITIONING & MAPPING

Geophysical data have limited utility without accurate positioning. Positions may be used either for navigation (flying the sensor along a planned path) or for data positioning (recording the actual position of the sensor regardless of planned path). Also useful is a good fit-for-purpose photo image and DEM (ground elevation) and in some cases, ideally a DSM (vegetation tops elevation) of the survey area.

6.1   GPS Positioning

The most common method of positioning in UAV applications is to triangulate a location based on satellite transmissions known as Global Navigation Satellite System (GNSS). This is the generic term which includes a number of nationally sponsored satellite networks including those listed in Table 14.

Table 14 Global Navigation Satellite System

GNSS System	Sponsor Country
GPS	USA
GLONASS	Russia
Galileo	Europe
BeiDou/BDS	China
NavIC/IRNSS	India
QZSS	Japan

The network(s) used will depend on the capabilities of the specific hardware in operation.

Timed radio pulses are transmitted from the satellite and received at the rover antenna. A minimum of four satellites is required to provide a unique location solution. With one satellite, the location could be anywhere on a sphere around the satellite. With two satellites, the location is on the circle formed by the intersection of the two transmission wavefronts. With three satellites, the location is reduced one of two generalized points. The three transmission wavefronts may not intersect perfectly but will form two recognizable point clouds somewhere on the circle described above. A fourth satellite is required to eliminate the ambiguous point cloud solution. Additional satellites add to the point cloud of potential solution locations, allowing you to improve accuracy by eliminating outliers and averaging the remaining points.

Triangulation accuracy (reducing the size of the point cloud of possible locations) relies on the constant speed of the transmission pulse as it travels through space. Atmospheric conditions slow the transmission and introduce inaccuracy in the location solution. Signal reflection off of hard surfaces (solid ground, buildings, etc) may produce multiple arrival times and introduce "multi-path" error. The practice of introducing jitter to the transmission times to intentionally reduce accuracy for strategic military purposes (known as Selective Availability) was discontinued by US Department of Defence (DoD) for GPS in May 2000.

Ambiguity due to transmission delays is typically addressed by measuring the delay at a known control point and then using this information to correct the signal prior to calculating a location. This is known as a differential correction. A time delay is calculated for each satellite so that the point cloud of locations converges at the known base station location. These time delays are then transmitted to the rover (on the

drone or drone magnetic sensor) and applied before a new calculation is made at the rover location. This assumes that the time delays experienced at the base station are similar to those experienced at the rover. The accuracy therefore depends largely on the proximity of the control point to the rover (closer base stations offer more relevant correction data). Distances greater than approximately 30km begin to lose relevance because the local conditions at the control point vary too much from the rover location. A wide variety of systems, both public and commercial, exist to provide differential corrections. In North America, the Wide Area Augmentation System (WAAS) is a network of 38 control points providing free differential corrections via satellite link. Similar networks with ground-based transmitters are operated by the US and Canadian Coast Guards. Commercial networks offer fee-based differential corrections with more control points to allow for greater accuracy and often world-wide service. Private operators can also establish their own control point at the project site for even greater accuracy and flexibility.

Positioning accuracy is typically given as the circular error probability (CEP) in units of meters. This is the mean error radius – 50% of the measurements will have a positional error less than this number. Assuming bivariate normal distribution, 93.7% will have an error less than 2CEP and 99.8% will have an error less than 3CEP. GNSS accuracy will vary from 15m to 0.02m CEP. GNSS receivers with only Upper L-Band reception typically perform with 5m CEP and will not achieve the same levels of accuracy as dual-phase receivers regardless of the differential quality. The size of the antenna, however, is very small and can be used in devices such as phones and watches. Dual-phase GNSS reception will improve raw accuracy to approximately 2m CEP. Differential corrections of some form are typically required to improve accuracy below this level. This requires not only a GNSS antenna, but an additional system to receive and process the differential corrections in real time. WAAS will improve accuracies to about 1m, but this is strongly dependent on your proximity to a control point. Commercial differential providers offer various levels of service from meter accuracy (CEP ~1m), to sub-meter accuracy (CEP ~0.2m) to centimetre accuracy (CEP ~0.02m). Note that vertical positioning errors are approximately two or three times the nominal horizontal errors due to the lack of satellites below the horizon.

6.2   Real Time Kinematic (RTK) Positioning

On-site control points with a base station receiver may be configured to provide real time kinematic (RTK) differential corrections via a radio modem link to the rover. Even if multiple repeaters are used, this typically places the base station within close enough range to the rover that it will provide centimetre level accuracy. Depending on the strength of the radio modem transmissions, Federal Communications Commission (FCC) licensing (or equivalent in non-USA jurisdictions) may be required to operate such a system. Thus, RTK provides two benefits:

- Real-time navigation of the drone to a pre-determined survey plan
- Geo-location (geotagging) of the magnetic measurement data.

6.3   Post-Processed Kinematic (PPK) Positioning

Alternatively, both the rover and base station may be configured to record the raw GNSS data and the differential correction can be applied post-mission for post-processed kinematic (PPK) differential. This requires additional software but removes the requirement for a continuous data uplink. PPK thus provides only one benefit:

- Geo-location (geotagging) of the magnetic measurement data.

NOTE: It also means that although the final data positioning may be extremely accurate, an alternative differential solution may be required for navigation depending on the project requirements. The two (RTK and PPK) are not mutually exclusive, and PPK may be used as a backup to fill data gaps where the RTK data link was lost.

6.4   IMU Positioning

Inertial measurement units (IMU) modules are part of all modern autopilot technologies on drones. IMU measure accelerations due to movement and are common in handheld gaming systems. When coupled with a digital compass, they are often used to measure platform orientation (pitch, roll, yaw) where this information is important to the geophysical data. Because they rely on movement and are independent of satellite connections, they can also be used to supplement GNSS data in GNSS-denied environments such as urban canyons, under tree canopy or inside buildings. Accuracy tends to degrade over time at a rate dependent on the quality of the instrument (drift), so frequent reconnections to the GNSS satellites are recommended. Tactical grade IMUs using gyros have the lowest drift parameters but are large, heavy and tend to interfere with magnetic and electromagnetic readings. Smaller Attitude Heading Reference Systems (AHRS) offer improved cost, power and form factors in exchange for poorer performance during periods of prolonged GNSS signal loss. If the sample rate of the IMU is faster than the update rate of the GPS, it can also be used to interpolate between regular GNSS updates. This may be useful to increase the frequency bandwidth of the recorded positions where high accuracy is required on rapidly or erratically moving platforms.

All of these measurements are based on the assumption that accuracy in an absolute sense is required. Most GNSS errors drift over long periods of time as satellites migrate across the sky. In many instances, relative accuracy (precision) is all that is required. If a project can be completed within a few hours, the relative accuracy may be more important than the absolute accuracy. This may be the case for survey technologies with very wide footprints such as Light Detection and Ranging (LiDAR) or photogrammetry. This may mean that the entire project site is shifted, but there are few mis-ties in positioning between adjacent lines. Surveys which span several longer periods or require reference to external or third-party data sources will require higher levels of absolute accuracy.

6.5   Laser Positioning

Although not easily translated to UAV platforms, and not used in commercial drones, an alternative to GNSS is laser positioning using one or more robotic total stations (RTS) and is mentioned only for completeness. This method uses a fixed laser to track the location of a reflective prism mounted on the rover. The base then transmits or stores locations with centimetre level positioning accuracy. This system requires line of site to maintain lock on the prism, although most models will search and reacquire the prism if line of site is temporarily lost. Another variant on laser positioning is the Simultaneous Localization and Mapping (SLAM) technology. This is a LiDAR based system that maps a point cloud of the surrounding area and creates a virtual model. This model is then used as a reference to continually update the position of the rover within the model environment.

6.6   Altimeters, Heighting and Terrain Models

Altimeters may measure height above sea level (or height above ellipsoid [HAE] for GNSS units) or height above ground level (AGL) and should be recorded in all aerial operations. These readings are often critical to operations in controlling navigation.

Commercial off-the-shelf (COTS) drones use barometric altimeters. GNSS data is fused with barometric altimeter measurements for robustness, but the main source of altitude information for navigation is from the barometric altimeter. This is except when in RTK mode, in which case altitude measured with the RTK receiver prevails over barometric altimeter readings. This is standard designed functionality for commercially available civil drones.

Higher ground clearance operations typically use GNSS-based altitudes for simplicity, whereas lower operations typically require a more precise measure of ground clearance. In addition to the utility of altitude for navigation purposes, most geophysical methods are extremely sensitive to height above the target. This sensitivity may be mitigated to some degree by the data collection parameters but cannot be avoided.

A variety of technologies can be used to measure altitude. This may include GNSS, barometric, radar, laser and sonic. Sonic (ultrasonic) altimeters are not used in practice. They have very limited range and don't work over vegetation (grass), snow and other surfaces. GNSS measures the height above the ellipsoid (HAE), which is roughly equivalent to sea level. The accuracy will depend on the quality of the differential corrections being used.

Barometric altimeters on a drone are set to zero during the initialization of the drone and during operations, and use air pressure to measure height relative to the initialisation point. The accuracy will depend on the procedures used to account for changes in pressure due to weather, rather than altitude. Converting these readings into height above ground requires a digital elevation model (DEM) and a height of the drone initialization point above the DEM or in an absolute value.

The accuracy of the DEM will depend on the accuracy of the altitude control for the original measurement system, the original collection time required to make the model, and the resolution of the model compared to the variability of the terrain. For example, a DEM collected from a drone using RTK corrections will start with cm level errors, whereas one without could have several meters of error. As with horizontal positioning, if the entire DEM can be collected in only a few minutes, then the relative error may be sufficiently low that a higher absolute error can be tolerated. However, the DEM is most likely going to be used in conjunction with GNSS HAE data on subsequent days, and the shift in elevation due to higher absolute errors could be significant.

Radar, laser and sonar systems measure the height AGL. This may be more useful from a geophysical perspective depending on the nature of the survey and the type of processing required. Each has their own strengths and weaknesses. Typical radar systems operate at frequencies of 24 GHz well above the frequency of operation or interference for geophysical instruments have moderate accuracy but may struggle at very low altitudes (a typical dead zone is just a few centimetres. Laser altimeters in ideal circumstances of hard reflecting surfaces (e.g., concrete) have moderate accuracy (20-60 mm) but may struggle at very low altitudes and may require additional processing to remove the effects of trees and other vegetation.

Both radar and laser altimeters are not suitable for flight over forested areas. Radar altimeters will report distance to something between ground and tree tops. Over forested areas the laser altimeter reflections will jump between ground and trees/leaves, etc. They also often have trouble getting signal reflection off standing water and can pick up reflections off towed instrument platforms which may hamper navigation.

Sonic systems are less likely to interfere with geophysical instruments, have low weight and power requirements, but offer lower accuracy (0.4 m). In practice sonic systems are not suitable for navigation systems on drones.

6.7   Mapping of the Survey Area – General Considerations

Crucial or highly desirable prior to undertaking a drone magnetics survey is having a map of the site both in terms of a digital photographic image of the terrain and a digital elevation model (DEM), also known as a digital terrain model (DTM). The required resolution of the digital photographic image and the accuracy of the DEM depends on the height of the magnetic sensor above the terrain. The greater the sensor height above the terrain and tree tops, the lower the digital photographic image resolution and the lower the DEM accuracy that can be tolerated for safe flying. Also, the variable height of vegetation above the ground surface, covering the survey area needs to be known for safe flying purposes. The operator must exercise sensible judgement when adopting a fit for purpose combination of digital photographic image and DEM.

When the planned surveying height of the magnetic sensor is safely clearing the tops of all vegetation and other height hazards in the survey then use can be made of: -

- a Google Map or Landsat image with pixel resolution of 30m x 30m (freely available from USGS) to serve as a photographic image and

- commonly available terrain models such as the SRTM (Shuttle Radar Terrain Model) with accuracy of a few metres in elevation over relatively flat areas, can serve as a DTM. For mountainous areas the vertical error of SRTM data can be a few dozens of meters.

- Satellite differential GPS surveying to achieve sub-metre heighting

- Flight plan programmed elevation controlling the drone surveying altitude flying mode (Section 7.3).

UXO or archaeological surveying or high-resolution geological mapping purposes, the survey objective is to fly as close as safely possible to the terrain, to obtain high resolution magnetic survey data, and sub-decimetre location accuracy. For such applications, if the survey area is either still heavily vegetated or has isolated trees, shrubs and other obstacles to be avoided, then it is highly desirable to make use of: -

- A Google Map Image, or existing high resolution digital photo image or preferably an image from a purposely flown drone photogrammetric survey, and

- A tree canopy terrain model derived from tree-top elevation, such as produced by a well conducted drone photogrammetry survey and/or drone LiDAR survey of the area, either an existing survey or purposely flown by drone prior to the magnetic survey. The LiDAR survey can provide both vegetation top elevations, obstacle location and dimensions and ground elevation.

- Height control systems on the drone as discussed in Section 6.6, to regulate desired terrain clearance of the magnetic sensor.

- For very small targets and small line spacings such as used in Level 1 type surveys, strict control of the magnetic sensor's xyz location is essential. This may be achieved by mounting the sensor on a rigid frame close to the drone, but this will be inside the zone of the drone platform interference on the magnetic signal, necessitating the need for platform interference compensation (Section 10). Suspending a sensor on a long cable away from the zone of platform interference considerably reduces system noise, however it may be very difficult to precisely control the xy position of a sensor with use of a long tow cable.

6.8   High Resolution Mapping of the Survey Area

Many drone magnetics operators may choose to either have or employ a sub-contractor with a separate purpose made smaller drone (such as the DJI M300 and similar capability drones) with a photogrammetric

quality camera and that can also carry a LiDAR unit for a separate LiDAR survey. The operation and data processing and quality considerations of photogrammetric and LiDAR surveying also requires use of high accuracy RTK surveying capability with an antenna base station, radio link and a rover antenna on the drone,

This is a specialty and high-cost operation and the total specification of the data processing and processing for photogrammetry and LiDAR surveys is beyond the scope of these guidelines. The American Society of Photogrammetry and Remote Sensing (ASPRS) has published standards for high resolution photogrammetry and LiDAR surveying from a drone or aircraft (ASPRS, 2014) and if the highest standards are required, it is recommended these guidelines and standards be adhered to provide the centimetre or decimetre xyz location accuracy of a photo-image and a LiDAR DEM.

Often though a lower standard DEM/DSM (error <1 m) can be accepted for navigation purposes

7.   SURVEY PLANNING AND PREPARATION

Despite the fact that in some jurisdictions, landowners can veto airborne surveying, airborne geophysical surveys usually do not suffer from access problems common to ground geophysical surveys; they can therefore be planned and executed to achieve optimal results. Airborne surveys for Level 2 type surveys (geological mapping etc) are flown as straight parallel traverse lines at a given line separation and are usually accompanied by straight tie or control lines flown in a different direction with larger separation. The regular survey layout facilitates data processing and ensures consistent spatial resolution of the final data over the entire survey area. For other applications (e.g., Leve1 UXO/archaeology and Level 3 wells / pipelines etc) the regular parallel flight lines approach may not be necessary and therefore be customised.

The major advantage of any airborne survey is that the data are acquired as a spatially linked continuous time line. This facilitates rigorous quality control, especially for potential field surveys such as magnetics. Neighbouring observations have to measure very similar values because they are close to each other in time and space and are distanced from the closest magnetic source by the ground clearance. Therefore, any larger deviation of any observation from its neighbours has to be caused by either instrument malfunction or by disturbing signal emitted by the platform. Although the length of the continuous time line that can possibly be acquired by electro-motor propelled drones is somewhat limited, the data can still be quality controlled as long as the platform is not changing altitude whilst hovering at the same location.

However, even airborne surveys do not necessarily have free access to the entire surveys area. Access restrictions very much depend on the envisaged ground clearance, e.g., the distance between the platform and the Earth surface. The lower the ground clearance the higher the possibilities that obstacles in the survey area prevent the execution of the optimal flight plan. For an archaeological or UXO detection survey flown at only a few metres above the ground even smaller changes in vegetation height can become a problem, whereas for a geological mapping survey with say 40 metres clearance and 80 metres line separation only rugged terrain has to be considered. In populated areas legislation can also prevent ideal survey execution by raising 'virtual obstacles' in form of no-fly zones.

Subject to flight regulations (or the exemption thereof) combustion engine propelled fixed wing UAVs can essentially perform the same survey operations as conventional, manned aircraft. However, most drone operators prefer e-copter UAVs as platform and therefore have to plan with their limited endurance.

7.1   Getting the Survey Specifications Right

Before survey planning can even get underway, the first important task is to ensure the survey specifications are in order and fit-for-purpose, regardless of whether the drone magnetics survey will be carried out "in-house" or by a contractor. The survey specifications process and good practice is discussed in more detail in Section 9.3 and covers technical specifications for magnetics and navigation data acquisition and processing, QA/QC and deliverables. Good communications between the person that wrote the specifications, the survey geophysicist, the drone pilot and the client is essential to plan the survey well and to meet the survey objectives and client expectations.

7.2   Master Survey Plan

To achieve this, the creation of a master survey plan is strongly recommended. The master plan is to be used as a 'template' for the individual tiles, even in cases when adjustments have to be made ad hoc in the field due to unforeseen circumstances. The planning software will have to be able to align the 'daily' flight plan to the master plan. Figure 12 compares a perfectly flown tile-boundary (left) with a badly flown one (right). Albeit, the boundary of the survey shown in the right will not give levelling problems because of the well-placed tie line, it will give problems when gridding the data.

As said in the introduction airborne surveys are flown as straight traverse lines with tie or control lines at wider line spacing flown preferably perpendicular to the traverses. The latter is not an absolute requirement and tie lines may be flown at angles different to 90° to the traverses to accommodate the survey layout. The higher the tie to traverse ratio the better is the levelling results that can be achieved, common tie to traverse ratios are 1:5 to 1:10.

Whilst the traverse spacing has to be absolutely equidistant, tie line spacing may vary to accommodate size and shape of the survey area. When planning the tie lines, one should make sure that a tie line is placed at each survey boundary to ensure edge validity. Similarly, a tie line should be placed where two tiles overlap.

The main survey direction (traverses) is traditionally planned to be perpendicular to the dominant direction of the expected structures in order to facilitate the gridding process (interpolation between traverses). For ultra-high-resolution surveys this rule becomes less crucial due to the tight line spacing and the main line direction can therefore be chosen for logistical reasons. However, magnetic surveys at low magnetic latitudes (< 20° inclination) should avoid flying east-west. This is because at low latitudes anomalies are 'squeezed' perpendicular to the declination of the ambient magnetic field and interpolation between traverses flown in east-west direction can result in the distortion of especially smaller anomalies.
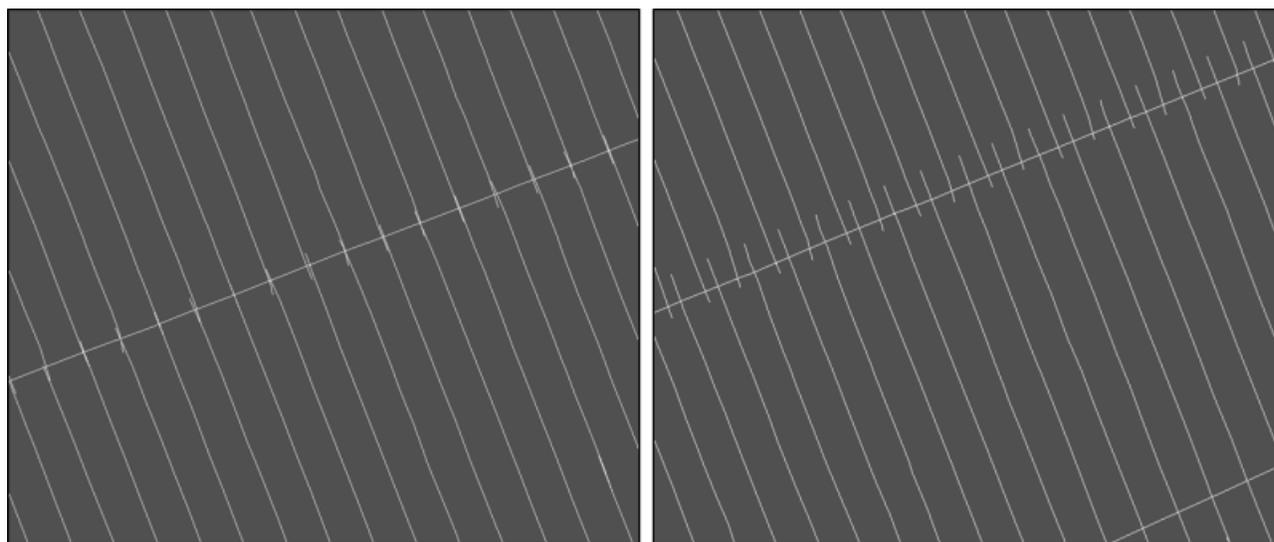
Figure 12   Comparison of a perfectly flown tile boundary (left) with a badly flown one (right).

In case the survey area is so large that the longest line cannot be flown forth and back to the operational base, the flight lines have to be split and the survey area is to be covered by many tiles. Lines from one tile should exactly continue the lines from the previous tile and overlap to neighbouring tiles should be ensured by at least twice the line separation. In addition, a tie line should be located at the split, if possible.

All surveys should further be planned slightly larger than the actual survey area; try to add a buffer of one to three times the nominal line spacing. Turns have to start outside the buffer zone in order to avoid manoeuvre induced noise in the production data. It is further advised to fly smooth 'U' shaped turns instead of a 'box', the smoother the turn the lower is the possibility to pick up manoeuvre noise at line ends, especially when the sensor is suspended below the platform. All excess data will eventually be cut for the final deliverables.

7.2.1   Comment

The authors acknowledge that the above may be impossible to achieve due to obstacles, curved survey boundaries and many other factors. However, the described ideal should be followed as close as possible.

7.3   Survey Altitude

Drone-borne magnetic surveys may be flown at fixed barometric/GPS height, at fixed height above terrain (which is always approximate, due to safety and operational considerations), or on a pre-planned loose drape. These differences are illustrated in Figure 13. Each choice has its own advantages and disadvantages.
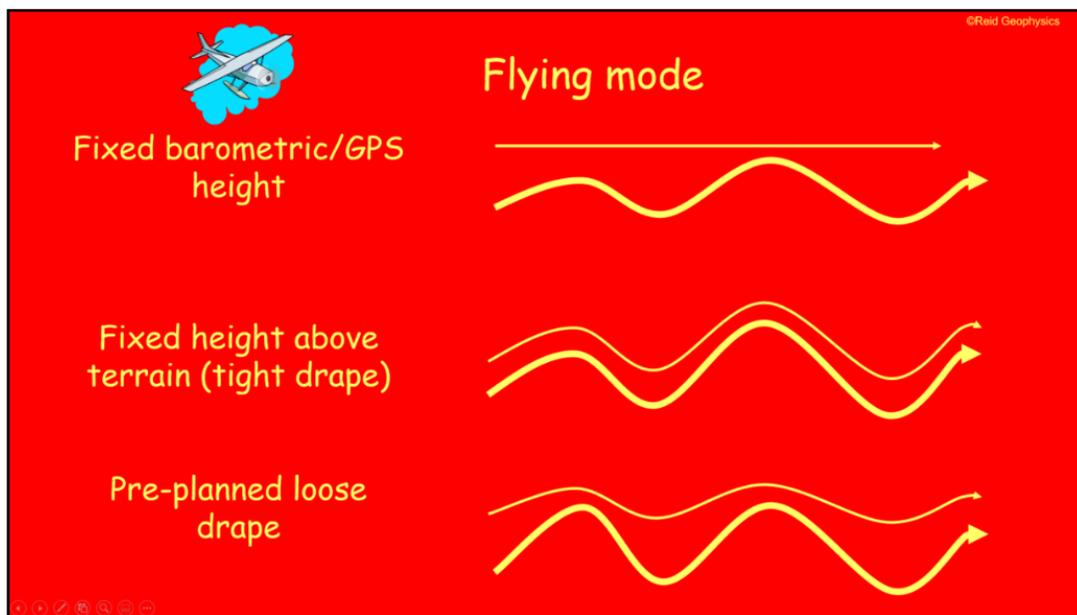
Figure 13   Survey choices with respect to terrain clearance.

For magnetic surveys it is important to fly neighbouring lines and traverses and ties at the same altitude. The reason for this is that variations in ground clearance, e.g., different distances to the magnetic sources, can significantly change the amplitude of the measured signal.

This is demonstrated in Figure 14 which shows the change in the amplitude produced by a monopole (vertical dipole with infinite depth extent) at the surface with increasing ground clearance. A navigational inaccuracy

in the altitude of 5 metres at a nominal ground clearance of 10 metres produces a variation (error) in the measured total magnetic field of around 50%, whilst the same altitude inaccuracy at a nominal ground clearance of 100 metres only produced a variation of 0.5%. In case gradients are measured the altitude related variation is 100% at 10 m nominal terrain clearance and 0.8% at 100 m.

Whereas Figure 14 is a sketch to illustrate the principle, Figure 15 gives a practical example of the detectability of small dipolar objects (UXO) of variable sizes. Small inaccuracies of the determination of flight height at levels below 5m above ground result in considerable variations of the flux density. In order to map the magnetic field of a small metal object buried in the ground, altitude accuracies in the order of 10cm and better are desirable.
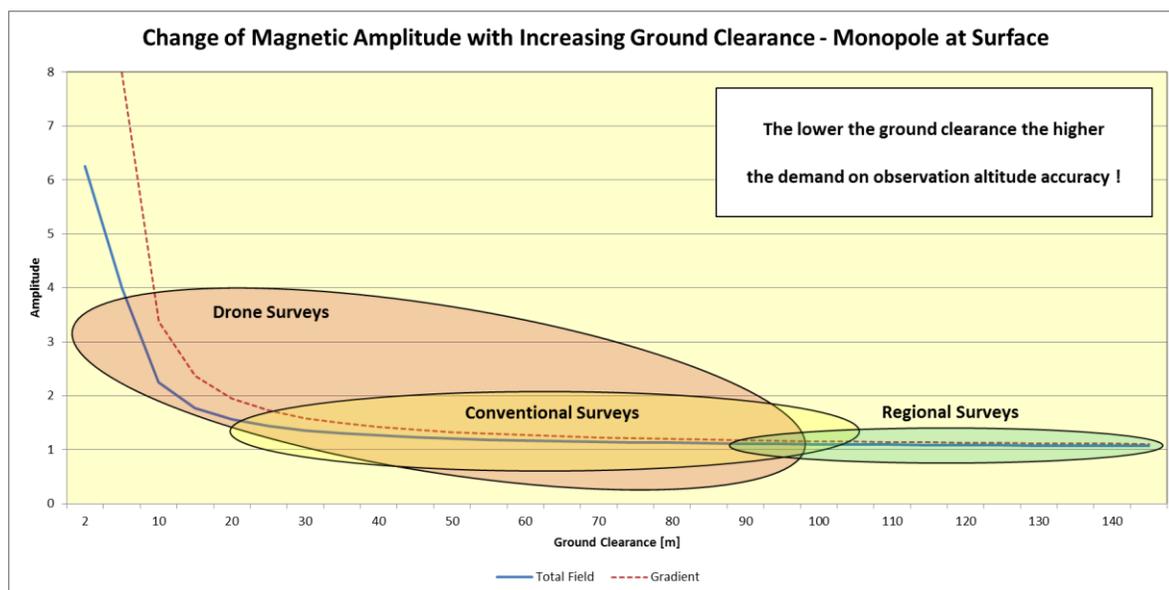
Figure 14   Change of magnetic amplitude with increasing ground clearance

(Closest distance to the next possible source).

The absolute accuracy of the ground clearance that needs to be adhered to, depends on the nominal ground clearance. The magnetic signal of a dipole falls off with the cube root of the distance between sensor and source. Hence, at an ultra-low ground clearance of a few metres, centimetre inaccuracies in the ground clearance can matter.

Standard GPS receivers exhibit accuracies in the range of +/-2-3m. In case higher accuracies are required positioning modules with integrated multi-band GNSS and RTK technology in a compact form, have to be employed to deliver centimetre-level accuracies.

Two methods can be employed to keep the ground clearance stable during survey: Automatic ground following systems using any sort of 'range finder' and following a pre-planned elevation based on GPS altitude, the latter is defined as drape.
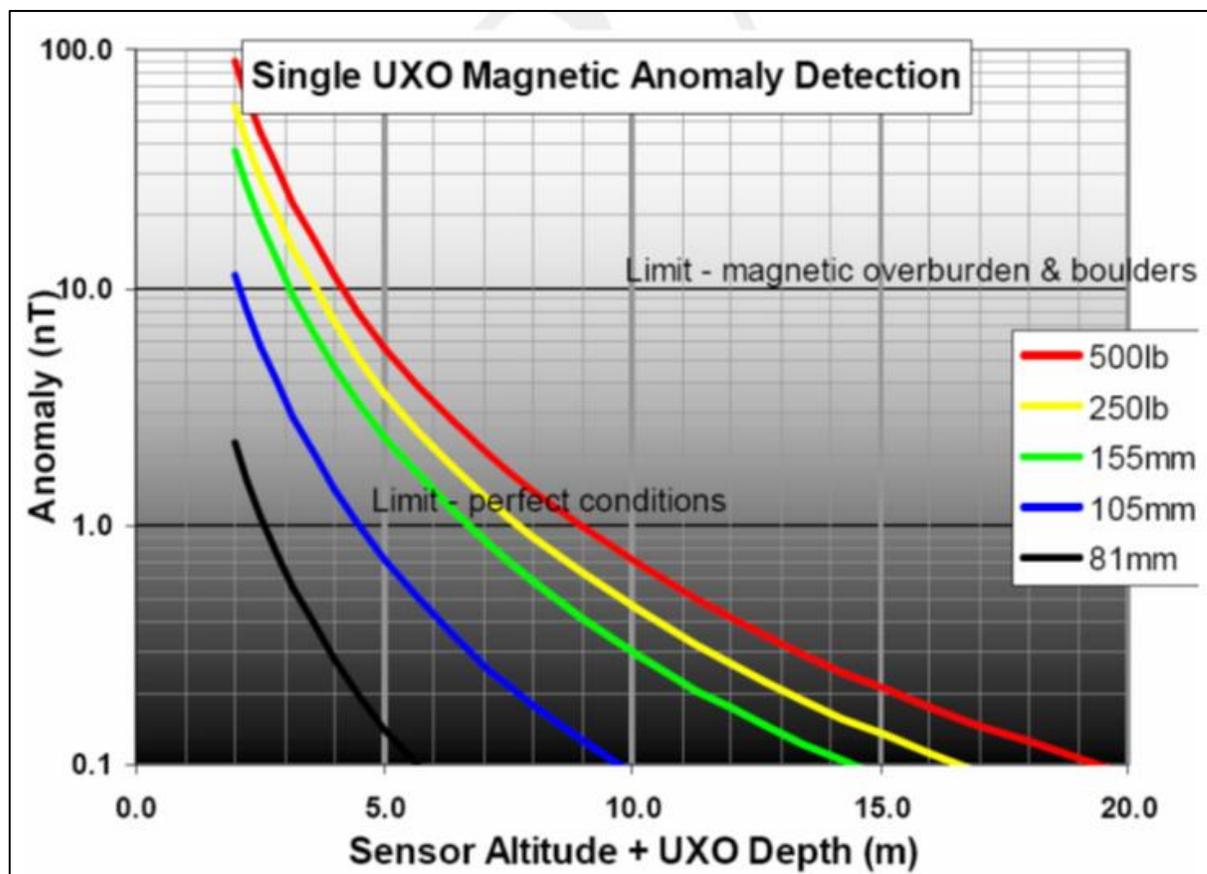
Figure 15   Detectability of small objects.

(Magnetic anomalies of specific objects and their fall off as a function of distance between sensor and ground. Depending on the sensitivity of a magnetometer used in a survey and the ambient noise, the magnetic signal of a magnetic object falls below a threshold at a given distance.)

7.3.1   Range Finder

There are different kinds of rangefinders: LiDAR (using laser or infra-red light to measure distance), Sonar (using ultrasonic sound), and Radar (using microwave RF), most common are Laser rangefinders. It is a low-cost optical distance measurement solution with a median 40m range under most operating conditions (over water the range can be only ~10 m; over concrete the range can be ~200 m), low power consumption, and small form factor. Downward facing rangefinders are automatically used in flight modes which have height control, such as for instance in the ArduCopter autopilot software: Altitude Hold, Loiter and PosHold Mode. Other systems with similar capability are available. Distances read by the sensor are input to the flight controlling software to keep the multi-copter at a defined distance above ground at 10cm level accuracies, however, real accuracy depends on speed, inertia of the drone, thrust/weigh ratio etc.

The type of 'range finder' utilised will however depend on ground conditions such as vegetation, surface water, sand dunes etc. At present there is no instrument available which would cover all cases, from desert to jungle to ice. Range finders will also only work for copter drones or for fixed wing drones in relatively flat country, not for fixed wing platforms in steep terrain, because fixed wing platforms require a minimum survey

speed and can therefore not follow steep terrain at very low altitudes (e.g., 1 m) but can operate in steep terrain, for example with 50m terrain clearance and 10 m/s speed.

Using a 'range finder' to follow the terrain has the further advantage of possible automatization, e.g., the flight plan for the drone navigation software needs only the two end points of each line (plus turn and ferry information).

7.3.2   Drape Surface

Drape surfaces (refer to Figure 13) in their simplest form are a copy of the digital terrain data, slightly filtered and lifted to nominal terrain clearance. Modern drape planning software incorporates the digital terrain data and the performance of the platform (climb and descent rates) to calculate the achievable drape surface. There are 2D drapes which produce the lowest ground clearance that can be flown by a specific platform for each line and 3D drape surfaces which calculate a vertical flight path for all lines, e.g., the possible elevations for traverses and ties are combined to ensure identical elevations at crossover points. Data flown on a 3D drape are the easiest to process but do result in an increased ground clearance compare to 2D drapes.

Flying a survey based on a drape surface does require the existence of digital terrain data with an adequate accuracy. For high resolution surveys this often means that the digital terrain data has to be acquired first by a photogrammetric or LiDAR survey. The drape grid has then to be converted into way-points which are fed into the navigation software. The number of way-points the navigation software can handle can influence the size of the area then can be flown as one survey or tile, since over rugged terrain more way-points will be required for accurate height keeping than over flat areas.

7.4   Nominal Line Separation

The optimal line separation is controlled by the achievable/practical average terrain clearance. Refer to Table 3 and Section 3, where line separation is tailored to the survey type (Levels 1 to 3)

The magnetic field is a potential field meaning that neighbouring observations are related to each other and cannot vary randomly. Reid (1980) showed that the total magnetic field is sampled sufficiently when flying at a line separation of twice the ground clearance. When gradients are measured the line separation should be equal to the ground clearance.

For ultra-high-resolution surveys, which try to map or locate small objects close to the surface, a line separation equal or slightly above the average terrain clearance is therefore sufficient for magnetic surveys.

7.4.1   Infill Surveys

When infill surveys are flown to increase the spatial resolution of existing data, the general rule of thumb is that a quarter of the line separation of the existing data yields the next 'quantum leap' in spatial resolution. When conducting an infill survey, the ground clearance has to be carefully considered: In particular if the ground clearance of the existing data is too high to support a quarter of the line spacing, the existing lines have to be re-flown as well at a lower ground clearance. On rare occasions the existing data might be downward continued but downward continuation of magnetic data can become mathematically unstable and can lead to erratic results.

8.   MAGNETIC SURVEY NOISE SOURCES

8.1   Noise and Survey Artefacts

Mounting a geophysical sensor on a moving platform can significantly increase the noise in the observed geophysical data. Most prominent example is gravity where the motion induced accelerations can be magnitudes larger than the geological signal. Other non-geological signal can be introduced into the geophysical data by disturbances emitted from the platform. All signals disturbing the geological response are referred to as noise. High noise levels can significantly lower the resolution of the geophysical data and therefore need to be eliminated or minimised as far as possible.

Strictly, noise is defined as a time varying signal that cannot be repeated. In airborne magnetics however we have to deal with two different types of disturbing influences. There is high frequency noise that would fall under the above noise definition and there are longer wavelength disturbances caused by attitude changes of the sensor and/or the sensor platform configuration. Let's name the former 'Instrument Noise' and the latter 'Manoeuvre Noise'. Manoeuvre noise also includes what manufacturers call the heading error of a sensor. The word 'Heading' would suggest directional effects only ('directional' as in-flight line bearing), but in reality, it does include variations of all three attitude angles of pitch, roll and yaw.

Instrument noise should not be mistaken as sensor noise (or sensitivity) given by instrument manufacturers (see Table 2; Section 0). These are measured in a laboratory environment and are by far lower than anything achieved so far in airborne geophysics (maybe with the exemption of the SQUID tensor magnetics).

Manoeuvre noise on the other hand does not follow the strict definition of noise. It comprises signals that alter the measured magnetic data depending on the attitude (Euler Angles) of the platform-sensor configuration or the attitude changes of the sensor itself. Attitude changes frequently occur in airborne surveys as the aircraft has to keep the planned flight path, thereby requiring constantly changing manoeuvres to do so. The typical wavelength of such manoeuvres is of a few seconds but does change with platform size and type. For suspended systems and low drag birds, it is often the pendulum frequency dictated by the length of the towing cable.

The manoeuvre noise is currently the biggest obstacle for drone-based surveys to achieve the quality of conventional aeromagnetic data. Many drone operators do not have access to compensation or calibration software and there are only a very few commercial versions available. Further, compensation only works well for systems with rigidly mounted sensors and the limited payload of (most) drones prevent long suspension distances to attenuate platform influences sufficiently.

In case the sensor itself is susceptible to attitude changes, suspending it does not solve the problem. The compensation of suspended systems is still in the developing phase or, if successful, is heavily guarded intellectual property. In conventional surveys suspension lengths of 30 metre or more are used, which cannot be achieved by smaller drones.

These noise sources and their importance on the quality of the final data is rarely highlighted. Often perfect-scenario datasets (e.g., static/stable sensors) are used to advertise noise levels and it can be difficult to understand what they may be in real survey conditions. Noise levels in real survey data may change as quickly as a gust of wind.

8.2   Instrument Noise

The extremely high sensitivities of modern magnetometers reported by the manufacturers are significantly lowered by mounting them on a moving platform which emits high frequency electromagnetic signals. The origins of these signals range from electronic equipment installed in the aircraft, moving parts in the platform engines and eddy currents induced in any electrical conductor moving through the ambient magnetic field.

The classic measure to quantify the noise level of airborne magnetic systems is the normalised 4th difference (Denisov et al., 2006). Standard threshold is 0.1 or 0.05 nT which may not be exceeded for a given distance. This noise measure was developed for conventional airborne magnetic surveys which, for ages, recorded data at 10 or 20 Hz.

This conventional threshold has however to be adapted to the sampling rate; a sensor with 1 kHz sampling has 10 times the 4th difference noise levels than a system recording at 10 Hz. This is demonstrated in Figure 16, which shows about 10 metres of data. The originally recorded 1 kHz data are shown on the left with the same section of data after reduction to 20 Hz being shown on the right; the recorded data are displayed in the top panel and their 4th difference in the bottom. Note the 4th difference scale in the left graph is about 10 times the scale in the right, confirming the above statement.
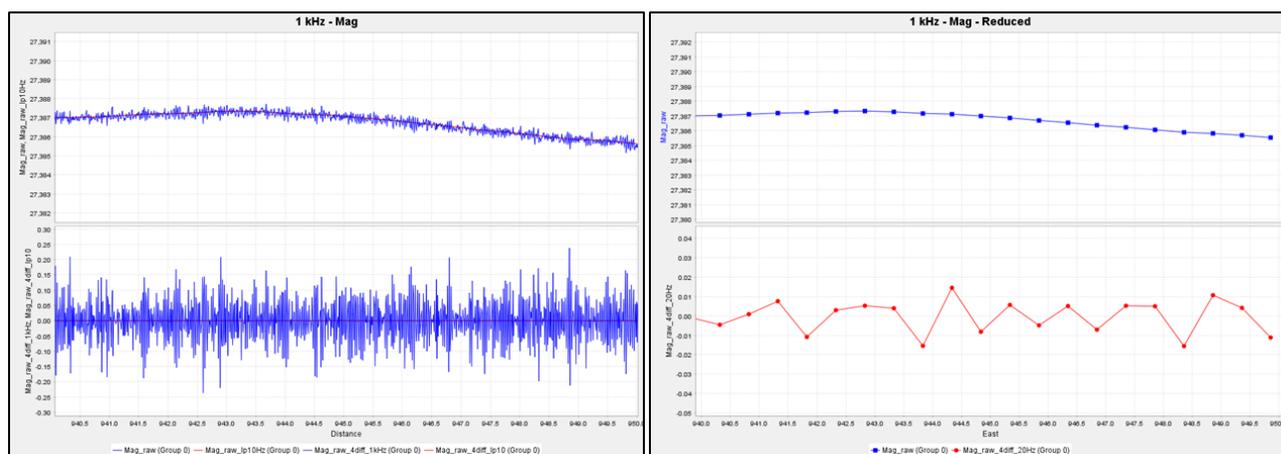
Figure 16   Measured magnetic data and their 4th difference.

Left: Original 1 kHz data. Right: Data reduced to 20 Hz. Approximately 10 seconds of data are shown.

8.3   Manoeuvre Noise

'Manoeuvre Noise' can be defined as all magnetic disturbances or inaccuracies that are caused by attitude changes of the moving platform-sensor system or by directional sensitivity of the employed sensor, or both.

There are two types of manoeuvre noise: The first is caused by the sensor itself when the recorded magnetic data change with the orientation of the sensor towards the ambient magnetic field, which is often referred to as 'Heading Error'. The second type is caused by attitude changes of the platform producing magnetic disturbances of varying magnitudes at the sensor position. Both types occur with rigidly mounted sensors as well as with suspended sensors and can reach magnitudes of 5 nT or more.

Strong attitude changes of the sensor-platform system can be caused by changes in survey speed, harsh movements of the platform (usually over steep terrain or to avoid obstacles) and obviously by wind. Naturally, rotary wing platforms are capable of stronger manoeuvres than fixed wing aircraft. That

manoeuvre noise has to be included in the overall noise estimate of each sensor-platform system is demonstrated below.

Figure 17 shows the high-pass filtered grid from an approximately 800 x 800 m window on the right and one example line on the left. The survey was flown at 25 m line spacing and 15 m ground clearance using as suspended fluxgate vector magnetometer. The survey was flown under favourable conditions over flat and cleared ground without any disturbing winds. As can be seen from the example consistent anomalies of amplitudes of 1 nT or less are identified.

The same system flown under very windy conditions can produce manoeuvre noise of more than 10 nT as shown in Figure 18. The line in Figure 18 is flown in an easterly direction; hence the variations in the north position are a good indicator of the swing of the bird. The recorded magnetic data and the north position are shown in the top panel and their high-pass filtered version in the bottom. As can be seen there is a very good correlation between the magnetic signal and the bird swing.

The line was flown with a total field magnetic sensor mounted on four cables 5 metres below the platform and the line is about 2.5 kilometres long. The top three panels show variations of the magnetic data: The raw data is followed by the high pass filtered version and the normalised 4th difference. The two panels in the bottom show the vertical fluxgate compass data and the recorded vertical accelerations.

The magnetic data in the first two thirds of the line are extremely noisy with the noise being perfectly picked up by the high-pass filter. However, the 4th difference does only indicate some noise bursts but would not mark the beginning of the line as completely faulty.

The vertical compass and acceleration data however show a bizarre behaviour in that they swap signs during flight. The only possible explanation of this behaviour is that the sensor actually flipped (somewhere in the turn to the left of the data shown), the platform then struggled to pull the flipped sensor along the line resulting in wild manoeuvres which in turn cause strong noise in the magnetic data. At about two thirds down the line the sensor flipped back into normal position and good magnetic data are recorded for the remainder
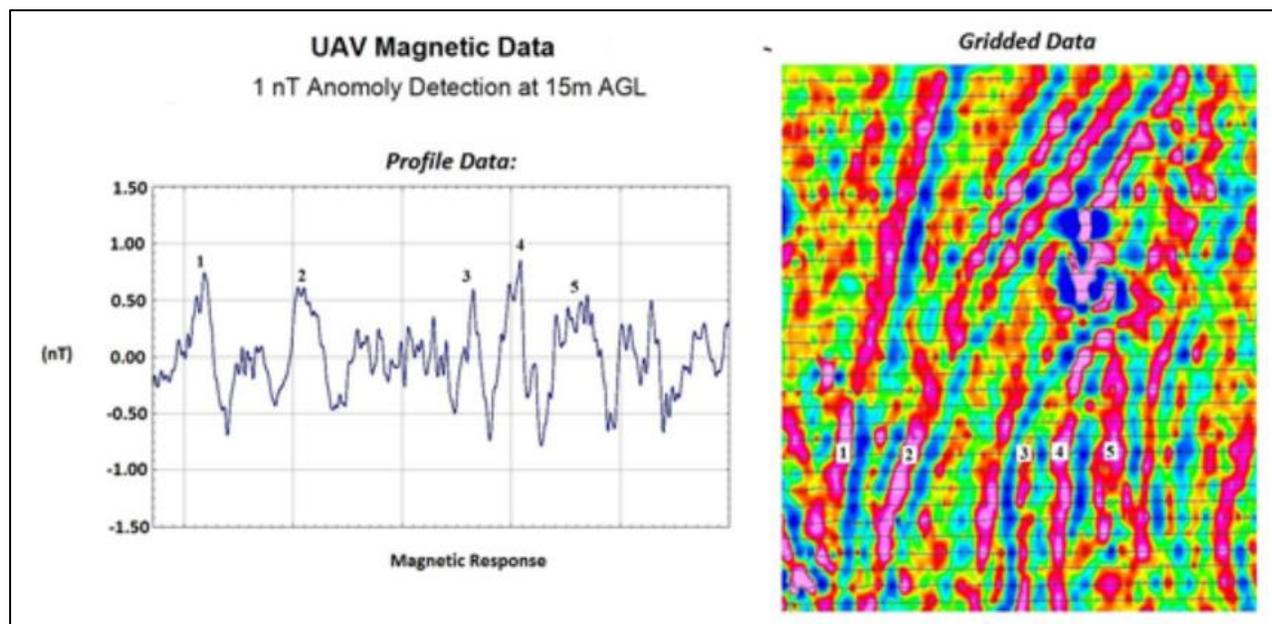
Figure 17   Example of a successful high resolution drone survey.

(Right: high pass filtered final grid data. Left: Line data. Source: http://www.thomsonaviation.com.au/uav/)
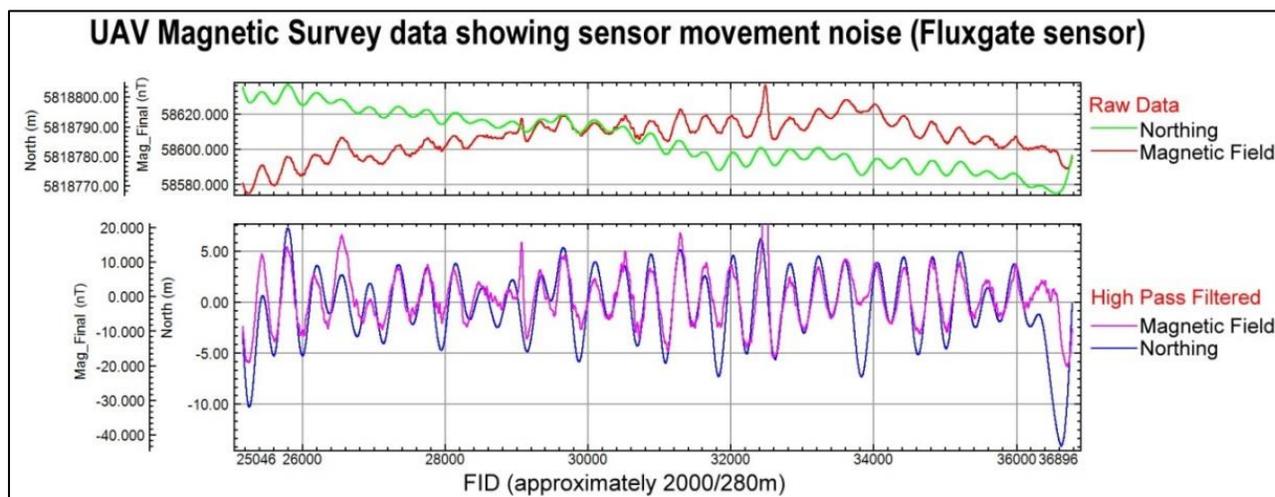
Figure 18   Example of an E-W line flown with the same system used to produce the data in Figure 12, but flown under very windy conditions.

(The top panel shows the recorded magnetic data (red) and the north position of the sensor with the respective high-pass filtered version in the bottom. Source: Paul Mutton – Touchstone Geophysics)

A further example of extreme manoeuvres and their influence on the magnetic data is given in Figure 19.
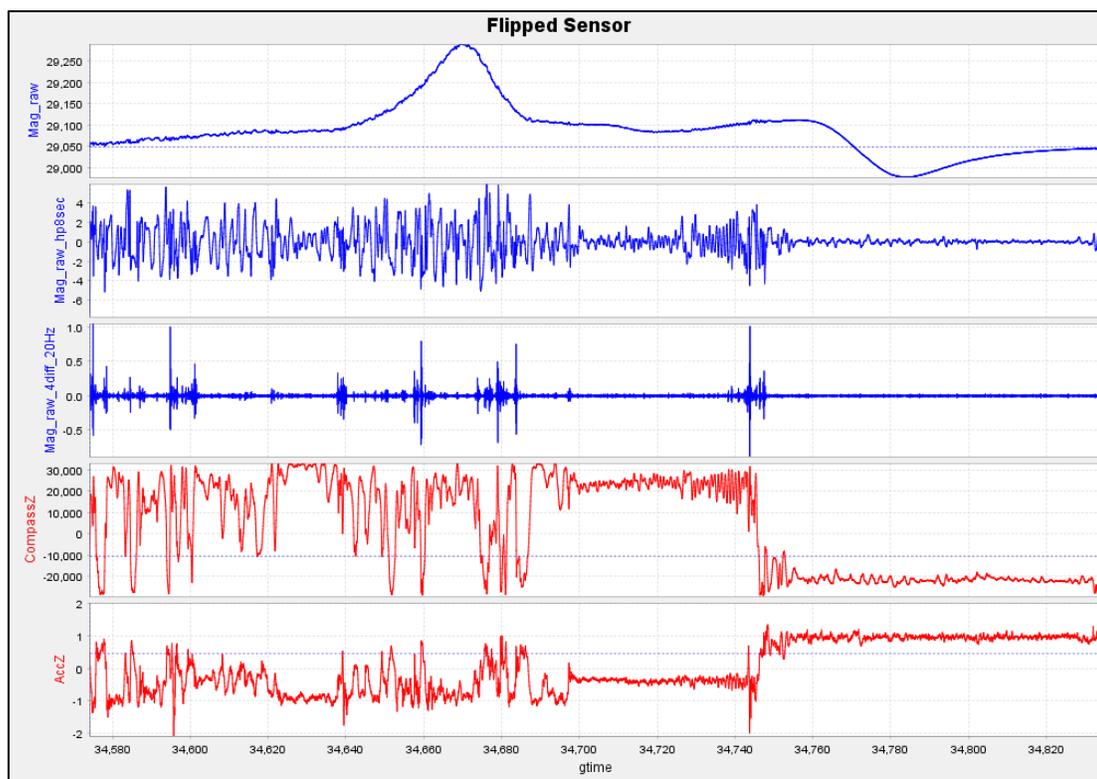
Figure 19   Example of extreme manoeuvre noise.

(From top to bottom: Recorded magnetic data, high-pass filtered data (8 seconds), 4th difference, vertical component of fluxgate compass, vertical component of acceleration.)

of the line. The lesson to learn from this example is that the conventional 4th difference noise is insufficient to detect manoeuvre noise.

Figure 20 shows about 450 metres of data affected by manoeuvre noise as an example. The diurnally corrected and IGRF removed data are shown in the top panel, followed by the 4 second (full wavelength) manoeuvre noise and the fluxgate compass channels. The red curve in the top panel shows the magnetic data after subtracting the 4 second manoeuvre noise. As can be seen in Figure 20, there are clear correlations between the manoeuvre noise and one or more compass channels. The data are acquired with the sensor suspended by 4 metres, and a pendulum of 4 metres length has a period of roughly 4 seconds. It can therefore be assumed that most of the manoeuvres are caused by the sensor swinging below the platform thereby constantly changing its attitude to the ambient magnetic field.

The manoeuvre noise in the example is obtained by a simple high-pass filter and may hence remove geological signal as well. It is therefore not suited as replacement for proper compensation. Compensating for platform influence is a standard process in conventional fixed wing airborne magnetic surveys; however, drone platforms cannot necessarily follow the same established procedures, especially when the sensor is suspended.
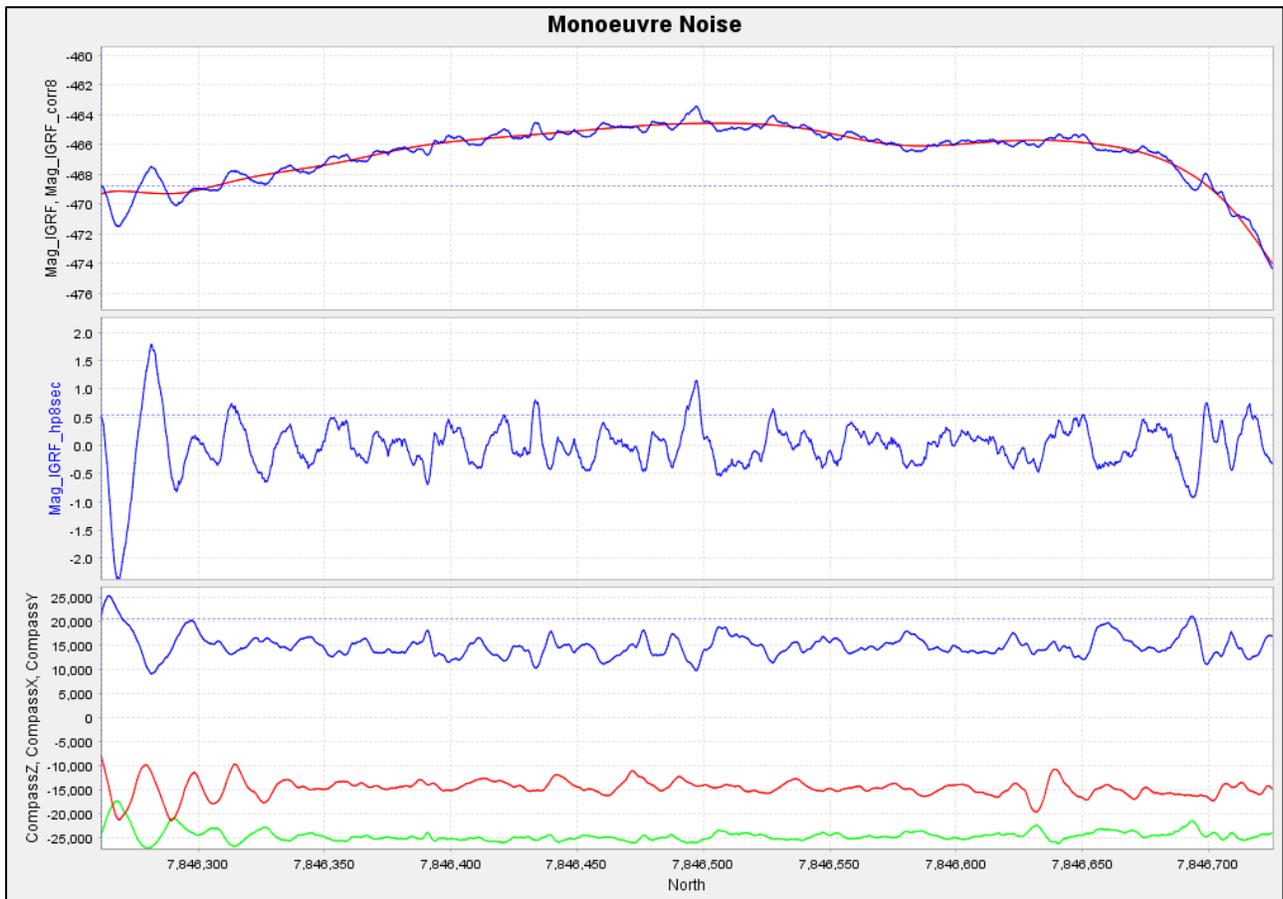
Figure 20   Example of data affected by manoeuvre noise.

(Top: Diurnally corrected and IGRF removed magnetic data before (blue) and after subtracting the 4 second manoeuvre noise. Middle: 4 second manoeuvre noise. Bottom: Fluxgate compass channels.)

It is therefore highly recommended to put effort and time into the development of alternative compensation tools able to remove manoeuvre noise from drone based magnetic data. They should preferably work directly from the production data and not require a high-level test flight, since this is not achievable by most drones. Modern pattern recognition and machine learning techniques might be able to solve the problem.

8.4 Electromagnetic Interference

UAV electromagnetic interference is a data quality issue frequently cited in literature by almost every publication on UAV aeromagnetic systems (Funaki and Hirasawa, 2008; Kaneko et al., 2011; Forrester et al., 2014; Funaki et al., 2014; Sterligov and Cherkasov, 2016; and Parvar et al., 2018). These electromagnetic interference signals can be divided into two dominant types based on their wavelength and overall effect within the gathered magnetic data. These two types consist of static and dynamic electromagnetic interference signals. Static interference is a non-oscillating magnetic field signal that results in a permanent or relatively long wavelength offset within the gathered magnetic data. These static interference signals can result from permanent and induced magnetization of ferrous components within the airframe (i.e., the permanent magnets in the electromagnetic motors) and DC currents within power supply wires. In contrast, dynamic electromagnetic interference is an oscillating signal of varying frequencies that can be caused by the rotation of the electromagnetic motors, DC and AC current fluctuations, and secondary eddy current fluctuations. These two main sources are discussed further in this section starting with the static and low frequency (< 10 Hz) electromagnetic interference signals.

Like early manned aeromagnetic surveys, the first and most common method used to avoid the electromagnetic interference generated by a UAV has been to position the magnetometer away from the platform's interference sources, most commonly by suspending the magnetometer below the UAV. Using this method, as shown in Figure 21 an optically pumped magnetometer with a sensitivity of 0.01 nT (blue outline) needs to be placed further outside the zone of static electromagnetic interference (blue shading) surrounding the multi-rotor UAV platform, than a fluxgate magnetometer with a lower sensitivity of 1 nT (red outline). This is due to the halo of electromagnetic interference having a higher amplitude closer to the multi-rotor UAV source and attenuating with distance. Note that the attenuation of the electromagnetic interference is nonlinear and decreases at a $1/r^3$ relationship away from the individual dipole signal sources on the multi-rotor UAV that can be on the order of 100s of nT (Parvar et al., 2018; and Tuck et al., 2018; 2021).

The diagram in Figure 21 provides an overly simplified and static view of what the magnetic interference amplitude halo would look like in 2D space surrounding the UAV in flight, dark blue for higher amplitude sources closer to the platform. This diagram assumes that there are several point dipole sources originating from the avionics, permanent magnets in the motors, electronic speed controller (ECS), and DC electrical cables on the platform and that these interference signal amplitudes attenuate with distance from the UAV. In the simplest form, this is a good approximation to aid in visualizing how these electromagnetic interference signals attenuate moving away from the UAV and where the magnetometer should be placed to target specific interference amplitude levels. However, when the full 3D electromagnetic interference halo of a UAV is mapped, there is undoubtedly a much more complex and interrelated electromagnetic interference system present consisting of static, low-frequency, and high-frequency electromagnetic interference signals. Studies such as Versteeg et al. (2007; 2010), Forrester (2011), Kaneko et al. (2011), Parvar (2016), Sterligov and Cherkasov (2016), Cherkasov and Kapshtan (2018), Parvar et al. (2018), Tuck et al. (2018; 2021), Krishna et al. (2021) and Walter et al. (2021a) have all mapped the static and low-frequency (< 10 Hz) magnetic interference signals that originate from the different components of various UAV platforms (fixed-wing, single-rotor, and multi-rotor). Each publication has demonstrated high-amplitude electromagnetic interference signals originating from point sources distributed around the UAV platform.
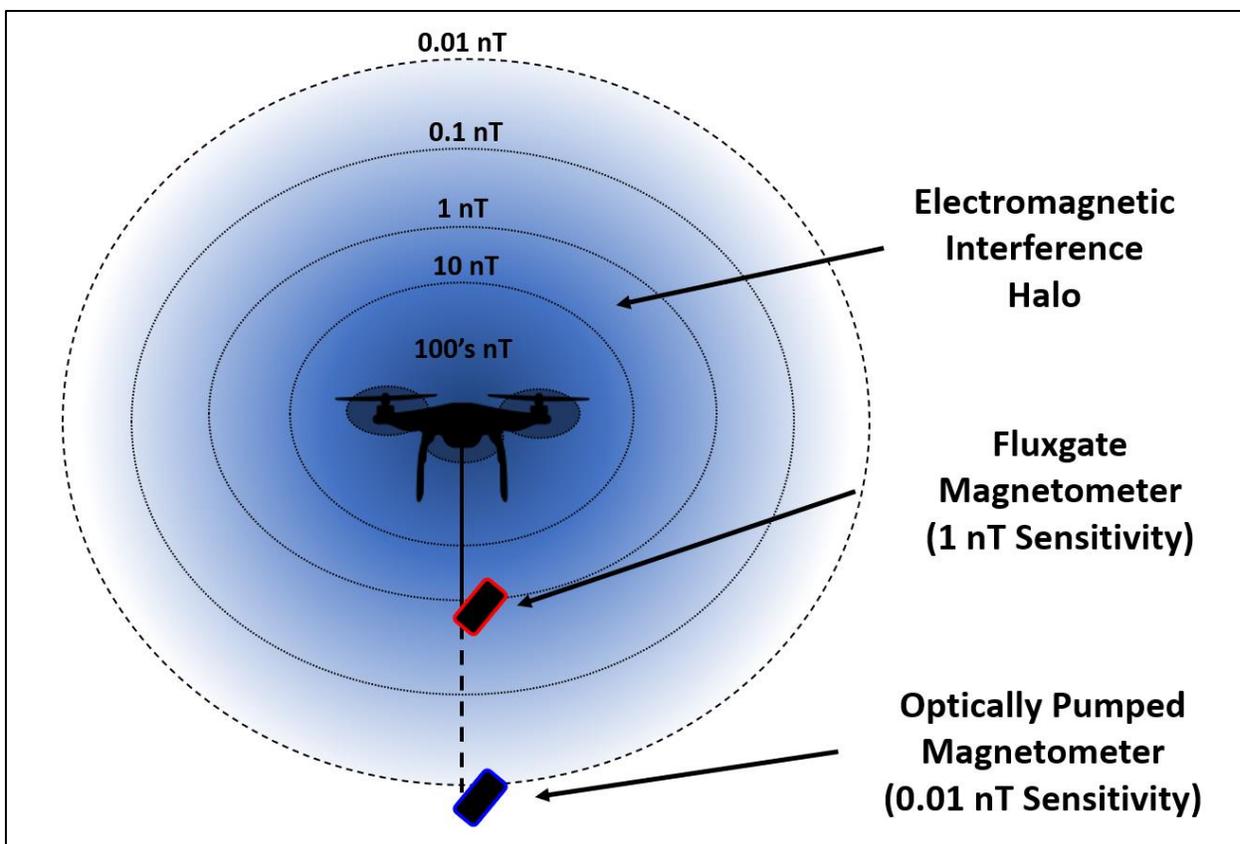
Figure 21   A simplified diagram depicting the halo of electromagnetic interference surrounding a multi-rotor UAV in flight.

(Note: the electromagnetic interference signal has a higher amplitude closer to the individual signal sources on the multi-rotor UAV, such as the avionics, wires, and electromagnetic motors.)

Specifically, Forrester (2011) mapped a 95 kg gas-powered fixed-wing UAV using a fluxgate magnetometer and identified three dominant sources of electromagnetic interference on the platform, which included the servos ~100 nT, the engine ~60 nT, and the avionics 30 nT. Sterligov and Cherkasov (2016) mapped a 10 kg electrical fixed-wing UAV and demonstrated that there are high-amplitude electromagnetic sources such as the electric motor ~800 nT, servos ~600 nT, and other ferromagnetic elements ~300 nT. Parvar (2016) conducted a 3D mapping of the underside of an 8 kg multi-rotor UAV and concluded that the maximum amplitude reached was ~350 nT. Tuck et al. (2021) mapped four different types of UAVs and demonstrated that the size and amplitude of the electromagnetic interference halo is linearly dependent on the amount of constant DC electrical current being drawn by the ESCs to power the UAV's electric motors. Tuck et al. (2021), shows a dipole anomaly generated when the multi-rotor UAV is powered. This anomaly shape mapped above the UAV, but also present below the UAV, is attributed to the constant DC current flowing to the ESCs to power the electromagnetic motors. These studies mapping the electromagnetic interference also demonstrate that there are differences between conducting these mappings when the UAV is off (mainly static and permanent magnetization components) or powered on (dynamic higher-frequency electromagnetic interference due to DC currents and other alternating sources).

Walter et al. (2021b) added to the previous investigations by characterizing the dynamic, high-frequency electromagnetic interference signals generated by a multi-rotor UAV both in a lab setting, as well as

throughout flight using the Geometrics MagArrow operating at 1 kHz. This study augmented the growing numbers of publications that have focused on mapping the static and lower-frequency (< 10 Hz) electromagnetic interference signals. The main finding is that the electromagnetic motors of the UAV, also known as permanent magnet synchronous motors, generate multiple high-frequency and high-amplitude electromagnetic interference signals. The dominant high-frequency electromagnetic signal is synchronous with the mechanical rotation frequency of the electromagnetic motor. Typically, this mechanical rotation electromagnetic signal frequency is observed around 45 – 60 Hz for most commercial UAV systems as shown in Figure 22 and can be observed varying slightly throughout flight based on the UAV's flight manoeuvres. For high-sampling frequency magnetometers such as the Geometrics MagArrow (1000 Hz), this high frequency interference signal can be observed directly in gathered data. However, for low-sampling frequency optically pump vapour magnetometers that sample at 10 – 20 Hz, this mechanical rotation electromagnetic interference signal will be under sampled and aliased in the recorded magnetic measurements.

The study of Accomando et al. (2021) also confirmed these high-frequency electromagnetic interference observations and compared different offset distances of the magnetometer below the UAV. Additionally, there are other higher frequency electromagnetic interference signals that are known to be generated by the UAV and can be predicted based on the configuration of the UAV's permanent magnet synchronous motors as explained in Walter et al. (2021b). Typically, the additional UAV generated electromagnetic signal frequencies extend up into the kHz frequency range under operating conditions and higher than the Nyquist Frequency (500 Hz) of most commercially available magnetometers and become aliased to lower frequencies within the gathered magnetic data. The most common and effective approach presently to mitigate the aliasing effects of these high-frequency electromagnetic interference signals has been to suspend the magnetometer below the UAV diminishing their amplitude. However, by suspending the magnetometer below the UAV will introduce a swinging interference signal within the data related to the swinging motion of the magnetometer bird throughout flight. The frequency of this signal is typically between 0.1 – 0.6 Hz and is explained in greater detail by Walter et al. 2019. Figure 22 shows both the mechanical rotation electromagnetic interference signal (F_{MR}) and the swinging frequency interference signal (F_{SW}) for a Geometrics MagArrow suspended 2.5 m below a DJI M600's airframe.

The need to map the extent and character of the electromagnetic interference in-flight during a surveying configuration has led to the adoption of the vertical buzz test as described by Walter et al. (2021a). This test aims to determine the vertical offset distance or the distance below the UAV where the magnetometer losses sensitivity to the interference signals. To avoid or limit the influence of the electromagnetic interference signals on gathered UAV magnetic data it is recommended to suspend the magnetometer at or near this determined vertical offset distance. While the vertical offset distance is often referenced at between 3 - 5 m for most commercially available UAVs, this will be unique for each UAV-magnetometer integration and should be investigated prior to conducting UAV surveys. Recent studies such as Phelps et al. 2022 have investigated compensating for the magnetometer swinging signals when it is placed outside of the electromagnetic interference halo. However, few attempts have been made to develop a robust compensation algorithm to correct for the dynamic electromagnetic interference signal interactions when the magnetometer is placed inside the electromagnetic interference halo. There are numerous considerations that still need to be investigated to develop a complete compensation algorithm and robust solution. These broadly include the magnetometer swinging through the dynamic electromagnetic interference, increased heading error signals, the aliasing high-frequency electromagnetic interference signals, DC and AC current variations, and eddy currents.
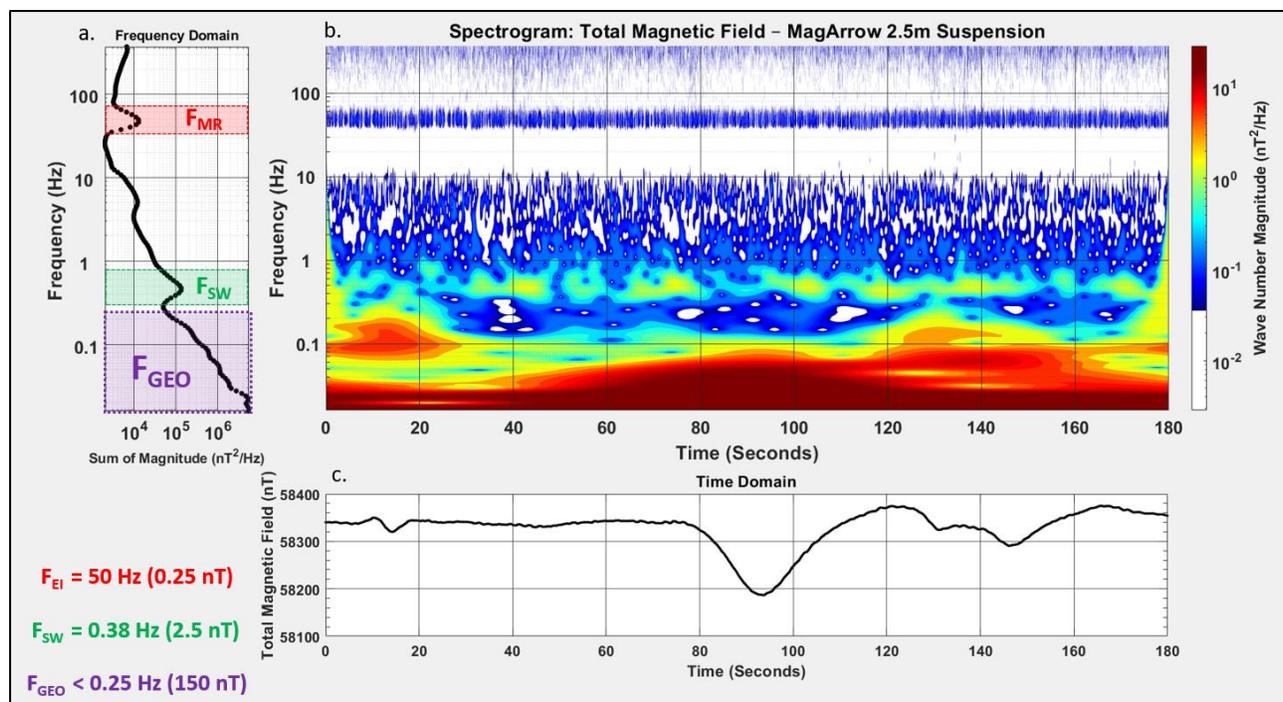
Figure 22   Frequency domain depiction of UAV electromagnetic interference for a flight line of UAV acquired magnetic data.

(Note: Frequency domain (a), scalogram (b), and time series (c) of one flight line demonstrating the two interference signals generated by a DJI M600 during flight and recorded by a Geometrics MagArrow (1000 Hz sampling frequency) suspended at 2.5 m below the airframe. The specific frequencies observed included the frequency of mechanical rotation (F_{MR} = ~ 50 Hz – red dashed rectangle), the swinging frequency (F_{SW} = ~ 0.38 Hz – green dashed rectangle), and the geologic target (F_{GEO} < 0.25 Hz – purple dashed rectangle).)

8.5   Artefacts

Noise usually appears as 'unconsolidated clutter' which can affect the resolution of the data. Depending on its magnitude, noise can only slightly obscure subtle geological (or anthropogenic) features or completely destroy the data. Noise can easily be detected (and sometimes quantified) in the final grids by using secondary products such as derivatives or hill-shading.

However, magnetic data can also contain artefacts which may reduce the quality of the final data. Artefacts are much more difficult to detect, because of their systematic nature. Artefacts are caused by badly executed survey operations, such as bad line keeping, or by processing errors especially in the tie line levelling step.

In case lines have to be broken for logistical reasons and there are navigation inaccuracies in the overlapping parts of two occupations, the gridding process can produce 'ringing'. This is because data acquired close to each other but having small level differences (due to bad height keeping for example) can produce strong gradients which in turn force the gridding algorithm to ring. In case individual lines require multiple occupations, the final grid can show small sharp but fake anomalies along the overlaps, in the case of two tiles (surveys) that are flown at different altitudes, tile boundaries may be visible in the final grid as rows of such small anomalies.

Long wavelength artefacts can be introduced by the tie line levelling process, when there are large misclosures at crossover points between traverses and ties. Large misclosure values can be introduced by mismatching altitudes of traverses and ties, or by incorrectly or not applied, heading or lag corrections. A faulty tie line for instance can produce a fake anomaly that is running parallel to the effected tie. Artefacts produced by tie line levelling are usually of a wavelength similar to the dimensions of the surveys area. And, whilst such artefacts may not affect smaller anomalies, they can prevent the successful merging of neighbouring surveys or tiles.

In case a survey is flown as many tiles, there are chances of level shifts between the individual tiles. If strong susceptibility contrasts exist in the survey area, or magnetic structures run parallel to the tile boundaries, such level shifts can be difficult to detect. The most prominent cause of (DC) level shifts is that the magnetic base station was moved during the survey and the differences in magnetic field strength between base station locations are not accounted for. Level shifts can also occur when the tiles are levelled individually. DC level shifts can be removed by gridding each tile individually, get the level shifts from a 'gridmerge' operation and correct the individual line databases. The data from all tiles can then be gridded simultaneously in one go.

A fourth class of artefacts occurs along the survey or tile edges, where the regular survey layout is not strictly adhered to. This can be the result of a tie line not being placed at the survey boundary, or be caused for instance, by starting the turns to the next line too early whilst still being in the actual survey area. Edge validity can easily be assured by simply designing the survey a bit larger than the actual area of interest, process the entire dataset and cut the final data.

8.6   Real World System Noise

Let's define the 'Real World System Noise' as the sum of instrument and manoeuvre noise. The best way to get a measure of the real-world system noise would be a small survey flown over a test area. The test area should comprise a magnetically quiet part and some distinct anomalies. The area should further be obstacle free but include terrain undulations to test height keeping and ground following capabilities. A high-quality detailed ground magnetic survey will have to be done as reference. The authors are aware of the fact that such test sites do not exist (yet). It would/should be a call to geological survey organisations worldwide to establish UAV test sites in the area of their jurisdiction. The authors are also aware of the fact that the result of the test surveys will be influenced not only by the quality of the acquired data but also by the processing techniques applied, which could be an added advantage.

A less time intensive way to establish the real-world system noise is flying a repeat line, an example of which is given in Figure 23: The repeat line was flown 12 times in alternating directions. The data show the deviation from the average of the 12 occupations with the black line indicating the standard deviation. The data are corrected for diurnal variations and the IGRF is removed. The repeat line was flown at a nominal terrain clearance of 15 metres. However, the line was located over some scrap metal found in the field. The strong deviations in the centre of the line are therefore likely to be caused by positional inaccuracies and do not reflect manoeuvre noise. The latter could be quantified from the line ends as about 3 nT (1 standard deviation range).

A repeat line may give some insight into the repeatability of a system (see the example in Figure 23), but falls short of quantifying the real-world system noise, because the data could be influenced by the underlying geology.
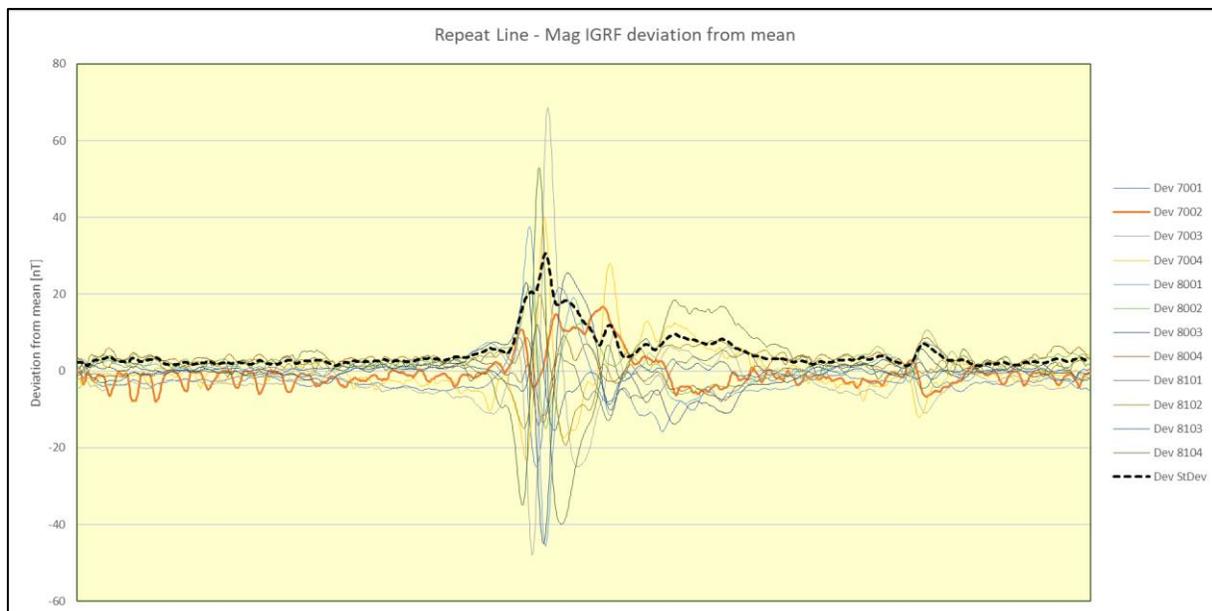
Figure 23   Repeat Line example.

(The coloured lines show the deviation from the average of 12 occupations. The magnetic data are corrected for diurnal variations and the IGRF is removed.)

In conventional airborne magnetic surveys noise test are done in a magnetically quiet environment simply by flying the test at high altitude. Unfortunately, drones cannot fly at 2 or 3 kilometres above the ground, but one should strive to conduct a noise test as high as possible and also avoid flying over magnetically active geology.

Another good way to assess real world total system noise is to look at the standard deviation of the differences between tie-lines and profiles (having applied all corrections to the data prior to the comparison): you get an "averaged" error reducing local influence of underlying geology, but this method is not as practical for in-field assessment (prior to processing). Section 9.1 outlines a simple method to determine system noise in the field

9.   SURVEY ACQUISITION AND QA/QC

Whether carrying out or supervising a drone magnetic survey or writing a specification for a drone magnetic survey acquisition process, it is important to have a way to ascertain under field conditions at the time of the survey, the total system noise of the UAV / magnetometer system carrying out the survey.

9.1   Recommended Repeatability Test for system noise assessment

In this section we recommend a simple test to establish the real-world system noise of a UAV based aeromagnetic survey using repeatability as a means for determining system quality. Such a test is primarily a quick way that clients can independently assess the noise levels of the magnetic survey system and the drone performance. Repeatability tests are non-commercial so they could be published by drone operators to demonstrate the repeatability (noise level) of their system(s) and/or they could be requested by clients to be performed prior to a survey operation. The test flight should not take more than 20 minutes to fly and should be repeated in case of changes to the platform-sensor system as well as significant changes in environmental conditions.

Repeatability flights measure the "real world system noise" across a broad spectrum of wavelengths and by analysing the deviation from the mean the flights do not need to be at very high altitude or in very quiet areas. Flying a 400m x 400m box flight pattern 6 times (3 clockwise and 3 anticlockwise) has been shown to be effective (Mutton, 2021) and only takes about 15 to 20 minutes. Ideally such a dataset can be made prior to awarding a contract (to demonstrate noise levels and data formats), prior to flying (to confirm system noise levels in local conditions), and during a survey if there is a substantial increase in the wind or any change to the system. The latter may be needed for clients to understand the effect of wind so that standby may be justified. Diurnally corrected noise levels at 1SD (one sigma deviation), 2SD, and 3SD at least can be used to quantify system noise levels and be compared to contractual requirements. Note that the test data needs to be diurnally and IGRF corrected. Critically, the data sampling frequency for tests must be specified and provided with required errors. Rapidly sampling (e.g., 500 Hz) can greatly increase apparent noise levels than lower sampling rated (e.g., 10 Hz) systems.

Figure 24 shows the results from such a repeatability test. The top panel (a) indicates the line path, the middle panels (b) and (c) show the deviation from the average for Lines 1 and 2 (Y-axis: ± 0.5 nT) and the bottom panel shows the variation in height for Line 1 (Y-axis: 1 m).

In a variation of the Figure 24 test which is flown on a plane, an improved flight to better test the drone and draping algorithm performance is show in Figure 25. In the Figure 25 variant, artificial terrain is added on two of the legs that represent very steep topography as might be expected in the survey area. High quality drone surveys may be flown at such a constant height that data does not need tie line levelling, similar to good ground magnetic surveys.

Note that the recommended tests (Figure 24 and Figure 25) are not yet established as a universal standard procedure. In some surveys the size of the box flown may need to be varied for different
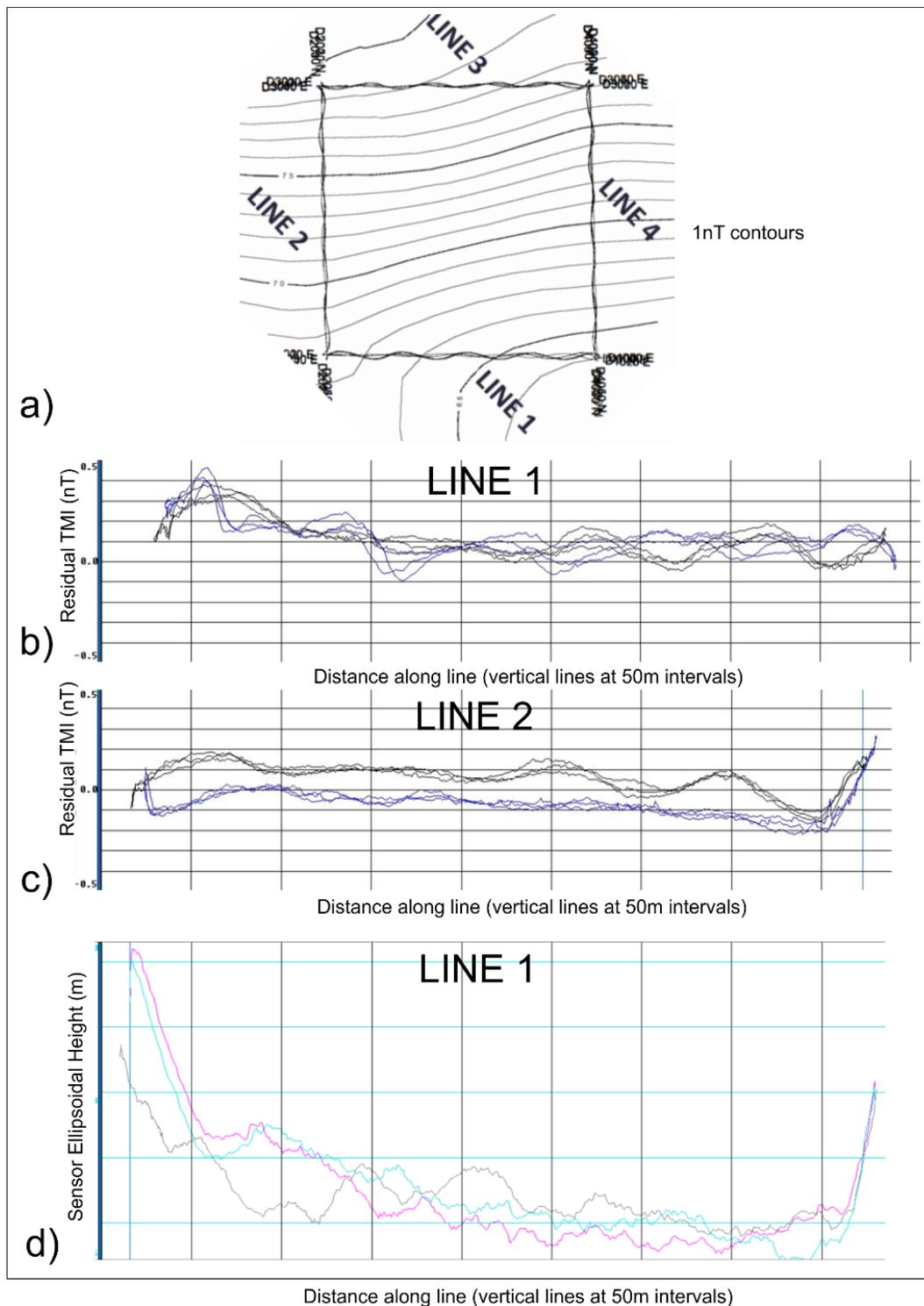
Figure 24   Repeatability Test Flight Data

((a) Flight lines of 400m x 400m box with contours of average magnetic field
b) Residual (survey data minus mean) magnetic data repeats from Line 1 showing approximately 0.2nT noise
envelop and no heading error.
c) Residual magnetic data repeats from Line 2 showing approximately 0.2nT noise envelope and 0.06nT heading
error
d) Elevation repeats for Line 1 showing about a 1m variation in flying height across 3 repeat lines)
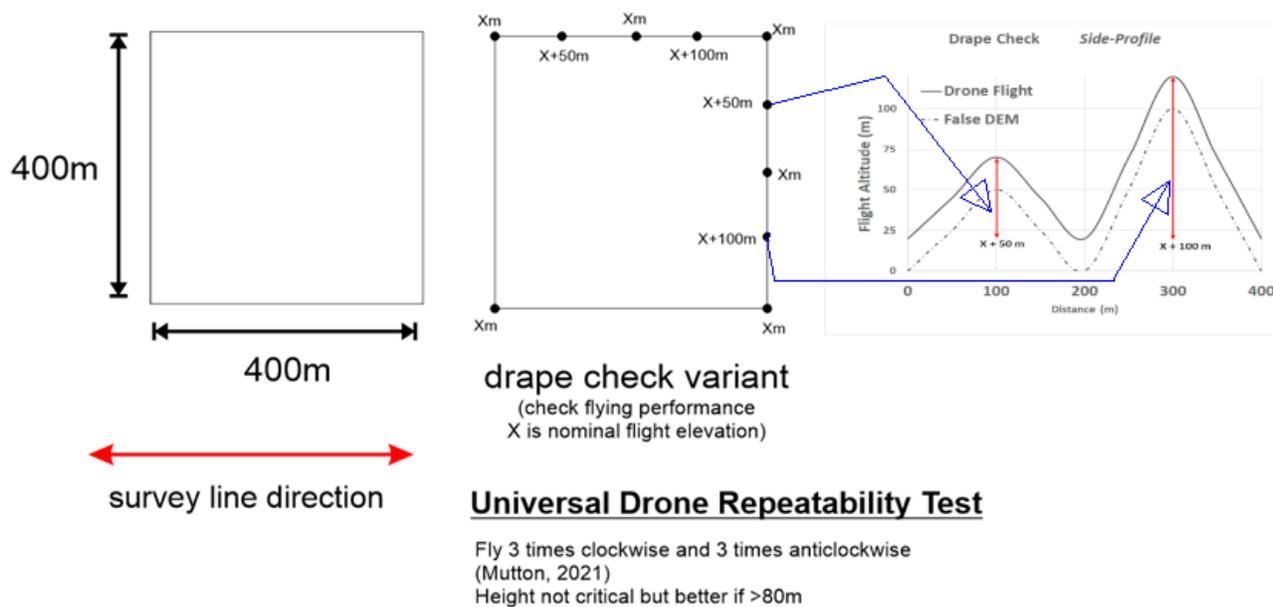
Figure 25   Repeatability Test with Artificial Terrain added

applications, e.g., the test box to be flown for an UXO detection or archaeological survey may have to be much smaller than the box for a geological mapping survey at 100 m line spacing.

In order to establish the universality of the tests, one will need a series of such tests performed by different platform-sensor systems under varying environmental conditions to determine the best proactive noise levels at a standard (e.g., 10 Hz sampling rate). Once established, any of the magnetic signal sigma deviations could serve as a contractual threshold similar to the Figure of Merit (FOM) established for conventional (manned) airborne magnetic surveys. Height variations can similarly be defined in a standardised test.

9.2   Pre-mobilisation check for draping algorithm and drape quality

For very steep area surveys, the worst of the survey area's topography can be simulated in a flight at the contractor's test range prior to awarding of the contract to check drone and draping algorithm performance. This may identify a potential issue otherwise missed and ensures all care is taken to ensure safe flying with the draping algorithm employs. An example is shown in **Figure 26**.
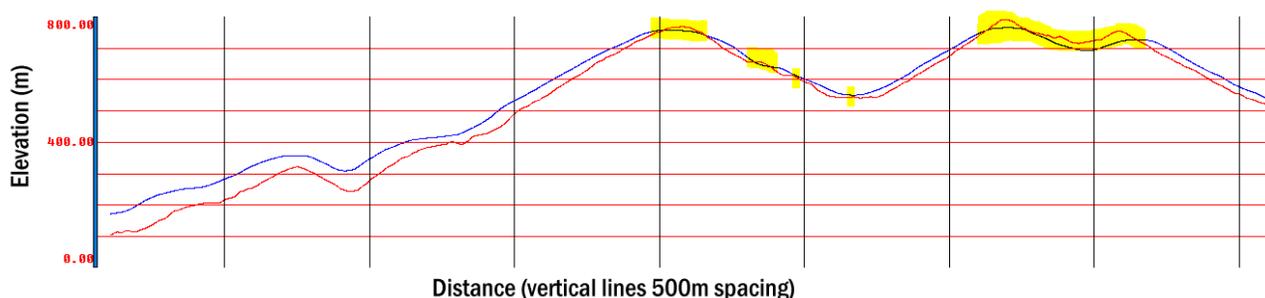
Figure 26   Example of a survey line flown on a test range with simulated topography and problems

(Problems with the drape are highlighted in yellow where the sensor height (blue) dipped below the topography (red))

9.3 UAV Magnetics Tendering and QA/QC Considerations

The tendering and awarding of a survey contract should include survey specifications, details for data quality assessment during the survey and deliverables expected.

9.3.1 Technical survey specifications

Technical Specifications must include the following: -

- Survey line direction, line spacing, area, and nominal flying height must be defined
- Vertical and horizontal datums must be defined. Most drones fly based on the WGS ellipsoid but most DEM's use a geoidal datum. These can be offset by tens of meters and mix-ups have been calamitous such as a drone crash or surveys requiring repeating due to flying too high.
- A request for the supply of a recent repeatability test (Section 9.1) should be requested to check system noise levels (noise envelope), system elevation control, drape performance, and supplied data format/fields. This is a critical check for the client.
- Sensor sampling frequency and maximum survey speed.
- Tolerance for breaks in survey lines due to (a) dead-zones and (b) GPS dropouts (recommend 20m for both – otherwise require reflys)
- Tolerance for sensor deviation off line (recommend 2m or 20% of line spacing, whatever is smaller)
- Tolerance for drape variations when no obstacle is being avoided (recommend 5%-10% of survey height).
- Tolerance for noise envelope (Figure 24) on repeatability of flight data as a deviation from mean after compensation, diurnal, and heading correction (In 2021 recommend <0.5nT for 3SD – 99.5% for geological surveys).
- The DEM to fly the survey must be agreed. Contractors may wish to acquire their own.

- The draping algorithm must be tested with the chosen DEM prior to awarding of the contract and mobilisation as per Section 9.2 and Figure 26.

- The following are additional considerations, that should be included in a contract.
- Who has responsibility for survey equipment damaged/loss during survey? (Normally, this is the responsibility of the contractor).
- Are tie lines necessary? (If in doubt carry out tie lines which can be good insurance unless QA/QC proves otherwise)
- What are the conditions for standby due to wind? (This should be based on safety considerations, drone stability and on the noise envelope as defined by repeatability tests)
- Weather standby conditions? (Frost, Snow, Rain, Temperature…)
- Survey speed/sampling?
- How should in-survey data be provided for noise and sensor clearance assessment tests (Section 9.1).

Specifications related to navigation

Horizontal navigation or line path following specifications usually allow deviations from the planned line path or line separation in the order of 15 to 25% over a certain distance. The reason for this is mainly to ensure regular survey layout for gridding, because lines too wide apart can stress the interpolation algorithm and produce 'blurred' areas between two failing lines or, in the case of neighbouring lines being too close together, gridding can produce ringing artefacts. Best practice requires that in no case should two neighbouring lines cross each other.

Vertical navigation specifications are either defined as a percentage of the nominal ground clearance or in absolute terms when following a predefined drape surface.

It should be noted here that the requirement for navigation accuracy for both, horizontal and vertical directions, sharply increases with tighter line spacing and lower ground clearance. For a UXO detection survey for example (Level 1 survey), the navigational accuracy should be in the decimetre range or better.

9.3.2   Quality checking

QA/QC considerations for the client or client representative should include the following:

- Repeatability test flight data needs to be reviewed before commencing survey (Section 9.1) for system noise level assessment and when weather degrades.
- Daily sensor clearance maps should be made/supplied to ensure good drapes are being achieved.
- Daily production report should be supplied to client or agent.

9.3.3   Survey Deliverables: -

Delivered survey and tie lines must all be assigned unique ID's, and must include:

- Location (XYZ) of survey point with time stamp.
- Raw Magnetic field after compensation (if compensation was necessary)
- Magnetic mag diurnal correction
- Heading correction (if applied).
- Final magnetic data after compensation and corrections.
- Note of processing applied (e.g., resampling, filtering), with estimate of survey noise levels from repeatability tests (1SD, 2SD, and 3SD from mean)

Optional extras (recommended) may include: -

- Raw sensor data with no compensation or heading correction.
- Located magnetic data after tie line corrections and micro-leveling.
- Grid of levelled Total Magnetic Intensity (TMI), ground clearance.
- Image of greyscale 2VD (Second Vertical Derivative) of the levelled TMI for QA/QC.

9.3.4   QA/QC considerations for the client or client representative,

Overall QA/QC considerations for the client or client representative includes the following: -

- Repeatability test flight data needs to be reviewed before commencing the survey.
- Daily sensor clearance maps should be made/supplied to ensure suitable drapes are being achieved.
- Daily production report should be supplied to client or agent.
- Plot of normalised 8th difference to monitor system noise (see Figure 27)
- Histogram of sampling distance / confirm maximum distance is within contract
- Flight path vector plots – showing required coverage, adherence to planned flight paths and good overlap plus tie-lines going over these overlaps (for tie-line levelling)
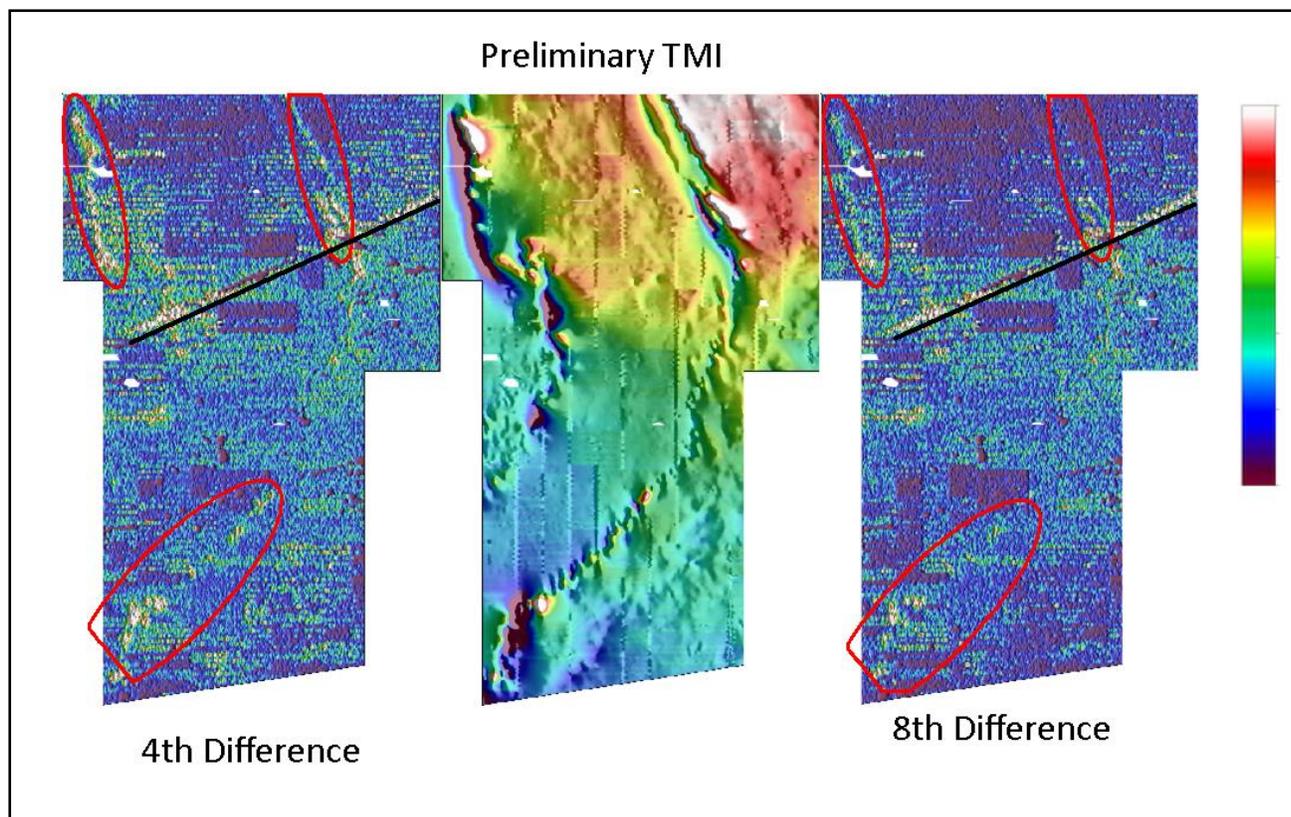
Figure 27   Comparison of Normalised 4TH versus 8TH difference for QAQC of TMI

(NOTE: The black lines indicated a "cultural" powerline, and the red polygons highlight geologic signal in the preliminary TMI. The centre image is the TMI, on the left being the 4th normalised difference, and the 8th on the right. Due to the generally lower flying height of the UAV, shorter wave-length geological signal is recorded in the data. The 4th difference (left) is still showing geological signal at this stage. Going to an 8th difference (right), the overall geological input is reduced, whilst still retaining higher-frequency cultural (e.g., powerline) features in the display.)

10.   COMPENSATION AND CALIBRATION

The first and arguably most important step towards high quality, noise and artefact free airborne magnetic data is to remove all platform influences from the measured data. And, as a matter of fact, all commercially available airborne platforms do emit DC and/or AC electromagnetic radiation, be it manned aircraft of UAVs (refer to Section 8.4).

Platform influences do originate from magnetic equipment installed in the platform, most prominently engines and electro motors, charging currents from batteries or alternators and eddy currents generated by the motion of the platform trough the ambient magnetic field. The magnitude and direction of the disturbing (electro-) magnetic fields also depend on the direction of the ambient magnetic field of the Earth and the attitude (Euler angles) the platform-sensor system has with regard to that field.

As a first measure to reduce platform influences, the magnetic sensor is placed as far as possible from the main sources of magnetic disturbance (engine / motors) by mounting the sensor in a stinger (or nose boom or wingtips) or by dragging the sensor in a 'bird' which is suspended (far) below the platform.

The platform influences are measured during a so-called compensation or calibration flight for various manoeuvres (attitudes) in the four cardinal survey directions and correction coefficients are calculated, which are then applied to the measured data. The corrected data from the compensation flight can be used to calculate the so-called Figure of Merit (FOM) which specifies the noise level of the platform-sensor system. FOM values are usually part of airborne magnetic survey specifications.

There are two common types of magnetic sensors used in airborne geophysics: Total field magnetometers and fluxgate vector sensors (Section 0; Table 2). Whereas the noise or inaccuracies of optically pumped total field magnetometers is far below any noise threshold required for aeromagnetic surveys, fluxgate magnetometers used in vector sensors have a couple of 'characteristics' that require special attention in order to produce reliable data. The compensation/calibration of both is therefore discussed separately (Sections 10.1 and 10.2).

10.1   Total Field Systems

The optically pumped magnetometers usually employed for airborne magnetic surveys do produce very reliable data at sampling rates of up to 1 kHz with an extremely low noise envelope but some sensors may be susceptible to attitude changes (see Table 2). When the sensor is rigidly mounted to the platform however compensation does remove both, platform influences and the 'Heading Error' of the sensor itself.

10.1.1   Conventional Compensation

In conventional (manned) airborne geophysics with a rigidly mounted magnetic sensor the platform influences are obtained during the so-called compensation flight. A series of pitch (±10°), roll (±5°) and yaw (±5°) manoeuvres, each lasting for about 5 to 6 seconds, are flown in the four cardinal survey directions. Leliak (1961) developed a series of 18 (2 redundant) equations which are used to calculate compensation coefficients for each manoeuvre in each survey direction.

Compensation software, often based on Leliak's original work, is mostly developed by the contractors for proprietary use. The authors are aware of only two commercially available software tools for conventional compensation.

The compensation flight has to be undertaken for each survey in a magnetically quiet environment to exclude any influence of surface geology. In practice this is guaranteed by flying at about 3000 metres above the ground. The regional changes of the magnetic field are removed by applying a high-pass filter to the recorded data.

Figure 28 gives an example of a compensation flight. The raw and compensated magnetic data and their high-pass filtered version are shown in the top and middle panel respectively with the manoeuvres, indicated by the (fluxgate) compass data, shown in the bottom. Data from the entire compensation flight (box) are displayed including turns.

The so-called Figure of Merit (FOM) describing the noise level of the platform-sensor system is calculated from the compensated and high-pass filtered data by summing the peak to trough values (sometimes the RMS) for each manoeuvre in each direction. Common FOM specification is 1.5 nT but compensation for some aircraft achieve FOM values of 0.5 nT or less. A FOM value of 1.2 nT means that the platform influence for each manoeuvre in each direction is 0.1 nT on average. This should be matched by drone magnetic systems if possible. It should also be noted that compensation does involve DC shifts as well as the removal of manoeuvre noise.

Note that there are ongoing research activities to replace the compensation of magnetic data based on the Leliak equations with more modern mathematical techniques such as machine learning. These techniques are based on production data and not on a compensation flight. They may therefore be useful for suspended systems in general and specifically drone surveys. The authors are however not aware of any published results.
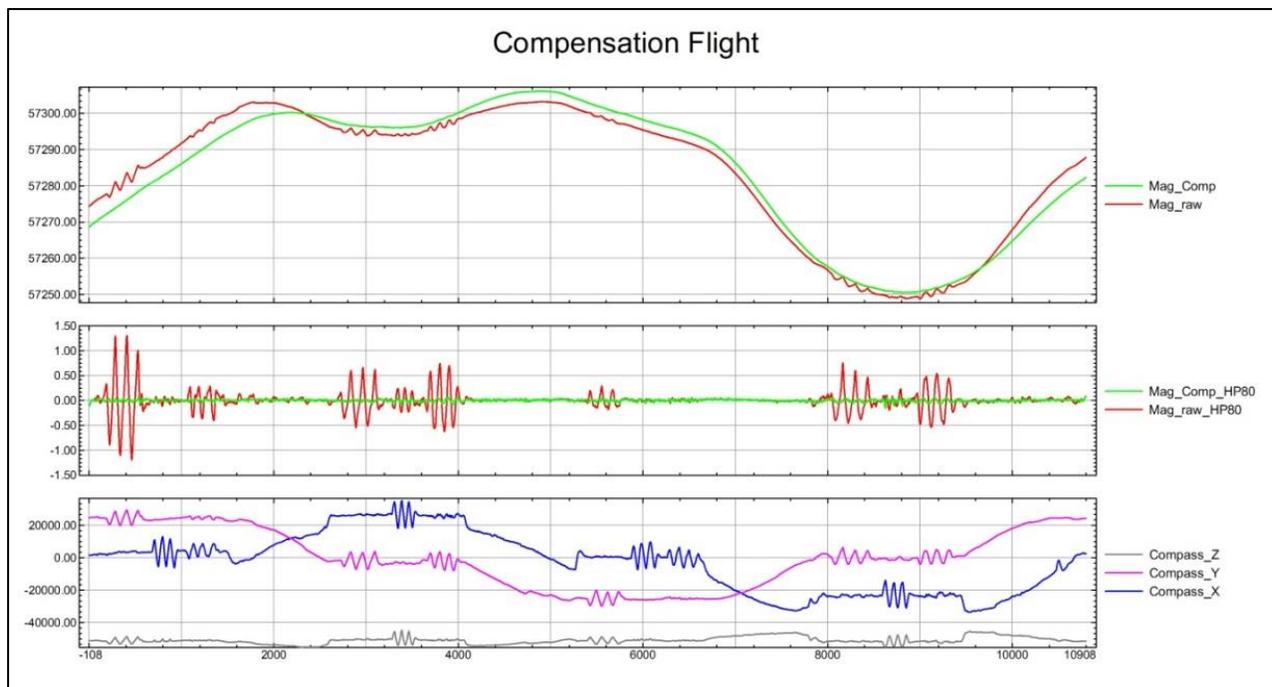
Figure 28   Example of a compensation flight.

(Top: Raw and compensated magnetic data. Middle: High pass filtered (8 sec) raw and compensated magnetic data. Bottom: Fluxgate Compass data. Note, all four directions are shown, including turns.)

10.1.2   Compensating Drone Systems

It has to be stated first that there is currently neither an agreed compensation routine nor is there compensation software available that provides consistent and reliable results for UAV based magnetic systems which could be used to classify the noise level of the platform-sensor system. The authors are aware of very promising research activities in this field, but none of these have reached a final or generally approved status. Therefore this chapter is rather a discussion than actual guidelines.

The conventional compensation strategy is not, or only partially, applicable to UAV base systems due to a variety of reasons: -

- The required 'magnetically quiet environment' by simply flying at high altitudes cannot be achieved by drones.

- Fixed wing UAVs are theoretically able to fly the required manoeuvres of ±10° pitches and ±5° rolls and yaws. It is however questionable whether these can be programmed into the navigation software.

- Rotary wing UAVs (copters) are capable of much larger attitudes (Euler angles) and large pitch and yaw angles can and do occur during production. So far nobody has proven that Leliak's equations are suitable to compensate such large-angle manoeuvres.

- Copter UAVs with a suspended sensor are the most frequently used systems for drone based aeromagnetic surveys. Any compensation algorithm for such systems has to therefore, not only to compensate the manoeuvres of the entire platform-sensor system, but also for the sensor motion with regard to the platform. No algorithms have yet been developed for this task and it is highly questionable whether the accuracy of the GPS receivers in both, platform and sensor, is sufficient to accurately calculate the position of the sensor within the coordinate frame of the platform.

- Further, smaller drones are not capable to support a high drag bird which would stabilise the bird's position. To achieve some stability the sensor is mounted either on four cables (Geometrics) or on a semi-rigid hose pipe (GEM).

- It should also be noted that the manoeuvrability of a copter drone is much higher than that of a fixed wing platform, however this manoeuvrability can result in pendulum motion of the sensor by sudden changes in speed or direction.

10.2   Vector Magnetic Systems

10.2.1   Fundamentals of Vector Magnetics

Fluxgate magnetometers have some important advantages over other types of magnetometers commonly used in geophysical exploration: much lower costs, low weight (100 gm) and the low power consumption.

Further, fluxgates are standard sensors on satellites. The orientation of the components of fluxgate sensors and the direction of the magnetic vector in space are maintained with the aid of a star imaging camera. Due to the long base line between fixed stars the absolute orientation of the fluxgate components in space can be determined with extremely high accuracy.

It is however important to empasize that fluxgate magnetometers are not absolute measuring sensors. Fluxgates have no physical principle that directly measures the "true" total intensity of the Earth's Magnetic Field, as is the case for scalar magnetometers. A fluxgate magnetometer requires calibration with respect to the "true" TMI at a location. But, three component fluxgates are one of a few magnetometers, which in

principle allow determination of the vector of the Earth' magnetic field. In many cases fluxgates are used as scalar magnetometers. The Pythagorean (https://en.wikipedia.org/wiki/Pythagorean_theorem) is applied to the three components to derive the TMI.

10.2.2   Vector magnetometer calibration

There are two different principles to calibrate a fluxgate magnetometer:

1. **Vector calibration** involves comparison of the output of the three components of the fluxgate magnetometer with the intensity of a scalar type magnetometer in combination with the determination of the direction of the fluxgate components measured versus time. The problem of in-flight vector calibration consists in the lack of knowledge of the accurate direction the components Bx, By, and Bz in space with respect to the Earth reference frame. VECTOR CALIBRATION of fluxgates involves estimating the "true" TMI of the Earth's magnetic field vector and its direction with respect to the Earth's reference frame. But the determination of the magnetic field direction in space requires keeping track of the angular rate of the components and monitoring of changes of the direction by means of high-definition and low drift angular rate sensors. It is required to resolve the absolute angles with an accuracy of at least 0.01°. Only Laser gyros, e.g., of Honeywell, can achieve this resolution. But Laser gyros are heavy and extremely costly and therefore inefficient for use on multi-copters.

2. **Scalar calibration** is the method to determine the TMI by neglecting the direction of the fluxgate components in space. Scalar calibration involves only the comparison of the intensity of the magnetic field against a scalar reference magnetometer, e.g., Overhauser-, or Cs-vapor type, or the local value of the international geomagnetic reference field (IGRF), does not make use of the direction of the magnetic field.

There are four errors which are inherent in a fluxgate sensor: -

- The scaling factors of the three components are not identical.

- The off-set is not zero (i.e., zero output does not correspond to zero ambient field).

- Non-orthogonality, i.e., the angle between two components is not perfectly 90°.

- Temperature drift.

As a consequence, the TMI strongly depends on the orientation of the fluxgate sensor in space. The application of the Pythagorean assumes the fluxgate components are mathematically identical and perfectly perpendicular to each other. Each component is physically differentiated from the others, by the scaling factor and offset, and non-orthogonalities between the components. These errors are predominant causes for the strong deviations of the TMI with regard to the sensor's orientation in space.

In order to eliminate these errors, set up a sensor model function that quantitatively describes these errors. Then use a least square approach to minimize the differences between components, which yields a TMI regardless of the orientation of the sensor in space. This procedure is called scalar calibration and fits nine model parameters (3 scaling factors, 3 offsets, 3 angles) to the intensity of the regional magnetic field. The TMI represents a point on the surface of a sphere, and the vector length corresponds to the radius of the sphere. In the uncalibrated state the vector length changes with the orientation of the sensor, describing a surface which equals an ellipsoid. This is demonstrated in Figure 29

Fluxgate sensors are subject to temperature drift, which strongly impact the quality of the magnetometer output. High quality fluxgate magnetometers measure the temperature both inside the fluxgate sensor and
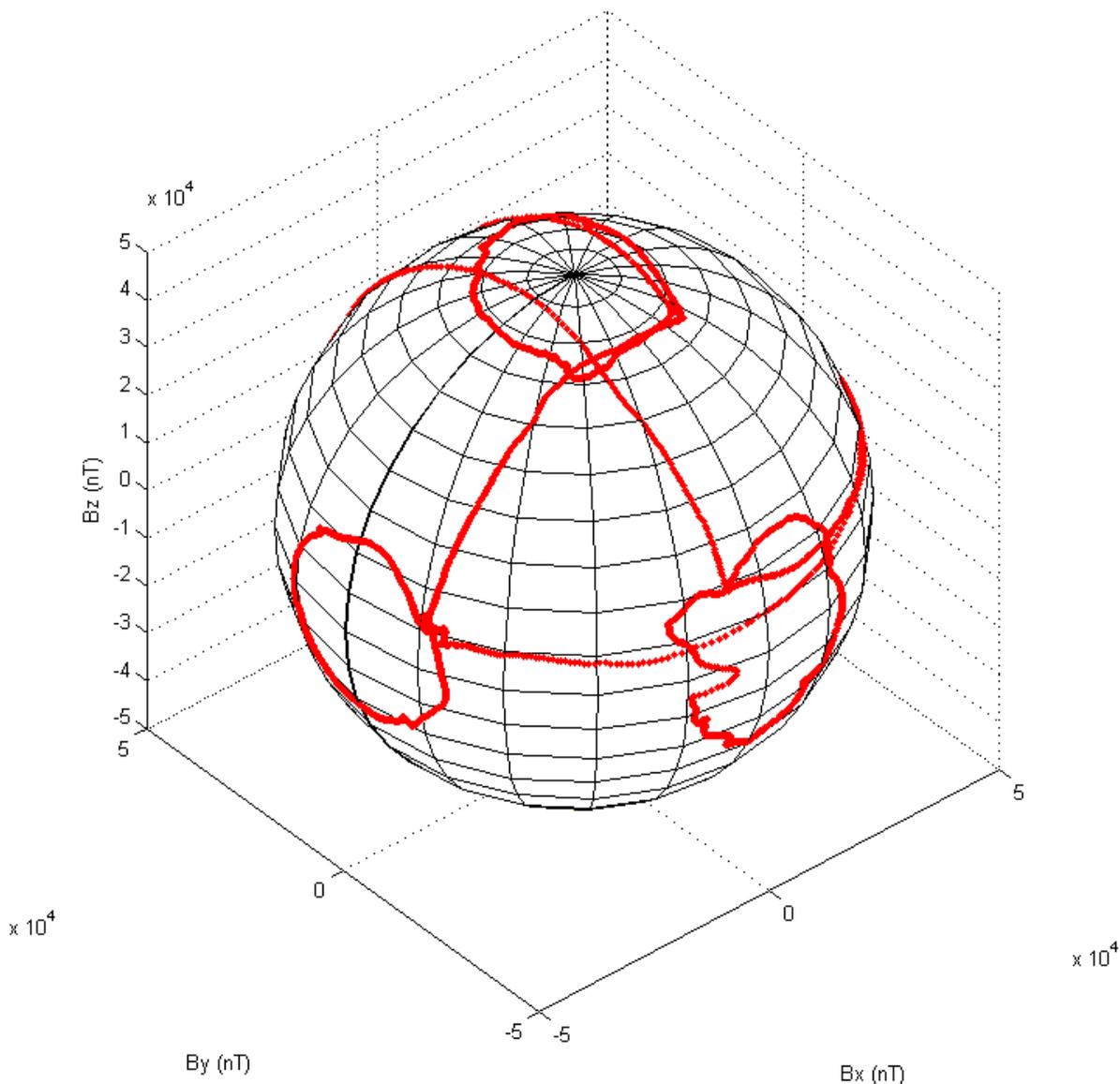
Figure 29   Changes in the vector magnetic components during calibration.

(Note: The surface of the sphere represents a constant TMI vector regardless of the orientation of the fluxgate sensor.)

on the electronic board to enable temperature drift corrections using a polynomial fit over a large temperature range.

Figure 30 shows an example of on ground calibration of a fluxgate sensor calibration routine.
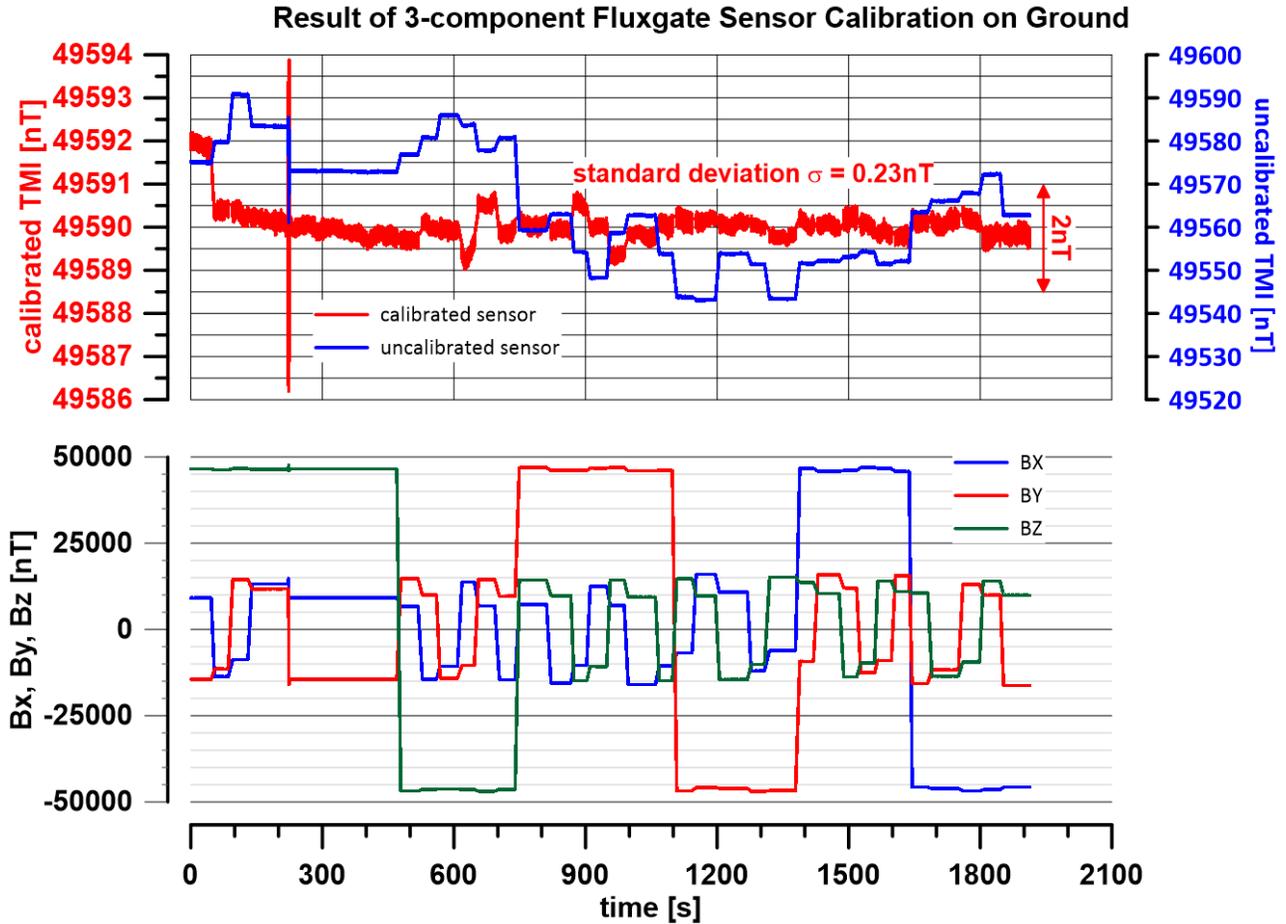
Figure 30   Vector Magnetic calibration on ground example.

(Note: Unfiltered Total Magnetic Intensity values before (blue) and after calibration (red) vs. time (upper panel). The data contain 50Hz ambient noise. Note, the scales for the uncalibrated and calibrated values are different.)

Upper panel: Application of the Pythagorean to the raw magnetic measurements of the components result in the total magnetic intebsity which is strongly depend on the direction of the fluxgate sensor (blue line). The heading error corresponds to about 50nT. After calibration (tranform from ellipsoid to sphere) and application of the nine parameters the heading error is almost eliminated and exhibits ±1nT and a standard deviation of about 0.23nT.

Lower panel: Components of the fluxgate sensor Bx, By, Bz vs. time. The fluxgate sensor is rotated stepwise by 90° about each axis. The changes of the values of each component reflect the changes in the direction of the component with respect to the Earth's magnetic field.)

11. PROCESSING AIRBORNE AND UAV MAGNETICS DATA

11.1   Background

The acquisition of magnetic data from an airborne platform, dates back to WW-II. Since then, a variety of processing techniques and data quality requirements were developed to eventually achieve sub-nT accuracy of the final data. Drones or Unmanned Aerial Vehicles of various types became available (and affordable) in the last decade. Although some do differ from standard fixed or rotary wing platforms geophysics does not, hence drone based geophysical data require identical or similar processing steps as data acquired on conventional (manned) platforms.

The required data quality obviously depends on the survey objective. Data consistency and noise levels have to be of a level that is (significantly) lower than the anticipated magnetic anomalies in order to allowing un-ambiguous detection or delineation of the objects to be identified. A survey that aims to identify different zones in a dump site for instance will require a much lower detection threshold than a survey looking for UXOs. Similarly, mapping carbonatite or BIF geological targets requires a lower detection threshold than a survey looking for inter-sedimentary structures with low susceptibility contrasts.

Therefore, magnetic properties of the host environment have always to be taken into account when determining the detection threshold.

Depending on the survey objective or detection threshold some processing steps described in this chapter may not have to be applied at all or, on the other side of the accuracy range, have to be applied with extreme care.

All common airborne platforms in use do emit electromagnetic radiation, be it DC or AC, and therefore influence the measured magnetic data and some magnetic sensors do have a directional error. In addition to these disturbances the variations of the ambient magnetic field also influence the observed data.

It is the role of processing to remove all influences from the measured magnetic data which do not originate from the target/geology itself. This should be done based on the principles of physics as far as possible. A workflow for the processing of 1 kHz drone data is illustrated in Figure 31. The coloured boxes refer to the standard tools available for the processing of airborne magnetic data. The following sections describe the steps in detail.

The very important step of calibration or compensation is discussed in Section 10.

11.2   Base Station Data

The ambient magnetic field varies during the day due to variations of the external magnetic field which are caused by the Earth rotating in the solar wind. Diurnal variations are normally in the range of 20 to 50 nT but can reach up to several 100 nT. Magnetic data acquired when strong and short wavelength diurnal variations occur - so called solar storms - are not trustworthy and have to be repeated.

The diurnal variations are recorded by a fixed magnetic base station. Usually, the daily variations are recorded by rather simple (cheap) instruments which can have a significant noise, noise which should not be migrated into the production data. Therefore, base station data have to be de-spiked and low-pass filtered. The filter lengths depend on the quality of the recorded data and on the distance between the base station
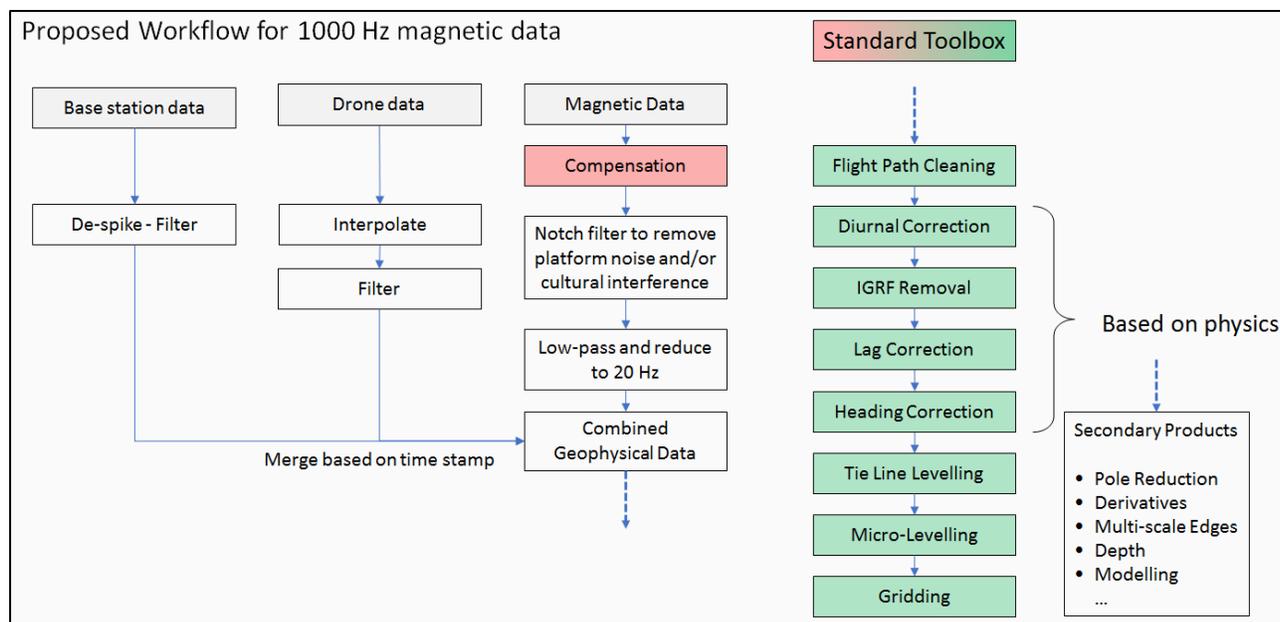
Figure 31   Proposed work flow for the processing of 1 kHz drone based magnetic surveys.

location and survey area. The reason for the latter is that high frequency diurnal variations as recorded by the base station may undergo phase shifts over longer distances.

11.2.1   Specification of base station data

The sampling rate of simple base station magnetometers is best set to between 1 and 10 seconds. Shorter sampling rates often increase the instrument noise and longer sampling may prevent correct filtering. The recorded data are then de-spiked using a non-linear (Naudy) filter followed by a standard low-pass filter. Filter lengths of 10 to 60 seconds are common. The base station data have also to be checked for anomalies caused by 'inquisitive visitors' of any kind. Affected parts have to be cut and interpolated.

The allowed diurnal variations are specified typical in the form of X nT over Y minutes (over linear background). Common specifications are 2 nT over 2 minutes, 5 over 5, or 10 over 10.

The base station should be located at a fixed position during data acquisition. Should a location change be unavoidable the DC difference of the magnetic field at the two locations has to be measured. If only a very few locations changes occur, the difference can be 'eyeballed' by comparing the grid from the production data corrected from one base station location with the grid from data corrected by the second base location.

11.2.2   Comment

Diurnal variations can also be removed by tie-line levelling, but this requires tight tie line spacing. (See for example Coyle et al, 2014).

11.3   Drone Data

The flight logs recorded during operation are referred to as 'Drone Data'. They comprise GPS and acceleration data as well as the recorded platform attitudes (pitch, roll and yaw) also known as 'Euler Angles'. Whether or not these data are required depends on whether the GPS unit linked to the magnetic sensor does record these data as well or not.

In case lines or parts of lines show elevated noise levels in the magnetic data, Euler angles can help to identify whether or not the noise is caused by strong platform manoeuvres. If yes, pitch, roll and yaw statistics can be used to identify possible re-flights and/or to apply corrections established during a test flight.

In older GPS units, the GPS signal is broadcasted only once a second, hence GPS related data have to be interpolated to the sampling rate used by the magnetic data logger. In most drones with more modern GPS units, the signal is broadcast at 10 times per second. Interpolation of the GPS locations to the magnetic data sampling rate can either be done by the flight log software in real time, or in post-flight mode.

Whether filtering of the drone data is required or not, is determined by their noise levels.

11.4   Magnetic Data

Magnetic sensors have always had high internal sampling rates, but the standard counters reduce the raw-raw data to sampling rates of 10 or 20 Hz. Recently, magnetic sensors are available that output the data at sampling rates of up to 1 kHz (or more), which requires some additional processing steps to be performed.

(Compensating the raw magnetic data for platform influences is described in Section 10.)

The acquired high-rate data allow for the application of notch filters, which can either remove platform noise of a specific frequency or cultural noise. Noise of a specific frequency present in the recorded data, can easily be identified by examining the power spectrum of a sortie. Then a notch filter has to be designed to remove the specific frequency band.

Note that culture interferences by active mining operations or electric railways can influence magnetic data up to a distance of 20 kilometres or more.

After cleaning the high-rate data the data can be reduced to a lower sampling rate in order to minimise the data volume (a 1 x 1 km survey flown at 20 m line spacing can easily produce 1 GB of raw data). A sampling rate of 1 kHz translates into a point-to-point distance of a few centimetres only, depending on survey speed. At say 5 m ground clearance the magnetic field is therefore vastly oversampled with a sampling rate of 10 or 20 Hz being absolutely sufficient to reflect the changes in the magnetic field.

Note, before de-sampling the data to a lower sampling rate they should be low-pass filtered with an appropriate filter length.

11.5   Data Merging

After all data have been corrected or 'treated' they have to be combined into one database. Base station and drone data will be merged with the (resampled) magnetic data.

The merging operation is based on the time stamp (and date if necessary). Hence it is of outmost importance that all data have the correct time stamp. One of the main functionalities of the GPS system, is to provide such a global time standard. Experience however shows that the GPS time stamp is sometimes 'manipulated', hence the times of all three data records should be thoroughly checked before survey.

However, the GPS signal is broadcasted once a second with the milliseconds required for 1 kHz data being interpolated via the internal clock of the data logger, which may not have the best accuracy. It can (and does) therefore occur that a one second record contains 999 records and the next 1001 or that duplicate time stamps are recorded. This might result in data merging problems.

11.6   Standard Toolbox

The following chapters describe the standard processing tools that have been applied to airborne magnetic data for decades. Note that not all of these processing steps may be necessary. Also, the order in which the various processing steps are undertaken can vary. Figure 32 gives an example of the processing chain. From left to right: Raw magnetic data, compensated data, diurnally corrected and IGRF removed data and final data after levelling and micro-levelling. (Note the small sharp anomaly in the centre west of the image is partially altered/reduced by micro-levelling.)
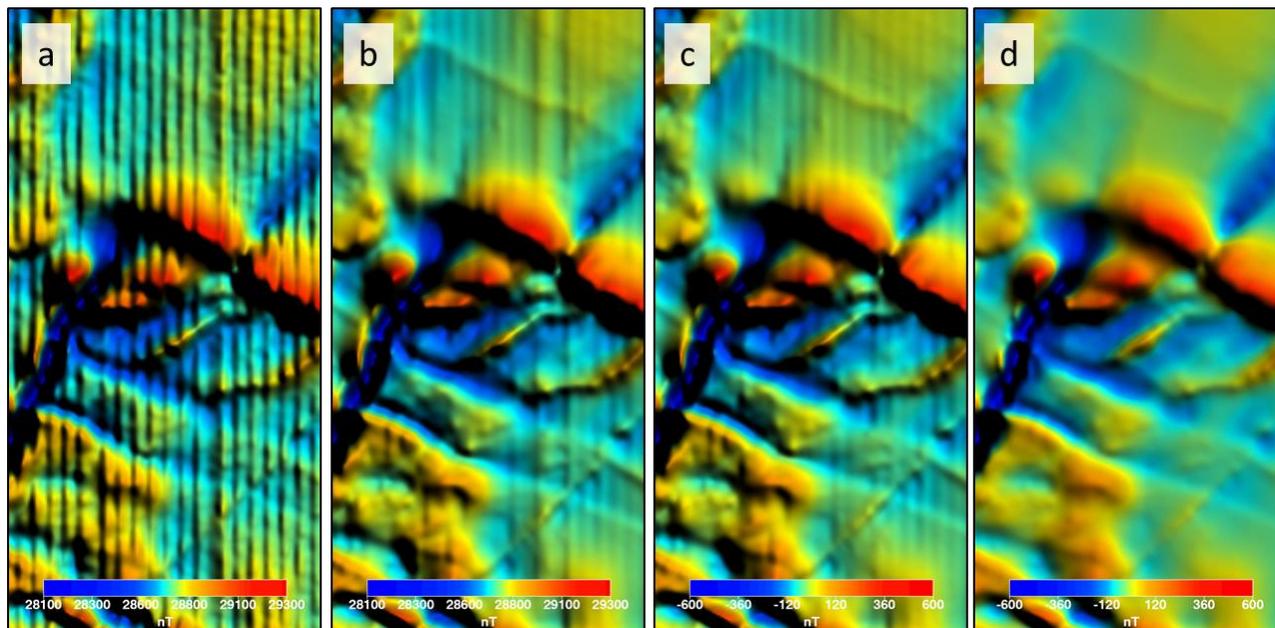
Figure 32   Examples of data improvement by processing.

(a) raw magnetic data, b) compensated data, c) after diurnal correction and IGRF removal, d) levelled and micro-levelled data.)

11.7   Flight Path Cleaning

The logging software of drone systems records all data from the start of a flight to the end, including ferries and turns. Both, ferries and turns, may not be flown at nominal survey height. Especially in turns the data can be affected by manoeuvre noise and, depending on the magnetometer used, data dropouts may occur.

Therefore, the production data have to be separated from ferries and turns, which are deleted. At the same time unique line numbers should be assigned to traverses and ties and each sortie will be given a unique flight number. Also, to be cleaned are overlaps where lines are covered by multiple occupations.

Flight path cleaning is usually a manual process but there is clever software that can do it automatically. Nevertheless, the results should them be imported into a geophysical processing package and checked visually. Figure 33 compares am undisturbed flight path with a flight path strongly affected by obstacles (radio towers). The flown flight lines are shown in grey with the clean lines in blue, nominal line spacing is 20 metres.

After the cleaning step, quality control (QC) channels will be calculated such as the 4th difference of the magnetic data as the main noise measure, point to point distance, survey speed, line separation etc. Another QC check that is recommended is the normalised 8th difference, because as drone surveys are flying lower,
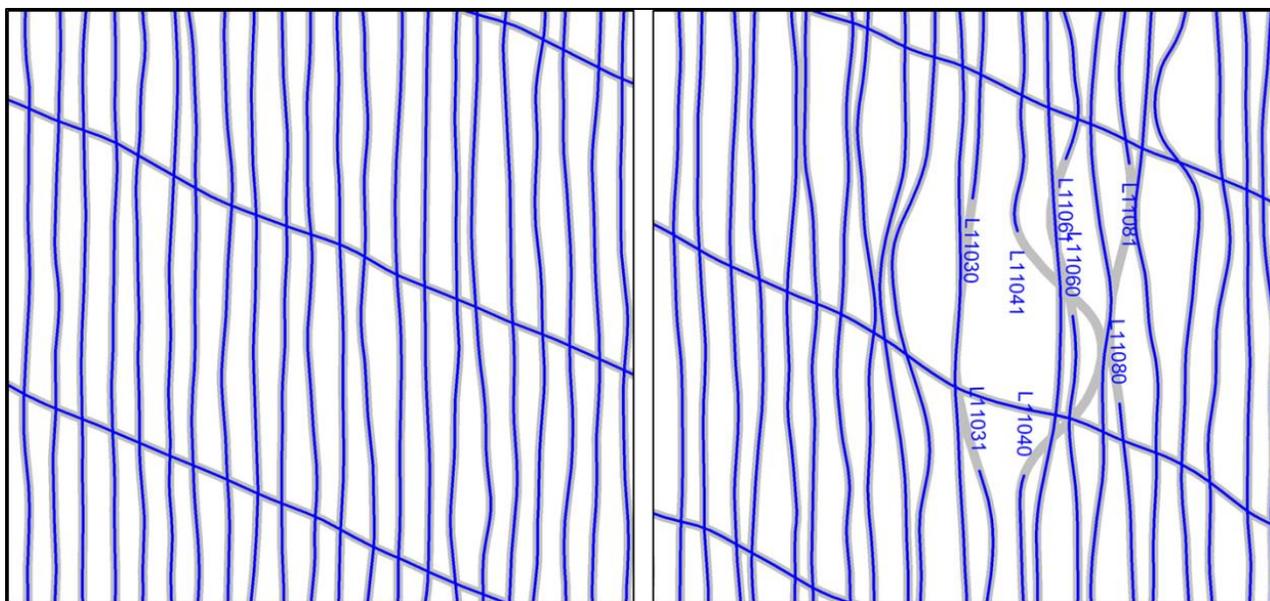
Figure 33   Undisturbed flight path vs a flight path affected by anthropogenic obstacles.
(Flown lines in grey and cleaned flight path in blue. 20 m line spacing.)

there is more short-wavelength geological signal which can still be present in the 4th difference (when generated as a grid/ image). The QC channels have then to be inspected to identify lines or parts thereof that have elevated noise levels, jumps or fail nominal specification in any way. This can be done semi-automatically by checking the statistics of the respective QC channel per line and/or by visual inspection.

11.8   Diurnal Correction

The recorded base station data are de-spiked and filtered, merged with the rover and subtracted from the production data. To maintain the absolute level of the production data a base value is removed from the diurnal variations, usually the average of the base station data. Note that the base level needs to be the same for the entire survey, unless the base station location is changed.

11.9   IGRF Removal

The International Geomagnetic Reference Field (IGRF) describes the ambient magnetic field. It varies spatially, including elevation, and in time.

For very small survey areas the spatial variations of the IGRF are almost negligible, but time variations should be taken into account. IGRF variations in time are also referred to as secular variations, implying a rather slow rate of change. In some parts off the world however, these 'secular' variations translate into more than 50 nT change per year or about 1 nT per week which can negatively affect the final product in case larger surveys are flown over a long time.

It is therefore suggested to calculate the IGRF for acquisition time and altitude and remove it from the diurnally corrected data. Do not remove the average IGRF after final processing; this could create problems when merging data from neighbouring surveys.

11.10   Lag Correction

The difference between the recorded platform position and the actual position of the magnetic sensor is referred to as lag or parallax. A lag mostly occurs as the distance between the navigational reference point (GPS antenna) and the magnetic sensor but it can also be caused by an electronic lag when the time it takes to record the data is larger than the sampling rate.

The lag is quantified by a lag test, which involves flying forth and back at low level over a sharp magnetic anomaly (railway line, bridge, hangar etc.). The recorded magnetic data are shifted with regard to the coordinates until the peak anomalies of both lines flown in opposite directions coincide. The lag test can be flown in any direction.

For drone operations the magnetic sensor is either mounted rigidly beneath the platform at a small distance or suspended on cables several metres below. In the first case the lateral distance between GPS antenna and magnetic sensor is very small; hence one would not expect any lag to occur. Suspended systems usually have their own GPS built into the magnetic sensor unit and should therefore have no lag either.

The Lag can be determined empirically to a relatively high accuracy from gridded data: Pick a sharp and strong anomaly running perpendicular to the traverse direction, if its crest appears ragged with 'saw-teeth' spaced at line separation one has to correct for lag. Apply a lag of X fiducials, re-grid and compare the raw to the lag corrected grid. Iterate the lag correction until the crest of the anomaly is smooth.

11.11   Heading Correction

A heading correction is required in case the platform compensation does not remove all DC effects.

The parameters for the heading corrections are obtained in a test flight taking the form of a cloverleaf. The cloverleaf is flown in the cardinal survey directions and the correction values for each direction are obtained from the central crossover point as the difference between the directional reading and the overall average of the four occupations. Note that the magnetic data have to be diurnally corrected to obtain correct heading values. Refer also to the repeatability test where the heading correction can be obtained (Section 9.1; Figure 24)

The heading correction is applied to the production data based on the actual bearing of the platform or sensor along the lines. Corrections for bearings not exactly following the cardinal survey directions are calculated by interpolating between the four directional heading values.

Note: The heading test should be undertaken in a magnetically quiet environment. Manned aircraft simply fly the heading test at high altitude, usually 3 km height (since above this height the aircraft must be equipped with oxygen supply). Such heights are not achievable with a drone platform; hence care has to be taken to fly the test over magnetically inert geology (refer to the repeatability test - Section 9.1; Figure 24).

For UAV copter platforms the question arises which 'bearing' the heading correction should be based on: The 'Track' direction recorded by the GPS position or the 'Compass' data recorded by the GPS fluxgates (if delivered). This has to be considered carefully since 'Track' and 'Compass' directions can differ significantly.

11.12   Tie Line Levelling

Despite all efforts to correct the recorded data based on principles of physics there usually are still errors in the data which occur due to a variety of influences, data errors, drift, different bases station locations etc. The main source of line-to-line differences however is that neighbouring lines are flown at different altitudes.

Tie line levelling tries to remove these as well as possible, in order to produce a consistent high-quality grid for interpretation. All tie line levelling methods are based on the difference between traverse and tie readings at crossover points, the so called misclosures or misties. Crossovers and misties have to be calculated first. Filters may be applied for misclosure calculation to avoid unrealistic correction values from outliers in the data. The crossover database also stores the gradients of the data which may be used to exclude crossovers in high gradient areas where smaller navigation inaccuracies can lead to larger misclosure values.

11.13   Zero Order Levelling

The simplest and least obtrusive levelling method is zero order levelling; entire lines are simply DC shifted by the average of their misclosures. One can only shift the traverses to the ties, or do a full iteration by shifting the ties to the traverses first and then shifting the traverses to the corrected ties. DC shifts in potential fields do not affect the anomalous or relative values of the data along each line.

11.14   Polynomial Levelling

The classical method in tie line levelling is polynomial levelling which involves the calculation of corrections as least squares fit along flights, tie lines and traverses. These curves plot misclosure either spatially or against time. Again, one can level traverses to ties only or first level ties against traverses and then traverses against the corrected ties. A more complete polynomial levelling regime would consist of:

- Level all ties to the principal tie (which has to be carefully selected) assuming that it has no error.

- Correct each flight assuming that the tie lines are correct. This step is sometimes described as 'Drifting the acquisition lines by flight to the tie lines'.

- Correct the individual acquisition lines assuming that the tie lines are correct; this can be described as 'Drifting the acquisition lines individually to the tie lines.

- Correct the individual tie lines again assuming that the acquisition lines are correct. This is an optional step intended to remove any last residual errors.

The above steps can be iterated a couple of time, but too many iterations can be harmful to the data. Further, if the above procedure is undertaken after the crossovers are sorted in time, as opposed to spatially only, potential drift in the data is removed. Diurnal variation can be seen as 'drift' and can be removed by tie line levelling. To do this accurately however tight tie line spacing is required (see for instance Coyle et al, 2014.)

Note: All steps in this levelling regime can have levelling parameters applied individually to each step. Parameters include the window width, e.g., the number of crossovers before and after the current crossover which are taken into account for polynomial correction, the width of the smoothing window and lastly the degree of the applied polygon. The parameters have to be carefully adjusted to the data quality and the magnitude of the misclosures and the polynomial degrees are best kept as low as possible to avoid overcorrection.

11.15   Loop Level

The loop closure method (Green, 1983) repeatedly adjusts the signal values in the acquisition lines to minimise overall misclosure for the dataset and distribute the residual errors.

The misclosure of a target crossover is examined including its four neighbours along the traverses and ties. First, the correct value for each crossover is estimated as the mean of its two signal values, and then the

proposed correction of the target crossover is adjusted using the current estimates for the neighbouring crossovers. After calculating a new current estimate for the target crossover, the next crossover will be the target crossover and the same adjustment is performed. This is continued until all crossovers are adjusted.

The same process is then applied to all crossovers in reverse order. This two-way pass makes up one loop closure iteration. Iterations are repeated up to a specified number or when the average change for crossovers falls below a specified level.

Practically, the loop level method reduces all misclosures to zero. Loop levelling is not frequently used in airborne magnetics because it tends to overcorrect. For datasets with large differences between traverse and tie readings, it may however be useful.

11.15.1   Warning

Tie line levelling is the single most important source of long wavelength artefacts or inaccuracies.

11.16   De-corrugation / Micro-levelling

De-corrugation or micro-levelling is a technique that can remove line parallel striations which remain after tie line levelling.

De-corrugation isolates anomalies along the traverse line direction by applying a low-pass filter along this direction and a perpendicular high-pass filter to the grid produced from the tie-line levelled data. Common filter settings are a low-pass filter length of twice the tie line spacing and a high-pass filter length of twice the line separation. Shorter wavelengths in the acquisition line direction or longer wavelengths in the tie line direction comprise a high risk of eliminating real anomalies. Some de-corrugation software also allows restricting the amplitude up to which corrections are detected and applied.

Best de-corrugation results are achieved by using space domain or convolution filters because they do not require all the preparatory steps required for Fourier operations. The latter can result in edge inaccuracies due to the de-trending and filling steps especially in odd shaped grids. Nevertheless, results similar to the de-corrugation process described may be achieved by the application of directional cosine filters in the frequency domain.

Both techniques can output either a correction grid (residual) or a corrected grid. The de-corrugated grid has then to be migrated back into the line database, a process referred to as micro-levelling. Again, filters can be applied in order to avoid ringing in the vicinity of small but strong anomalies.

11.16.1   Caveat

De-corrugating / micro-levelling geophysical data can remove 'geology'! Refer to the small sharp anomaly in the centre west of the image of Figure 32(d), which is partially altered/reduced by micro-levelling. Regardless of which de-corrugation method is used, one therefore has to always visually inspect the correction grid to determine whether it contains structures that could be related to geology. In such case, the filter parameters and the maximal correction amplitude have to be adjusted.

11.17   Gridding

Most interpretations of airborne geophysical data are based on grids, not line data.

A grid is a geo-located raster dataset that contains information fully covering the survey area. Whereas most techniques used in remote sensing or aerial photography already acquire complete coverage, airborne

geophysical data are measured along profiles and the profile data have to be 'converted' to emulate full coverage. This conversion process is called gridding. An example of the original line data and the resulting grid is shown in Figure 34.

Gridding interpolates all gaps between the lines to achieve complete coverage. This is not necessarily a trivial task, because one has to interpolate highly spatially sampled data along the lines over the relatively large distances between lines. Potential field data however, facilitate the gridding process by the fact that neighbouring data are related to each other and the potential field of a given assembly of sources has a minimum possible curvature thereby aiding the interpolation process. (Gridding data that can randomly vary from one point to the next, such as radiometric data, is different, because the interpolation process 'assumes' a continuity which may not be there.)

Aeromagnetic data are normally gridded to a cell size of a 4th or a 5th of the nominal line spacing. Gridding to a larger cell size will unnecessarily smooth the data whilst gridding to smaller cell sizes always has the risk of introducing gridding artefacts. Gridding is also the reason as to why overlapping lines have to be cropped carefully because data-points with slightly different values which are very close to each other can produce unrealistic steep gradients in the interpolation process, an effect called 'grid-ringing'.

Note: Any gridding process is a (serious) manipulation of the measured data. To judge whether a given grid is a good representation of the measured data one always has to look at both, line data and the grid.

Various gridding methods were developed to support different data acquired by different sampling schemes and at different sampling densities as shown in Table 15**.**

Table 15 Gridding methods.

GRIDDING METHOD	GRIDDING METHODOLOGY
Bi-directional spline (line data only)	Spline curves are fitted along and across lines. Measured gradients can be incorporated into the gridding process.
Minimum curvature	Fitting a 2D minimum curvature surface to the data.
Nearest neighbour	Simple triangulation process.
Boxing	The value of each cell is calculated from the average of its neighbours.

There are other gridding methods like Variable Density Gridding, which is designed to deal with data with variable resolution such as marine surveys or ground gravity data, or Kriging which tries to 'predict' a grid from sparsely sampled data based on geo-statistical techniques. The most common gridding methods used for total field airborne geophysical data are bi-directional splining and minimum curvature.

In addition to choosing the basic gridding method and the cell size one has to define a variety of parameters which can have a significant influence on the resulting grid:

- Spline type, e.g., linear, BiCubic or Akima splines
- Size of the minimum curvature kernel, usually 5x5 or 7x7 cells
- How to treat the data within one cell, e.g., average, closest, minimum etc.
- How to treat distance between data points and cell centroids, e.g., unity, inverse distance, square root
- Tension splines might be used in minimum curvature refinement (dangerous!)
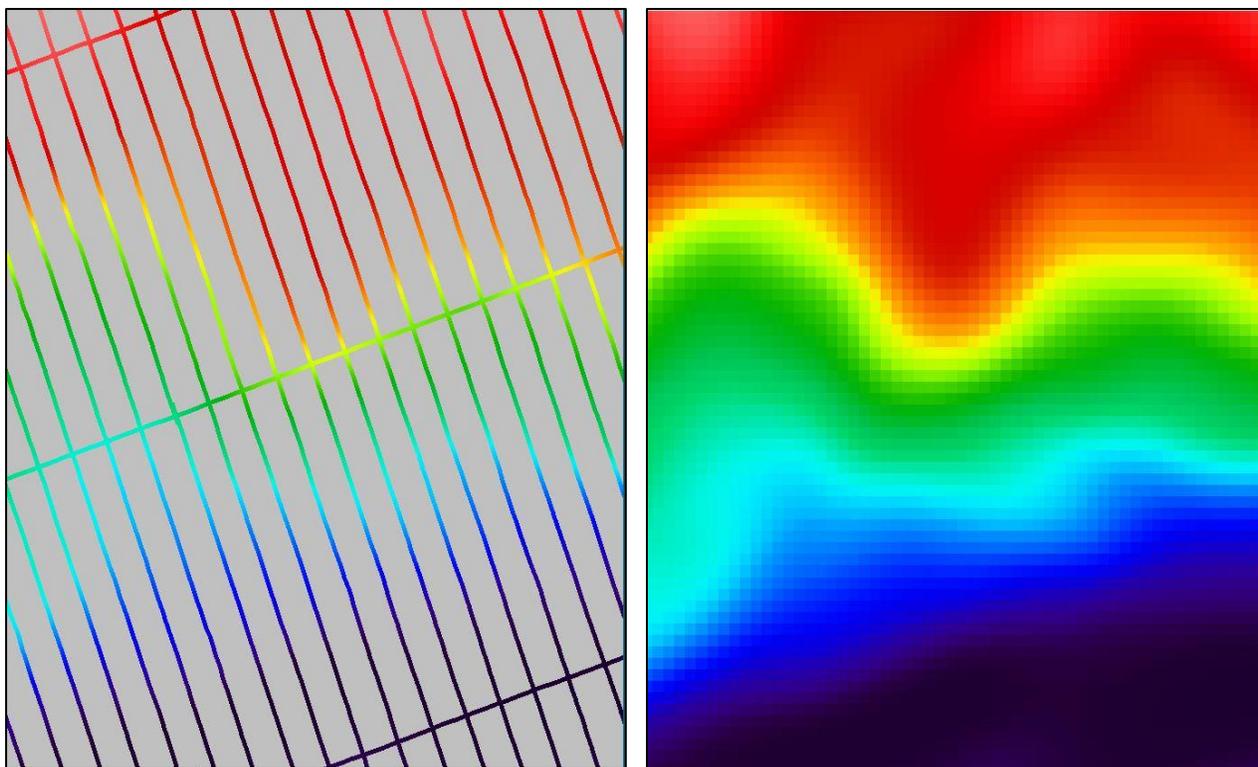
Figure 34   Gridding oblique line data.

When gridding oblique line data, it is advisable to rotate the grid so that grid north is aligned with the nominal line direction. The reason for this is that for oblique lines the ratio between line spacing and grid cells is distorted by a factor of up to 1.4 ($\sqrt{2}$) for line directions of 45°.

A grid (or raster image) is always arranged as square (or rarely rectangular) cells in north south and east west direction. Should the grid be rotated the actual dataset is still the same with the rotation angle supplied in the metadata. When imaging rotated grids the software reads the rotation angle and resamples the input grid into square pixels oriented East and North.

12.   IMAGING UAV MAGNETICS DATA

12.1   Introduction

After the hard work of collecting and processing high-quality magnetic data, the data needs to be presented as images suitable for human or machine interpretation. Such images can be as simple as profile plots, or as complicated as N-dimensional volumes. Whatever the imaging requirements, there are choices to be made. Some choices will make subsequent interpretation easier, whilst others may cause important information to be misunderstood or overlooked. Figure 35 shows examples of magnetics data displayed in different presentation modes.

12.2   Grids vs images

Grids are arrays of numeric values. Images assign colours to grid values to assist with geophysical interpretation.

Contour maps can also be used to display grid information. These can sometimes be useful when comparing one set of grid values with another set, or when looking for subtle features.

12.3   Choice of colour table

Colour tables are used to map grid values to output images. They may be monochrome, multi-coloured, symmetric or cyclical. Perceptually uniform colour tables are highly recommended compared to other common tables which over their range may, have a very uneven perceptual contrast potentially resulting in visual "flat spots" (i.e., resulting in hiding of a feature(s)), or have a discontinuity that induces the display of a false feature (see Kovesi, 2015). Figure 36 shows examples of magnetic data displayed with and without perceptually uniform colours. Some interpreters use different colour tables for different product streams (e.g., geophysics, terrain, satellite imagery). Personal preference and ease of communication to colleagues are important considerations here.

12.4   Choice of colour stretch

The colours displayed in an image can be linked to the underlying grid values in different ways to emphasise different features of the source grid. Common colour stretches include linear (often used to display all grid values with equal prominence), equal area (often used to spread the colour table equally between the grid values) and normal distribution (often used for grids uniformly distributed around a central value).

12.5   Directional shading

Directional shading (sun-shading) can be very useful to highlight geophysical features with a particular orientation. By implication, it will also draw your eye away from geophysical features with other orientations, so should be used with care.
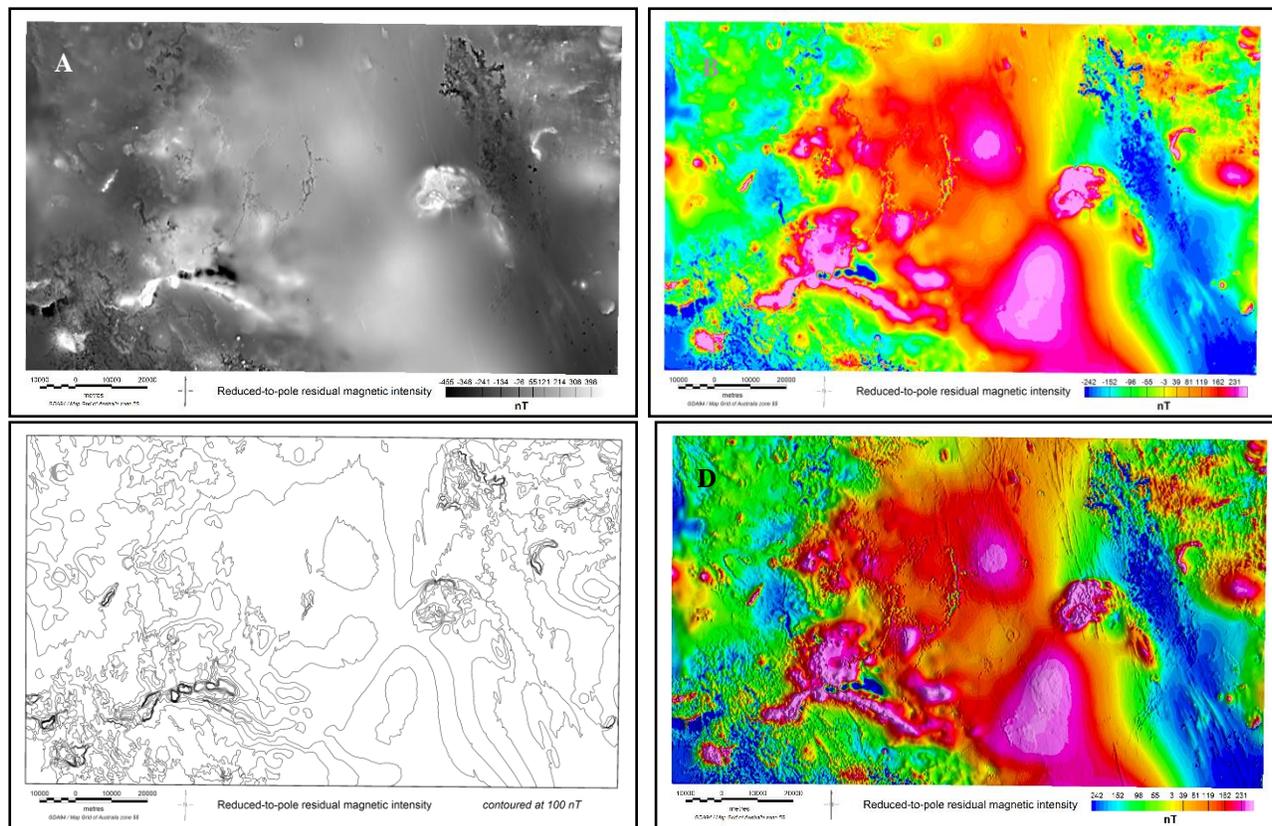
Figure 35   Geophysical magnetic data imaged in different ways to emphasise specific features.

(Examples shown are (A) linear monochrome (greyscale), (B) equal-area polychrome (rainbow), (C) contoured and (D) sun-shaded magnetic images from an airborne survey in Queensland, Australia (data courtesy of Geoscience Australia).

12.6   Combining images

Typical methods of geophysical image combination (see examples in Figure 37) include:

- Multi-plot: one or more sets of point or line data are overlain on a grid image

- Pseudo-drape: a grid image is overlain on a relief surface created from another grid image

- Ternary imaging: three images are combined using the RGB/CMY channels of the display sensor or print device

- 3D imaging: multiple overlapping images and data sets are simultaneously displayed and variably thresholded in 3D space.
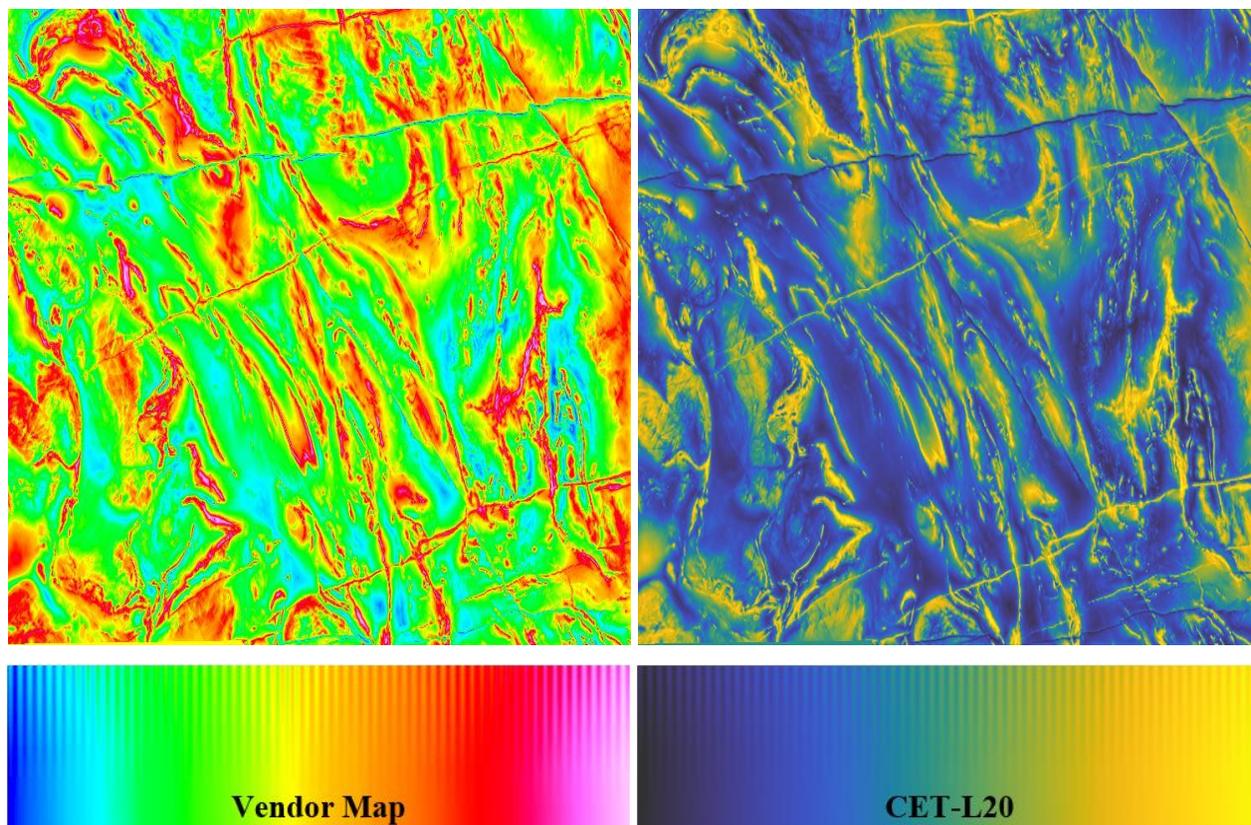
Figure 36   Comparison of default (left) & perceptually uniform colour tables (right).

(On the left is the result of rendering an aeromagnetic image of the Yilgarn region in Western Australia with the default colour map of a widely used geophysics package. On the right is the same data rendered with the perceptually uniform colour map CET-L20. The vendor map exhibits a large perceptual dead zone at green, a smaller dead zone at red, and false features at cyan and yellow." (Copied from Kovesi, 2015, https://colorcet.com. Accessed 9 Oct. 2022).
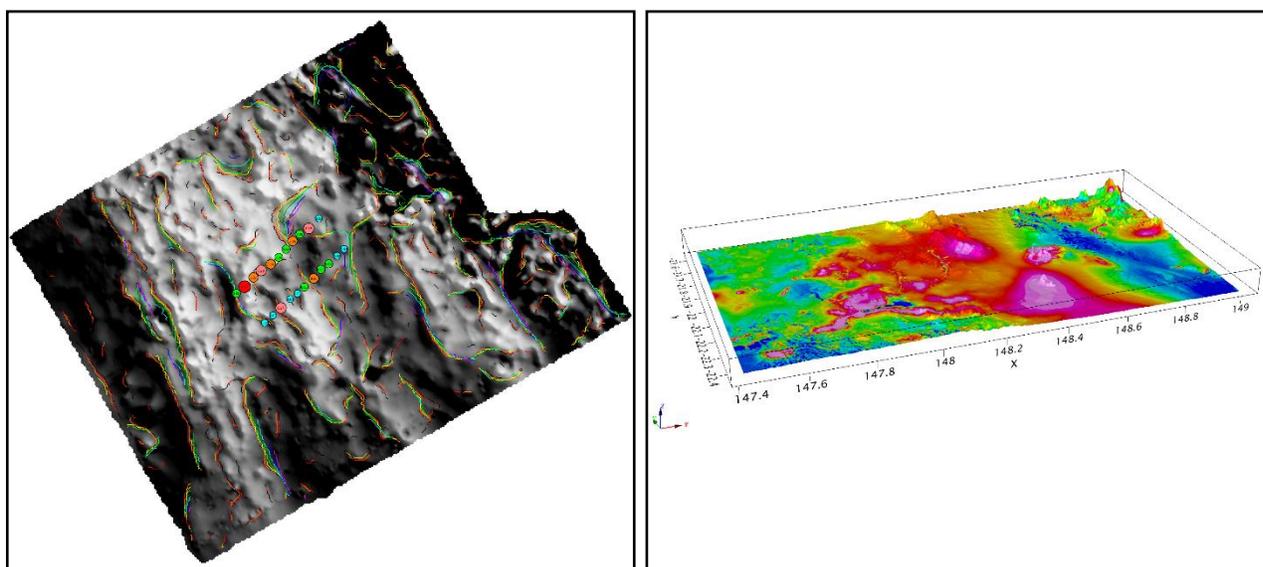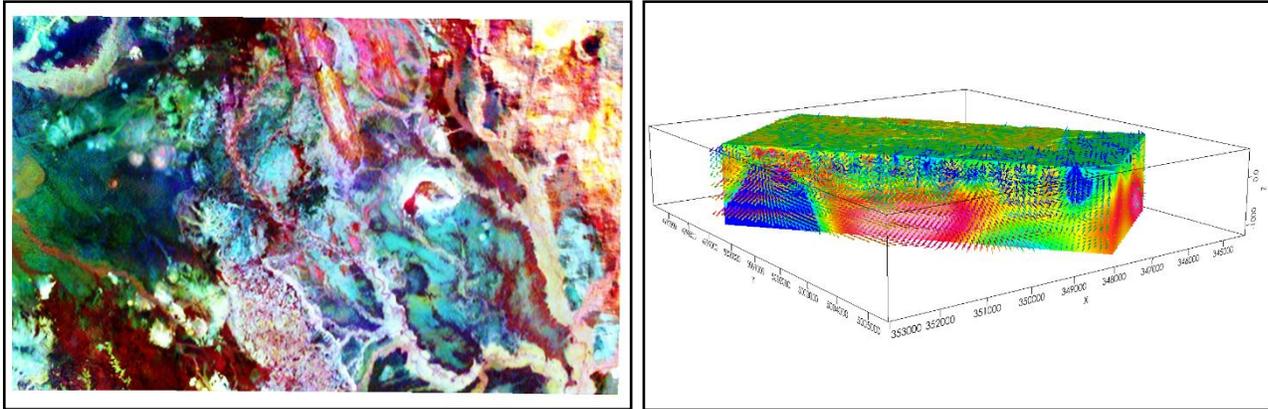
Figure 37   Geophysical magnetic data imaged in different ways to emphasise specific features.

((A) Multi-plot (B) Pseudo-drape (C) Ternary imaging (D) 3D imaging)

13. INTERPRETATION OF UAV MAGNETICS DATA

13.1 Introduction

Interpretation is the process of characterizing one or more parameters of the targeted sources, such as spatial position, depth, shape or magnetization, from the recorded magnetic field.

Two major challenges for interpretation are the dipole nature and inherent ambiguity of the magnetic field (Figure 38). A "magnetic signature" always has both a positive and a negative part (dipole) that are most of the time not symmetrical. These are the result of a complex interaction between the parameters of the source and that of the ambient magnetic field, such that an infinite combination of these parameters can give the same result (ambiguity).
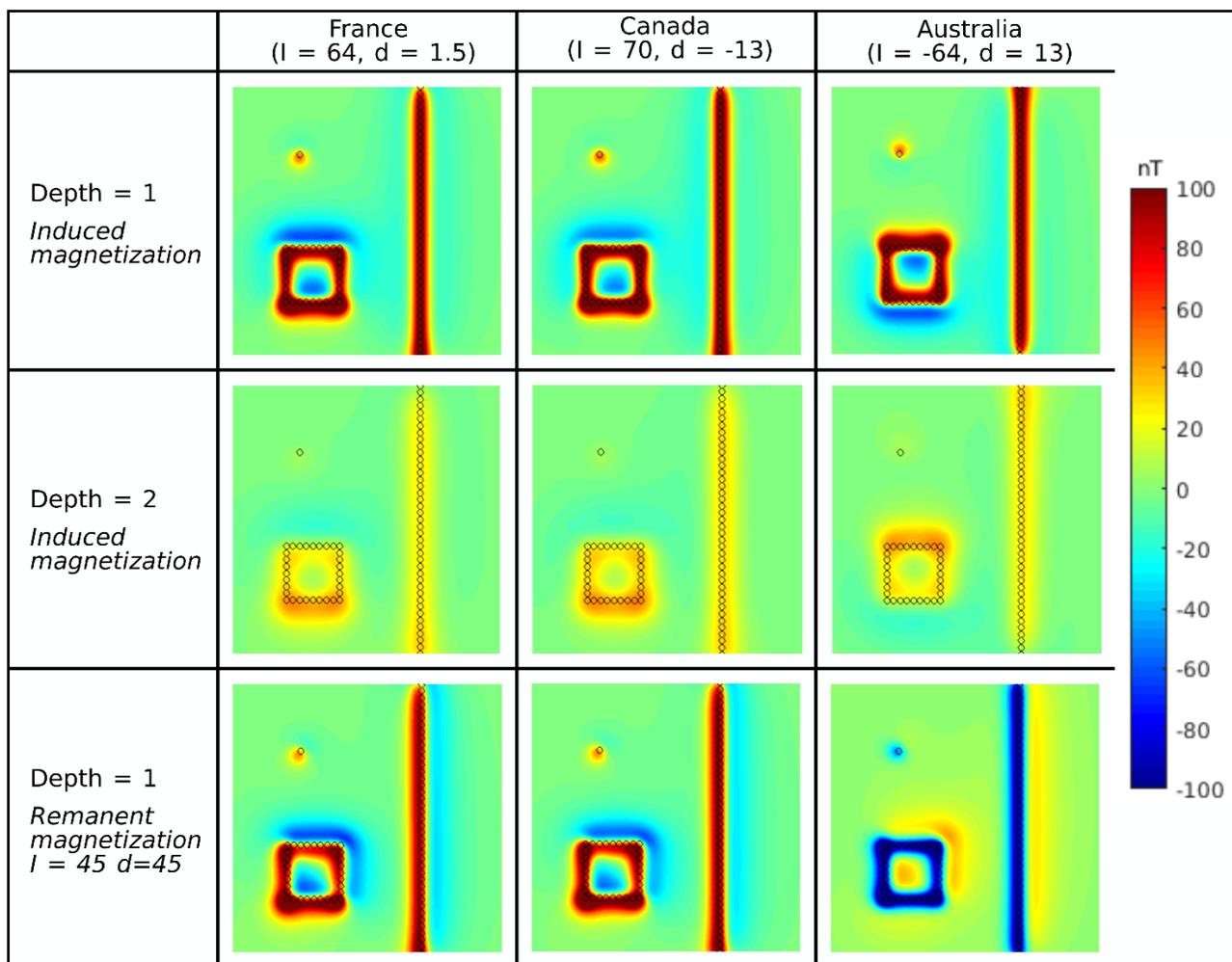
Figure 38   Illustration of the impact of the parameters of the sources (circles) on the magnetic anomaly: depth, shape, place on earth and remanent magnetization.

NOTE: I = magnetic inclination, d = magnetic declination, depth in arbitrary relative units.

In general, we mitigate these challenges by (1) applying suitable mathematical transformations to derive geometrical parameters of mapped objects and (2) by enforcing sensible modelling constraints to ensure geological integrity.

13.2   Magnetic anomalies

The magnetic field is a vector; it has both magnitude and direction as illustrated in Figure 1. Although some systems exist to record one or all of the orthogonal components of this vector field, many other systems simply record its scalar amplitude (or intensity). The output we work with for interpretation is often the total field anomaly, which is the difference between the magnitude of the measurements (ambient field plus the anomalous field) and the magnitude of the regional magnetic field (or the ambient field as given by an IGRF from the global model). NOTE: This computation (removal of the ambient field, the IGRF), gives a value which is an approximation of the projection of the magnetic field of the sources (the anomalous field) onto the regional magnetic field (Blakely 1995) and we will use it as such in further calculation. This approximation is correct only if the anomalous field is small compared to the regional (ambient) field. This is usually true except very close to extremely magnetized objects.

13.3   The importance of terrain

A terrain DEM is an important geophysical data set. It often gives clues to the underlying geology. It also helps develop exploration strategy, particularly in mountainous, boggy or otherwise challenging operating environments.

As discussed in Section 7.3 and illustrated in Figure 13, drone-borne magnetic surveys may be flown at fixed barometric/GPS height, at fixed height above terrain (which is always approximate, due to safety and operational considerations), or on a pre-planned loose drape. Each choice has its own advantages and disadvantages.

13.4   1D, 2D and 3D Interpretation

Different techniques with different degrees of automation or quantification can be used alone, in combination, and/or iteratively, to estimate different parameters according to context, application objectives and previous knowledge of the sources.

As measurements are commonly acquired along parallel profiles following terrain, interpretation techniques can be divided into three main groups: -

- Profile based interpretation (1D-space): almost continuous signal allowing us to assess the most subtle variations and shortest wavelengths, but sensitive to lateral effects (sources offline and/or not perpendicular to the profile might be hard to interpret). This profile interpretation approach ignores offline magnetic effects and assumes linear geology perpendicular to or at a known angle to the line direction.

- Grid based interpretation (2D-space): allows the assessment of the anomalies, and thus the sources, in both X and Y directions, but the gridding process smooths out the shortest wavelengths indicative of near-surface sources (e.g., surface magnetic objects, UXO, etc.) and heavily interpolates between profiles. It is also complicated to interpret contacts that change with depth (such as non-vertical limits).

- Voxel based interpretation (3D-space): allows the assessment of the sources with depth, but requires heavy computing power and/or good *a priori* knowledge of the sources to be geologically plausible/relevant/possible.

13.5   Forward modelling, inverse modelling and field transformations

The different interpretation techniques can also be divided into three categories by activity: -

- Forward modelling assumes the following steps: develop an assumed geologic model, compute its expected anomaly and compare it to the observed magnetic anomaly. The parameters of the model can then be modified until the results fit with the observations. Unfortunately, it can require a lot of iterations and a fit does not mean the results are correct due to the non-uniqueness (ambiguity) of the solution mentioned above.

- Inverse modelling allows computation of: parameters of the sources directly from the measured data with some assumptions (i.e., constraints) about physical properties and/or geometries of the source. The main difficulty is to get enough *a priori* information on the sources to have a well constrained problem.

- Field transformations comprise of: different techniques that are used to modify the signal according to potential field theory to emphasise certain parameters and attenuate others with few *a priori* assumptions. One must be prudent, as such transformations can mask some of the information or lower the signal/noise ratio.

13.6   Computation in the spectral domain

A good number of the described techniques cannot easily be computed in the spatial domain but only in the spectral (i.e., frequency) domain, i.e., the signal is synthesized by an infinite sum of weighted sinusoid (or periodic) functions. In other terms, the magnetic signal is transformed to be expressed not as a function of distance but as a function of wavelength through a Fourier transform (Figure 39). A consequence of Fourier transformation is that signal with a wavelength less than twice the sampling distance (distance between samples along a profile or between nodes in a 2D or 3D grid) is not accurately preserved, and that an incomplete anomaly at the border of a profile or grid (i.e., only part of the positive and or negative part are sampled) cannot be properly transformed and might lead to inaccurate results.

13.7   Specificities of drone-borne data

Compared to airborne and ground-based data, drone magnetic data has specific advantages to provide a high range of possibilities for survey design, altitude, resolution that can be driven by the interpretation objectives and not the technical limits. Disadvantages include limited payload, low endurance, and currently restrictive operating legislation. It is a fact that drones are filling the gap between different scales of measurement with their own different communities, guidelines and specificities. That said, we must always be careful when using interpretative tools that are common in ground or traditional airborne magnetics, that these tools meet requirements of drone magnetic data.

The following sections present an overview of the most common tools for drone-borne magnetic data interpretation. The list is not meant to be exhaustive, as specific tools could be designed and adapted for every survey according to the objectives and environment.
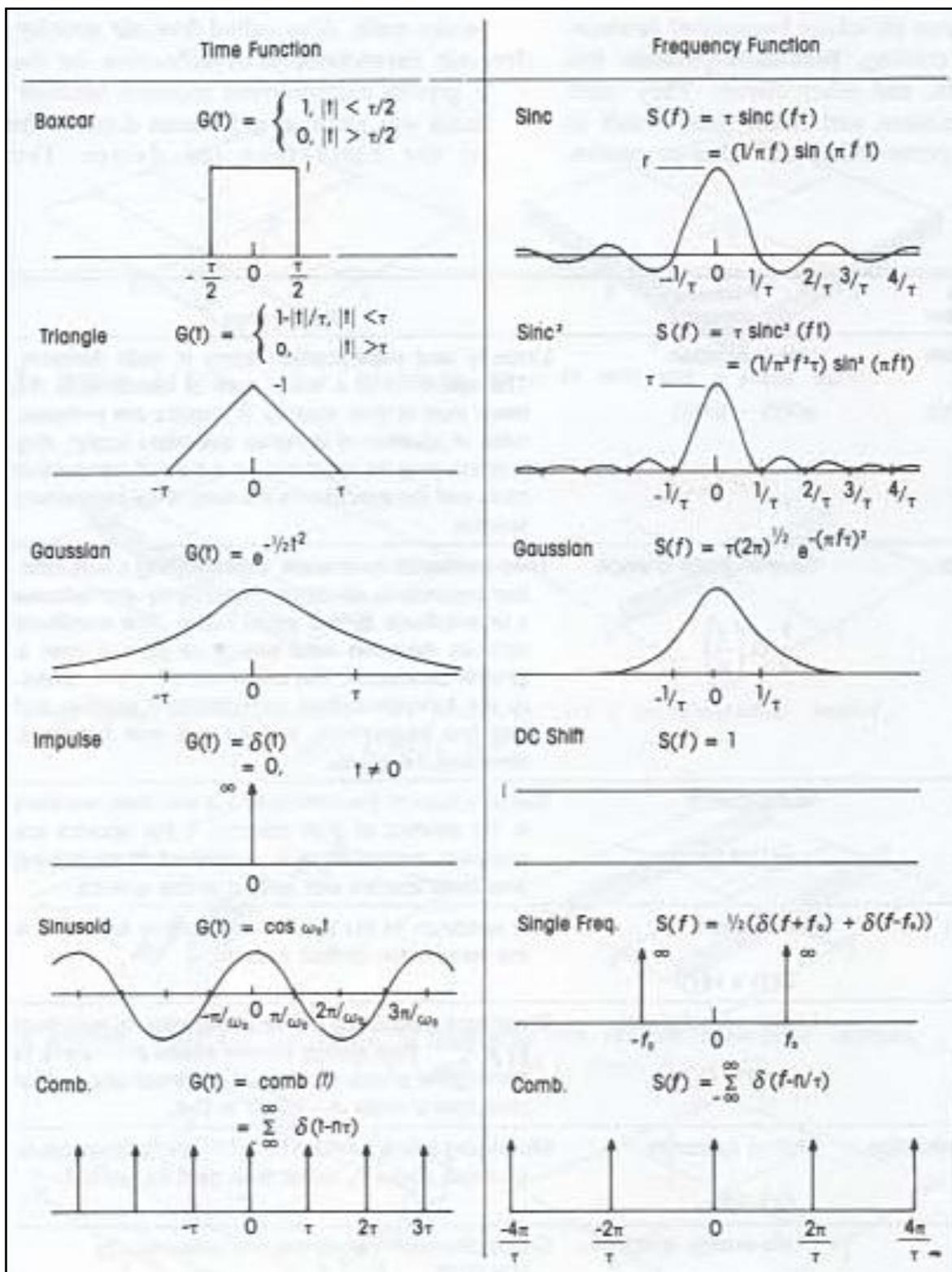
Figure 39   Fourier transform pairs.

(Copied from Sheriff, 2002).

13.8   Profile-based interpretation (1D data space)

Profile-based interpretation is less popular now than in the past, due to the advent of powerful computers capable of processing and imaging large 2D and 3D data sets within realistic timeframes.

Profile-based interpretation can nevertheless still be useful, for example during survey design when an approximate idea of the measured outcome is sought, as well as when modelling targets or horizons for which existing geological or seismic 2D models are already available.

Several "rule of thumb" depth estimation techniques, have been developed for magnetic profile data. These are slow to implement for large data sets, and need to be correctly applied (Atchuta Rao & Ram Babu, 1984).

More analytical 1D depth estimation techniques, including Werner Deconvolution (Hartman et al, 1971) and Euler Deconvolution (Thompson, 1982), can also be used.

13.9   Available 1D profile interpretive modelling software

Software packages such as Intrepid, ModelVision, Oasis Montaj, and Potent all provide interpretive modelling capabilities for 1D magnetic profile data.

13.10   Grid-based interpretation (2D data space)

Grid-based interpretation processes detailed below include:

- Lineament analysis
- Continuations
- Reduction to the pole
- Spatial Derivatives
- Analytic signal
- Frequency filtering
- Pseudo-depth slicing
- Depth estimation
- Forward and inverse modelling

13.11   Lineament analysis

One of the simplest yet efficient methods to interpret data is to point out graphically, anomalies forming lineaments. It does not require any *a priori* or knowledge on the sources. The pointing is usually done between the positive and negative maxima. The method does not give the accurate position of the source, but it indicates quite fairly that a contact of the approximate orientation is in the vicinity.

13.12   Continuations

As a consequence of Laplace's equation, it is possible to estimate the anomalies at another elevation than the elevation of the survey (Henderson & Zietz, 1949). This procedure, called continuation, can be done using different methods and can be in both downward and upwards directions (Figure 40). Downward continuation must be used carefully because it is prone to instabilities and amplifies the noise of the original data. Upward continuation acts as an attenuator of the signal and can be used to smooth out the shorter wavelengths (hence the shallower sources and noises) and target the main sources (e.g., deep geological features).
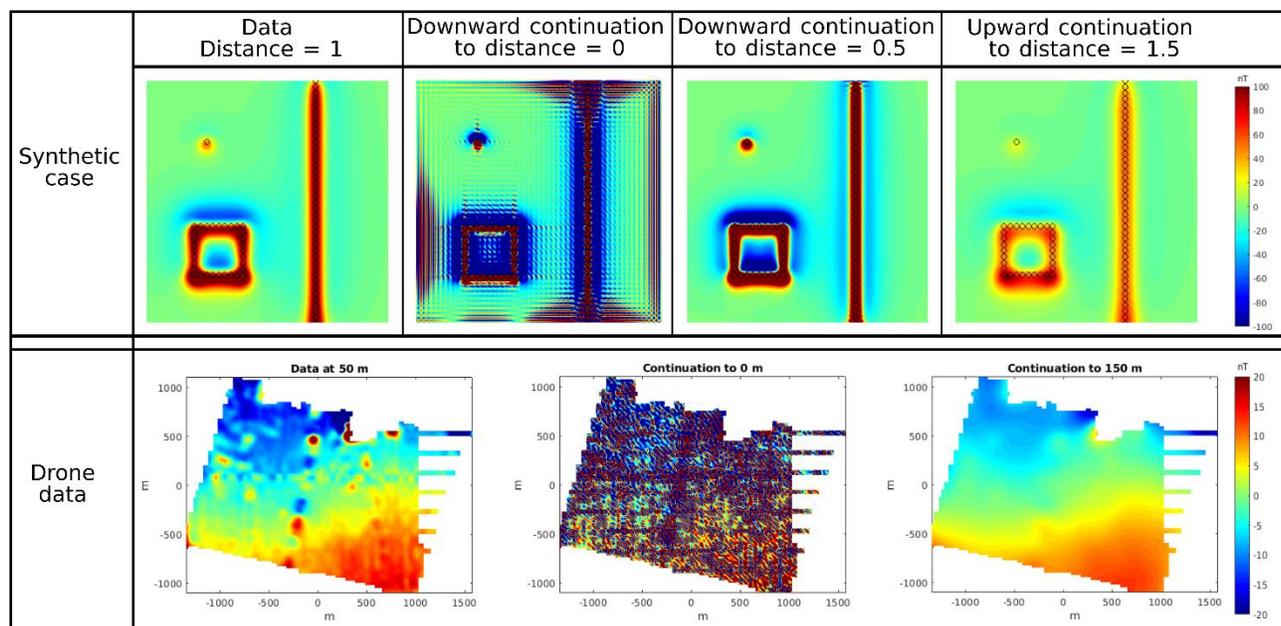
Figure 40   Illustration of the effect of upward and downward continuation on a synthetic case.

(Top, inclination = 64, declination = 1.5, only induced magnetization and Bottom, on real drone borne data (Rhine valley, France, survey 50 m above ground level): data at 50 m show the effect of different geological features, a N010 train line and a N090 power line, continuation to 150 m highlights the deep geological features, and continuation to 0 m (ground level) shows only noise)

13.13　Reduction to the pole

As seen before, magnetic anomalies are usually non-symmetrical, and one of the common issues in interpretation is to locate the sources precisely. A solution is the reduction to the pole (RTP) transformation that computes the signal as if the regional field and magnetization of the sources were vertical, i.e., a magnetic inclination of 90° (Baranov, 1957). As a result, the position of the sources is indicated by the maxima of the anomalies (Figure 41). In regions with low magnetic inclination (i.e., the ambient field is closer to horizontal direction than to vertical one) the reduction to equator (RTE) is used instead.

	Data	Reduction to the pole (RTP)
Induced magnetization I = 64, d = 1.5		
Remanent magnetization I = 45, d = 45		
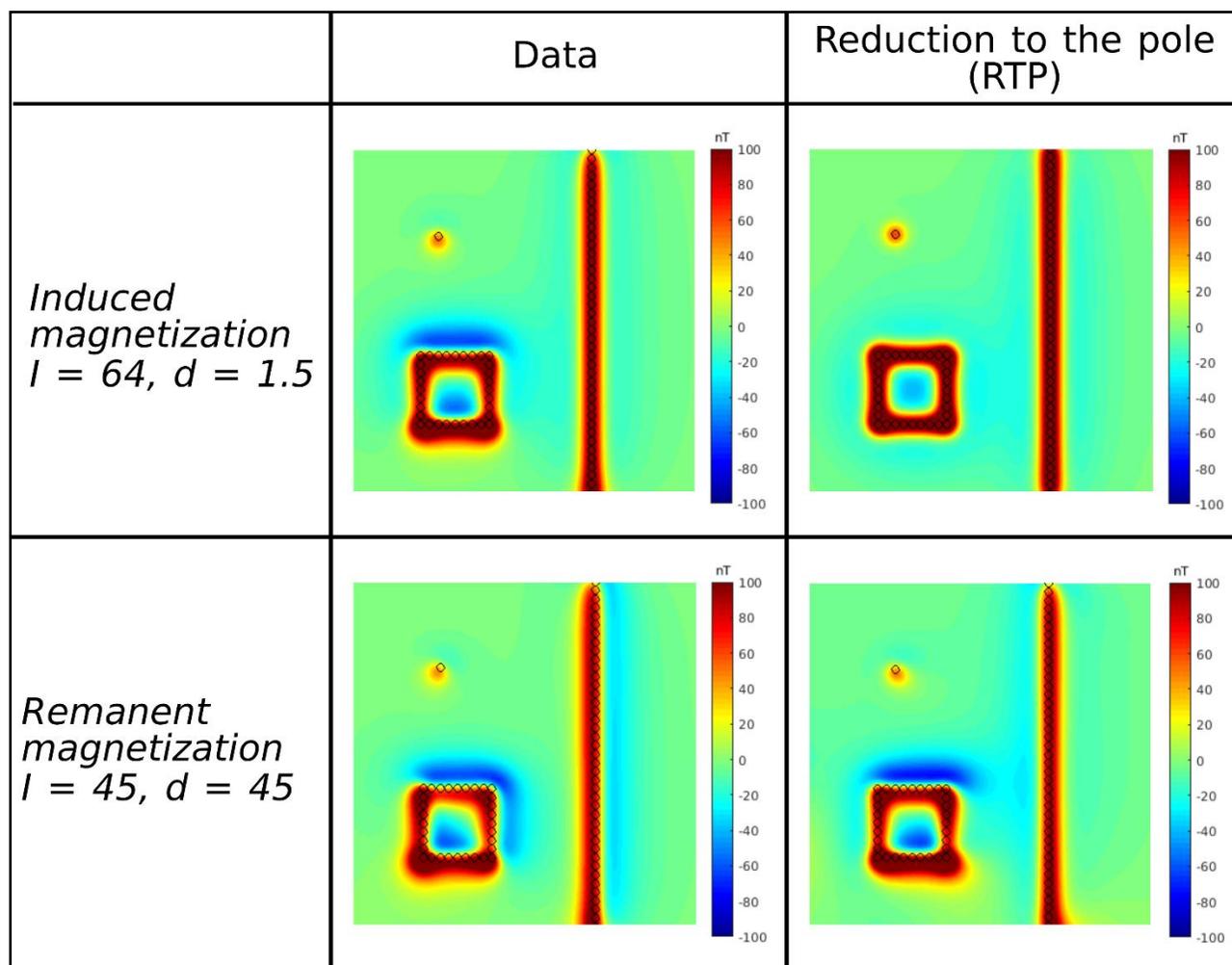
Figure 41　Illustration of the effect of reduction to the pole on a synthetic case.

(Top: induced magnetization. Bottom: remanent magnetization. Regional field inclination = 64, declination = 1.5)

To make the computation, the direction of the regional field and of the magnetization of the sources must be known. The direction of the regional (ambient) field is easily reachable by using the International Geomagnetic Reference Field (IGRF). Usually, the magnetization direction is set to be the same as the IGRF (i.e., only induced magnetization, or remanent magnetization in the same direction as the ambient magnetic field). If the sources present remanent magnetization in another direction/s, then the results of reduction to the pole can be unsatisfactory and misleading. A way to easily detect a problem on a reduction to the pole is to check for the presence of non-symmetrical anomalies on the output image.

13.14   Spatial Derivatives

Vertical and horizontal derivatives can be used to "sharpen" the anomaly (Figure 42). Vertical derivative accentuates shorter wavelengths and attenuates longer wavelengths (kind of the opposite of the upward continuation), and horizontal derivative sharpens the edges of the anomalies. Derivatives can be computed at any order, even fractional, to adjust the desired effect of enhancement. As they accentuate the shorter wavelengths, these transformations also end to accentuate measurement noise.
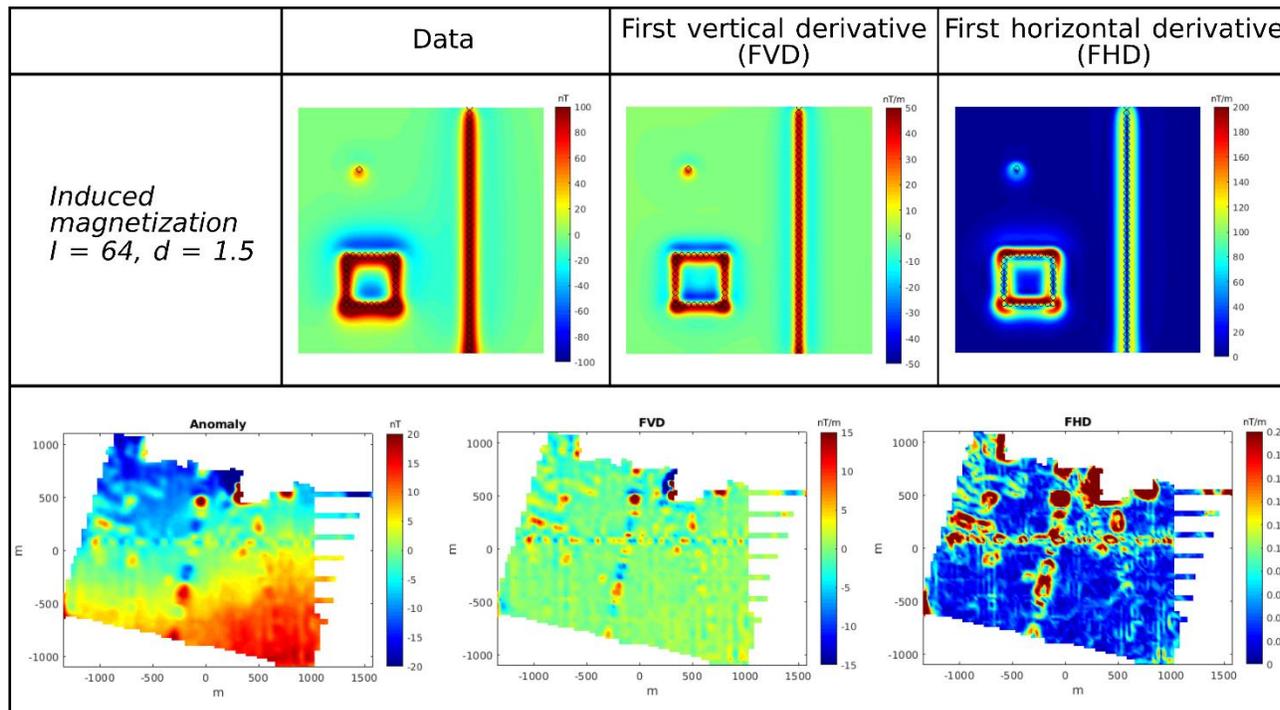
Figure 42   Illustration of the effect of first order vertical (FVD) and horizontal (FHD) derivatives on a synthetic case.

(Top, inclination = 64, declination = 1.5, only induced magnetization), and Bottom, on real drone borne data (Rhine valley, France, survey 50 m above ground level)

13.15   Analytic signal

3-D analytic signal (Roest et al., 1992), more correctly termed total gradient amplitude, is a popular tool to localize the sources without *a priori* information on the direction of magnetization (unlike the reduction to the pole), such as metallic objects (Figure 43). Unfortunately, the precision of the localization is dependent on the inclination of the regional field and the error for the horizontal position can reach up to 30% of the depth of the source (Salem et al, 2002).
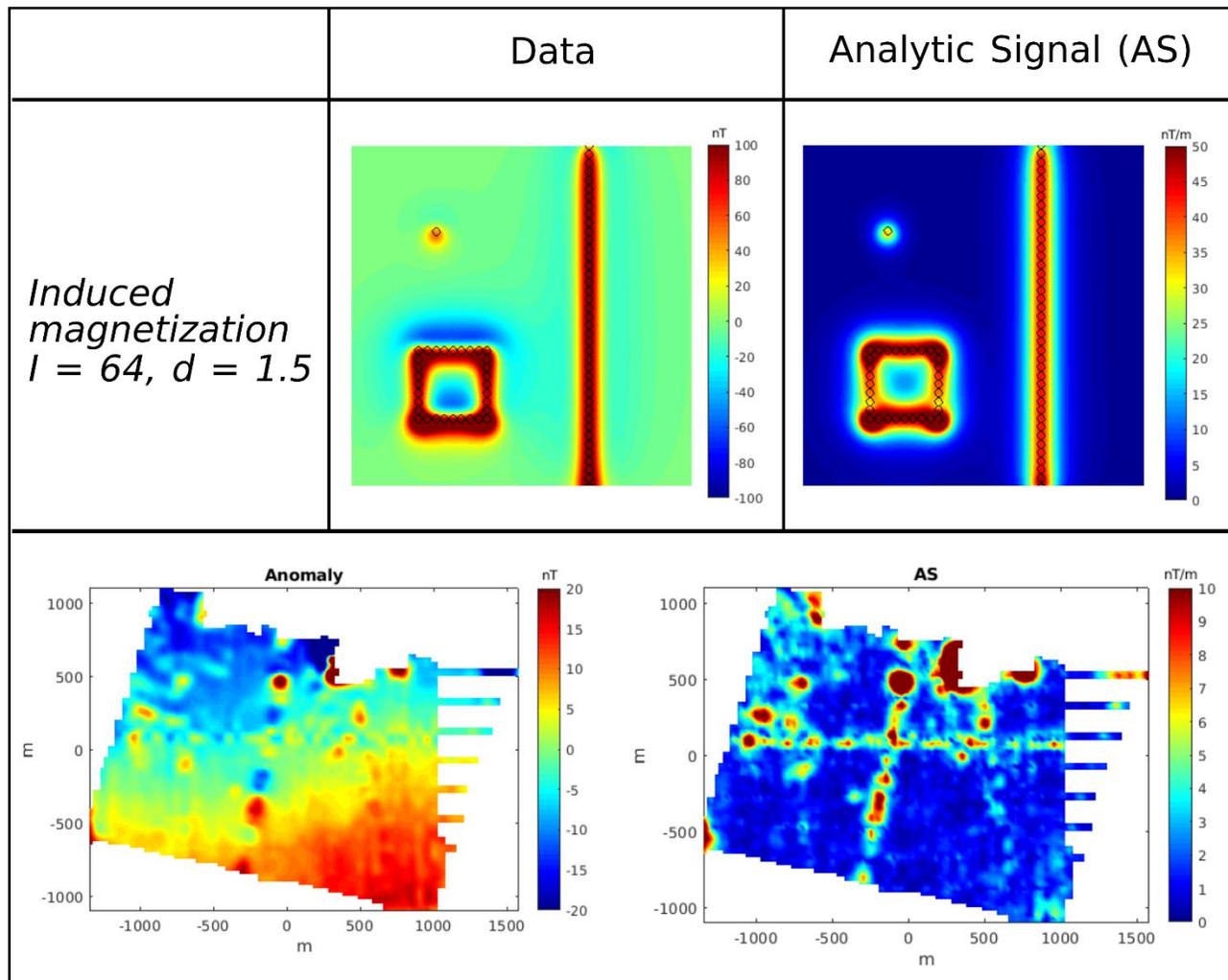
Figure 43   **Illustration of the effect of analytic signal (AS) on a synthetic case.**

(Top, inclination = 64, declination = 1.5, only induced magnetization), and Bottom. on real drone borne data (Rhine valley, France, survey 50 m above ground level).

13.16   Frequency filtering

As briefly discussed earlier, a spatial data set can be decomposed into its different frequency components using Fourier analysis by using an algorithm similar to that proposed in Cooley & Tukey (1965).

In general, high-frequency (short-wavelength) information originates from shallow sources. Low-frequency (long-wavelength) information often originates from deep sources, although it can originate from slowly-varying shallow sources as well.

By applying frequency filtering to magnetic data in a thoughtful manner, the response of shallow and deep features can be selectively amplified and attenuated to aid geophysical interpretation.

Typical frequency filters applied to magnetic data include low-pass filters, high-pass filters, and band-pass filters (Figure 44). In all cases, a cut-off wavelength and a roll-off rate need to be specified.
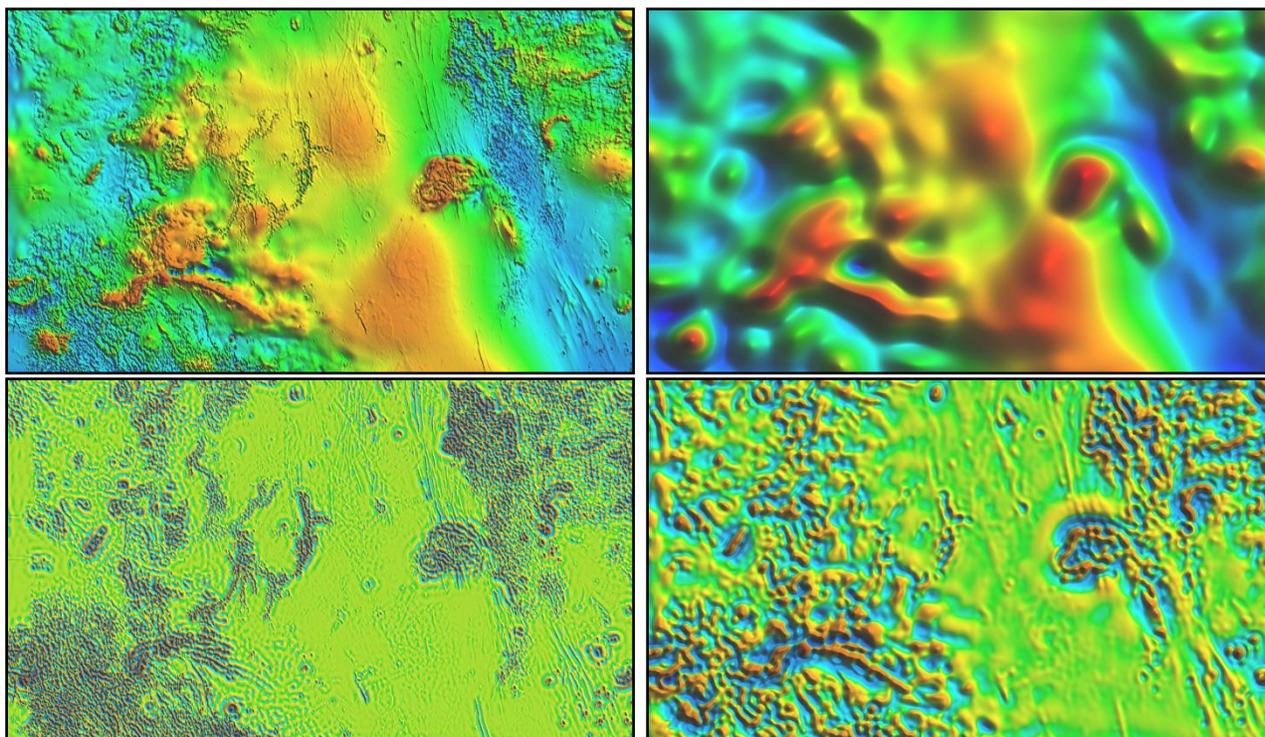
Figure 44   Illustration of the effect of spatial filtering on a magnetics gridded data set.

(Low-pass (B), high-pass (C) and band-pass (D) filtering applied to a magnetic data set (A))

13.17   Pseudo-depth slicing

Because of the inexact correlation between frequency content and source depth mentioned above, pseudo-depth slicing often produces more accurate results than frequency filtering. This follows the method outlined in Spector & Grant (1970) and produces a series of slices from successive magnetic ensembles within the subsurface. Spatial separation is still not exact, hence the term "pseudo-depth".

13.18   Depth estimation

Frequency filtering and pseudo-depth slicing have already been mentioned. Other methods of depth estimation using magnetic data include:

- Spectral fitting - depths to magnetic ensembles are estimated using the power spectrum (Spector and Grant, 1970)

- GridSLUTH - following the work of Smith et al. (2012), the GRIDSLUTH algorithm provides an estimate of source depth, strike angle and structural index from a magnetic grid by ray tracing spatial derivatives of the magnetic field on two height datums.

- Euler deconvolution – Euler deconvolution was first developed by Thompson (1982) and later extended by Reid et al (1990). Since then, it has been adapted and improved upon by Keating (1998), Mushayandebvu et al. (2004), and many others. This popularity is largely due to its great simplicity of implementation and use, making it the tool of choice for a quick initial interpretation. In many cases, maps of gravity and magnetic data (and transformations thereof) provide good constraints on the horizontal location of an anomaly source. Euler deconvolution adds an extra dimension to the interpretation. It estimates a set of (x, y, z) points that, ideally, fall inside the source of the anomaly. Euler deconvolution requires the x-, y-, and z-derivatives of the data and a parameter called the structural index (SI). The SI is an integer number that is related to the homogeneity of the potential field and varies for different fields and source types (Stavrev and Reid, 2007; *https://wiki.seg.org/wiki/Dictionary:Euler%E2%80%99s_homogeneity_equation*).

- Source Parameter Imaging (SPI) is a method for automatic calculation of source depths from gridded magnetic data (Thurston and Smith, 1997). These depth results are independent of the magnetic inclination and declination, so it is not necessary to use a pole-reduced input grid. SPI assumes a step-type source model.

- Multi-scale edge detection - following the work of Archibald et al (1999) and subsequent practitioners, multiscale edge analysis provides a means of estimating the location and dip of geological "edges" by contouring the total horizontal derivative of progressively upward-continued versions of a gravity or magnetic source grid.

13.19   Forward and inverse modelling

Forward modelling refers to the process of calculating a resultant grid from a postulated distribution of subsurface magnetic sources. Forward modelling is usually compared with the magnetic grid actually observed on site to test and refine the postulation.

By contrast, inverse modelling refers to the process of calculating a postulated distribution of subsurface magnetic sources, by matching the resultant grid to the magnetic grid actually observed on site.

Forward modelling and inverse modelling are complex mathematical procedures, often supported by mature technical software. But a good level of geophysical and mathematical understanding is still required of the end user if sensible modelling results are to be obtained.

13.20   Available 2D magnetics grid interpretive modelling software

Software packages such as Intrepid, ModelVision, Oasis Montaj, and EMIGMA all provide interpretive modelling capabilities for 2D magnetic grid data.

13.21 Voxet-based interpretation (3D data space)

A 3D volume of discrete element of magnetic susceptibility can be created from forward modelling of known environmental or geological parameters, or computed from inverse modelling of a measured magnetic data set. Such a volume is termed a voxet (VOlume ELement => VOxEL; VOxel sET => VOXET). Forward and inverse modelling both have value, and both can be difficult to implement.

Forward modelling is complicated by often sparse and occasionally conflicting subsurface information. Inverse modelling is complicated by the inherent ambiguity of magnetic measurements. A common workflow is to create a 3D model of magnetic susceptibility incorporating known subsurface information, and then invert the observed magnetic data to improve its accuracy.

Various weighting parameters and other constraints can be applied to improve the output of 3D inversion. These are advanced topics, and not discussed here.

13.22 Available 3D magnetic modelling software

Software packages capable of forward and inverse 3D magnetic modelling include GeoModeller, ModelVision, Oasis Montaj, and VPmg. Open-source libraries including SimPEG and Fatiando a Terra are also available.

13.23 Geophysical vs geological interpretation

As seen throughout all the previous sections, the interpretation of magnetic data is most efficient when constrained by other information. To move from a geophysical interpretation to a geological interpretation, the following additional information can be integrated into an overall strategy.

- Downhole geophysics or measurements on samples: provide geophysical properties of the sources, such as magnetic susceptibility,

- Integration of other geophysical datasets can provide information on source geometrical parameters, such as depth of sources with seismic data,

- Specialist geological collaboration the extensive knowledge on the sources can be very helpful to select between different assumptions,

- Ground truthing can be carried out; the information gathered through direct access to the sources on a small area (e.g., an archaeological excavation or an exploration drillhole) that can be later carefully extrapolated to the rest of the magnetic survey. and

- Iterative interpretation approach, such as combining the different methods, and going back and forth between magnetic data and external information, is often a very effective way to improve the overall interpretation.

14. CONCLUSIONS AND RECOMMENDATIONS

Drone geoscience is not "plug and play". That is, it is not a simple matter of going out buying a drone and all the equipment and software, putting it all together, flying the drone responsibly, acquiring the data, and processing it.

Each of these steps requires specialist knowledge and involves a learning curve, if quality data is to be delivered. In particular, we trust the guidelines have conveyed this point to both geophysicists, non-geophysicists, interpreters and clients and has helped in making that learning curve easier for all. Reading, understanding and intelligent use of the guidelines, will result in better decisions and actions, safer operations and quality data in relation to drone magnetics data acquisition processing and data delivery.

Drone technology and the technology of magnetics sensors, navigation equipment and associated data processing software is evolving rapidly. Version 1 of these guidelines is a start and it is recognized need feedback and revisions to refine these guidelines as quickly as possible. Version 2 based on user feedback and edits is planned for late April 2023.

The Drone Geophysics Guidelines website (https://www.guidelinesfordronegeophysics.com/) which will be live shortly after the Version 1 launch Webinar, hosts two Version 1 documents:

- **Drone_Magnetic_Guidelines Version1_13November2022.pdf** – The current Version 1, for general distribution and use and is intended to be a read-only file.

- **Drone_Magnetic_Guidelines Version1_13November2022.docx** – the current Version 1, intended to be edited in track changes (which are locked). Please take time to download and review and edit the document, use the Comments function in Word and suggest any improvements. **If your full name initials are MAJ for example,** save the file as:

  MAJ_ Drone_Magnetic_Guidelines Version1_13November2022.docx and upload it to the website.

Your suggested improvements to the guidelines are important and potentially valuable to the drone geoscience community. Please assist in updating the guidelines by the process as outlined above.

These guidelines will serve as a template for other geophysical sensor guidelines that are in preparation (i.e., radiometrics, electromagnetics, GPR etc.).

Specific conclusions messages relevant to the drone geoscience community stakeholders are as follows:

1. **Overal**l – the guidelines provide a safety framework and quality data approach and emphasize the importance of good upfront planning and written specifications as well as QA/QC during operations and adherence to best practices developed by the industry for processing airborne magnetics data, for achieving the objectives of the survey to be carried out.

2. **The quality of the drone data** acquired depends on the ability to minimise system noise, either by configuring the sensor to be suspended outside the influence of the drone platform and performing a simple noise and heading error assessment test or suspending the drone within the zone of platform influence and the minimizing noise in data processing and possibly pre-survey compensation and testing approaches. There is an inter-dependency of survey objectives, altitude (terrain drape or constant elevation), safety issues, navigation capabilities and sensor mounting that all affects final planned and achievable data quality and these guidelines have attempted to outline these inter-dependent factors.

3. **Instrument makers and software developers / sellers** – These guidelines would be useful to share with customers to ensure proper and intelligent, informed use of your equipment and software, a proper understanding of the effects of magnetometers interaction with the drone platform and the factors important for using the equipment and software to enable getting the best quality data out of the drone magnetic system.

4. **Drone pilots / owners** wanting to get into the drone geoscience (specifically magnetics) business– the guidelines give a broader understanding of the data you are partly responsible for collecting and highlights some drone magnetics specific safety considerations. The guidelines indicate the complexities involved in obtaining good data and processing it well and shows that it is bast to partner with a trained geoscientist skilled in the magnetics geophysical aspects of the work.

5. **Geophysicists** – regardless of your background in magnetics (ground or airborne) the guidelines show that it is possible to collect better magnetics data, closer to the terrain than is possible with a conventional aircraft but there is much learning to be undertaken to achieve that. Apart from drone operations learnings, many geophysicists will be new to magnetics data processing and will have operated only on processed data prepared by airborne contractors. The guidelines provide a start for the learnings in the data processing required.

6. **Interpreters and Clients** – The guidelines provide an understanding of how to evaluate if you have quality drone data or not and to possibly improve the data supplied. Most importantly they provide a benchmark that you are advised to measure your data quality requirements against. This will ensure that (legacy) drone magnetic data you are either forced to work with, can either be improved by specialist processing or understood for its limitations work with, It will also enable you to be more informed when choosing a contractor and it is advised to choose a contractor that can demonstrate clearly that they are adhering to these guidelines.

7. **Finally, the industry is urged:** (a) to refer to and promulgate these guidelines, (b) for UAV magnetics operators and geoscientists to study and follow them, (c) for clients for their own protection, to require that UAV magnetics operators and geophysical contractors follow and demonstrate adherence to these guidelines, and (d) for interpreters to educate themselves about these guidelines when ascertaining the provenance and quality of the UAV magnetics data they are interpreting.

15.   REFERENCES AND BIBLIOGRAPHY

15.1   References

Accomando, Filippo, Andrea Vitale, Antonello Bonfante, Maurizio Buonanno, and Giovanni Florio. 2021. "Performance of Two Different Flight Configurations for Drone-Borne Magnetic Data" Sensors 21, no. 17: 5736. https://doi.org/10.3390/s21175736

Alken, P., Thébault, E., Beggan, C.D. et al., 2021, International Geomagnetic Reference Field: the thirteenth generation. Earth Planets Space 73(49). https://doi.org/10.1186/s40623-020-01288-x (https://earth-planets-space.springeropen.com/articles/10.1186/s40623-020-01288-x#citeas. Accessed 30 September, 2022)

Archibald N., Gow P. & Boschetti F. (1999). Multiscale edge analysis of potential field data. Exploration Geophysics, 30:1-2, 38-44.

ASPRS, 2014, ASPRS Positional Accuracy Standards For Digital Geospatial Data, Edition 1, Version 1.0, November 2014. (https://www.asprs.org/news-resources/asprs-positional-accuracy-standards-for-digital-geospatial-data, Accessed 30 September 2022)

Atchuta Rao D. & Ram Babu H. V. (1984). On the half-slope and straight-slope methods of basement depth determination. Geophysics, 49, 1365-1368.

Baranov, V. (1957). A new method for interpretation of aeromagnetic maps: pseudogravimetric anomalies. Geophysics, 22, 359–383.

Blakely, R.J. (1995). Potential Theory in Gravity & Magnetic Applications. Cambridge University Press.

Brother Arnold. 1904. The letter of Petrus Peregrinus on the magnet, A.D. 1269. Translated by Brother Arnold. New York, McGraw Publishing, https://books.google.com.au/books?id=oCw4AAAAMAAJ&redir_esc=y.Accessed 23 October, 2022

Cabreira, T.M., Brisolara, L.B. and Ferreira. PR. Jr, 2019, Survey on Coverage Path Planning with Unmanned Aerial Vehicles. MDPI Drones 2019, 3(1), 4; https://doi.org/10.3390/drones3010004 (https://www.mdpi.com/2504-446X/3/1/4. Accessed 20 September, 2022

Cherkasov, S., and Kapshtan, D., 2018, Unmanned aerial systems for magnetic survey. Intech Open, 9, pp. 135-148. DOI: 0.5772/intechopen.73003

Christensen. U.,Olson, P. and Glatzmaier, G.A., 1998, A dynamo model interpretation of geomagnetic field structures. Geophysical Research Letters, 25(10), pp 1565-1568, May 15, 1998 (https://agupubs.onlinelibrary.wiley.com/doi/epdf/10.1029/98GL00911?src=getftr. Accessed 30 September, 2022)

Cooley, J. W. & Tukey, J.W. (1965). An algorithm for the machine calculation of complex Fourier series. Mathematics of Computation, 19, 297-301.

Courtillot, V. & Le Mouël, J.L. (1988), Time Variations of the Earth's Magnetic Field : From Daily to Secular, Annual Review of Earth and Planetary Sciences 16 (1), pp. 389–476, Doi:10.1146/annurev.ea.16.050188.002133.)

Coyle, M.; Dumont, R.; Keating, P.; Kiss, F.; Miles, W., 2014 - Geological Survey of Canada Aeromagnetic Surveys: Design, Quality Assurance, and Data Dissemination; Open File 7660; Geological Survey of Canada: Ottawa, ON, Canada, 2014, doi:10.4095/295088. (https://publications.gc.ca/collections/collection_2015/rncan-nrcan/M183-2-7660-eng.pdf. Accessed 30 September 2020)

Denisov, A., Denisova, O., Sapunov, V. and Khomutov, S., 2006, Measurement quality estimation of proton-precession magnetometers. Earth Planets and Space 58, pp707-710, doi 10.1186/BF03351971.

Dentith, M., & Mudge, S., 2014, Geophysics for the Mineral Exploration Geoscientist. Cambridge University Press. doi:10.1017/CBO9781139024358.

Forrester, R, 2011, Magnetic signature control strategies for an unmanned aircraft system, Master of Applied Science thesis, Mechanical and Aerospace Engineering, Carleton University, Ottawa, Canada. pp. 1-212.

Forrester, R., Huq, S., Ahmadi, M., and Straznicky, P. V., 2014, Magnetic signature attenuation of an unmanned aircraft system for aeromagnetic survey, IEEE/ASME Transactions on Mechatronics, 19, no. 4, pp. 1436-1446. DOI: 10.1109/TMECH.2013.2285224

Francke, Jan & Verezub, Olga & Macnae, James & Minty, Brian & Clark, David & Hammond, Giles & Hussey, Michael & Sabatini, Roberto & Aravanis, Theo & Pils, Tom. (2020). Developing UAV Mounted Geophysical Sensor Arrays. (https://amira.global/wp-content/uploads/Amira-P1204_Sensors-UAV_Public-Report.pdf. Accessed 9 October, 2022)

Funaki, M., Higashino, S. I., Sakanaka, S., Iwata, N., Nakamura, N., Hirasawa, N., Obara, N., and Kuwabara, M., 2014, Small unmanned aerial vehicles for aeromagnetic surveys and their flights in the South Shetland Islands, Antarctica, Polar Science, 8, pp. 342–356, DOI: 10.1016/j.polar.2014.07.001.

Funaki, M. and Hirasawa, N., 2008, Outline of a small unmanned aerial vehicle (Ant-Plane) designed for Antarctic research, Polar Science, 2, no. 2, pp. 129–142. DOI: 10.1016/j.polar.2008.05.002

Gilbert, W. (1600), De Magnete, Magneticisque Corporibus, Et De Magno magnete tellure ; Phyfiologia noua, plurimis & argumentis, & experimentis demonstrata, Peter Short.

Glatzmaiers, G. and Roberts, P. 1995, A three-dimensional convective dynamo solution with rotating and finitely conducting inner core and mantle. Physics of the Earth and Planetary Interiors 91, pp 63-75. Elsevier.(https://websites.pmc.ucsc.edu/~glatz/pub/glatzmaier_roberts_pepi_1995.pdf. Accessed 30 September, 2022)

Green, A,A,, 1983, A comparison of adjustment procedures for leveling aeromagnetic survey data. Geophysics 48 (6): 745–753. doi: https://doi.org/10.1190/1.1441504

Hartman, R.R., Teskey, D.J. & Friedberg, J.L. (1971). A system for rapid digital aeromagnetic interpretation. Geophysics, 36:5, pp 891-918.

Henderson, R. & Zietz, I. (1949), The upward continuation of anomalies in total magnetic intensity fields, Geophysics, 14 (4), pp 517–534.

Hood, P.A., 1964 - The Königsberger Ratio and the dipping-dyke equation. Geophysical Prospecting, 12(4), , pp 440-456

Kaneko, T., Koyama, T., Yasuda, A., Takeo, M., Yanagisawa, T., Kajiwara, K., and Honda, Y, 2011, Low-altitude remote sensing of volcanoes using an unmanned autonomous helicopter: An example of aeromagnetic observation at Izu-Oshima volcano, Japan, International Journal of Remote Sensing 32, no. 5, pp. 1491-1504. DOI: 10.1080/01431160903559770

Keating, P. B. (1998). Weighted Euler deconvolution of gravity data. Geophysics, 63:5, 1595-1603.

Kovesi, Peter. (2015). Good Colour Maps: How to Design Them. (https://colorcet.com)

Krishna, J., da Silva, E. L. S., Døssing, A., 2021, Experiments on magnetic interference for a portable airborne magnetometry system using a hybrid unmanned aerial vehicle (UAV). Geoscientific Instrumentation, Methods and Data Systems, 10, no. 1, pp. 25-34. DOI: 10.5194/gi-10-25-2021

Larmor, J., 1919, ''How could a rotating body such as the Sun become a magnet?'' Rep. Brit. Assoc. Adv. Sci. 159–160

Leliak, P., 1961, Identification and evaluation of magnetic-field sources of magnetic airborne detector equipped aircraft. IRE Trans. Aerosp. Navig. Electron. 1961, ANE-8, 95–105.

Mitchell, A.C., 1932, Chapters in the history of terrestrial magnetism, Terrestrial Magnetism and Atmospheric Electricity 37 (2), pp. 105–146, doi:10.1029/TE037i002p00105.

Mitchell, A.C., 1946, Chapters in the history of terrestrial magnetism, Terrestrial Magnetism and Atmospheric Electricity 51 (3), pp. 323–351, doi:10.1029/TE051i003p00323Mukherjee, S., Bell, R.S., Barkhouse, W.N., Adavani, S., Lelièvre, P.G. and Farquharson. C.G., 2022, High-resolution imaging of subsurface infrastructure using deep learning artificial intelligence on drone magnetometry. The Leading Edge, July 2022, pp 462-471. https://doi.org/10.1190/ tle41070462.1

Mushayandebvu, M.F., Lesur, V., Reid, A.B. & Fairhead, J.D. (2004). Grid Euler deconvolution with constraints for 2D structures. Geophysics, 69, 489-496.

Nabighian, M. N., Grauch, V. J. S., Hansen, R. O., LaFehr, T. R., Li, Y., Peirce, J. W., Phillips, J. D., & Ruder, M. E. (2005). The historical development of the magnetic method in exploration. In GEOPHYSICS (Vol. 70, Issue 6, pp. 33ND-61ND). Society of Exploration Geophysicists. https://doi.org/10.1190/1.2133784Noriega, G., 2022, UAV-based magnetometry — Practical considerations, performance measures, and application to magnetic anomaly detection. The Leading Edge, July 2022, pp 472-480. https://doi.org/10.1190/ tle41070472.1

Parker, E. N., 1955, ''Hydromagnetic dynamo models,'' Astrophys. J. 122, 293–314.

Parvar, K, 2016, Development and evaluation of unmanned aerial vehicle (UAV) magnetometry systems, Master of Applied Science thesis, Department of Geological Sciences and Geological Engineering, Queen's University, Kingston, Ontario, Canada, pp. 1-141. DOI: http://hdl.handle.net/1974/15234

Parvar, K., Braun, A., Layton-Matthews, D., and Burns, M., 2018, UAV magnetometry for chromite exploration in the Samail ophiolite sequence, Oman, Journal of Unmanned Vehicle Systems, 6, no. 1, pp. 57-69. DOI:10.1139/juvs-2017-0015

Phelps, G., Bracken, R., Spritzer, J., White D., 2022, Achieving sub-nanoTesla precision in rotary-wing UAV aeromagnetic surveys, Journal of Applied Geophysics.

Reid, A.B., 1980, Shot Note Aeromagnetic Survey Design. Geophysics 15(5), pp 973-976.

Reid, A.B., Allsop, J. M., Granser, H., Millett, A.J. & Somerton, I.W., 1990, Magnetic interpretation in three dimensions using Euler deconvolution. Geophysics, 55, 80-91.

Roest, W.R., Verhoef, J. & Pilkington, M. (1992). Magnetic interpretation using 3-D analytic signal. Geophysics, 57, 116-125.

Sheriff, R.E. (2002). Encyclopedic Dictionary of Applied Geophysics, Fourth edition. Society of Exploration Geophysicists. 429 pp.

Smith R.S., Thurston J.B., Salem A. & Reid A.B. (2012). A grid implementation of the SLUTH algorithm for visualising the depth and structural index of magnetic sources. Computers & Geosciences, 44, 100–108.

Spector, A. & Grant, F.S. (1970). Statistical models for interpreting aeromagnetic data. Geophysics, 35, 293-302.

Stavrev, P. & Reid, A.B. (2007). Degrees of homogeneity of potential fields and structural indices of Euler deconvolution. Geophysics, 72, L1-L12.

Sterligov, B. and Cherkasov, S., 2016, Reducing magnetic noise of an unmanned aerial vehicle for high-quality magnetic surveys, International Journal of Geophysics, no. 2016, 4098275, pp. 1-7. DOI: 10.1155/2016/4098275

Stern, D.P., 2002, A millenium of geomagnetism, Reviews of Geophysics 40 (3), pp. 1–30, doi:10.1029/2000RG000097.

Thompson, D.T. (1982). EULDPH – A technique for making computer-assisted depth estimates from magnetic data. Geophysics 47, 31–37.

Thurston, J.B. & Smith, R.S. (1997). Automatic conversion of magnetic data to depth, dip and susceptibility contrast using the SPITM method, Geophysics, 62, 807-813.

Tuck, L., Samson, C., Laliberté, J.,Wells, M., and Bélanger, F., 2018, Magnetic interference testing method for an electric fixed-wing unmanned aircraft system, Unmanned Vehicle Systems, 6, no. 3, pp. 177-194. DOI:10.1139/juvs-2018-0006

Tuck, L., Samson, C., Laliberté, J., and Cunningham, M., 2021, Magnetic interference mapping of four types of unmanned aircraft systems intended for aeromagnetic surveying, Geoscientific Instrumentation, Methods and Data Systems, 10, pp. 101–112. DOI:10.5194/gi-10-101-2021

Versteeg, R., McKay, M., Anderson, M., Johnson, R., Selfridge, B., and Bennett, J., 2007, Feasibility Study for an Autonomous UAV -Magnetometer System. Final Report on SERDP SEED 1509:2206 - Idaho National Laboratory, pp. 1-53. DOI:10.2172/923485

Walter, C., Braun, A., and Fotopoulos, G., 2019, Spectral Analysis of Magnetometer Swing in High-Resolution UAV-borne Aeromagnetic Surveys. IEEE Systems and Technologies for Remote Sensing Applications Through Unmanned Aerial Systems, pp. 1-4. DOI: 10.1109/STRATUS .2019.8713313

Walter, C., Braun, A., and Fotopoulos, G., 2021a, Conference Proceedings, 82nd EAGE Annual Conference & Exhibition, Oct 2021, Volume 2021, p.1 – 5 DOI: https://doi.org/10.3997/2214-4609.202113170

Walter, C., Braun, A., and Fotopoulos, G., 2021b, Characterizing electromagnetic interference signals for unmanned aerial vehicle geophysical surveys: Geophysics, 86, no. 6, pp. 1-12. DOI: 10.1190/geo2020-0895.1

Walter, C., 2021c, Optimization of UAV-borne Aeromagnetic Surveying in Mineral Exploration, PhD Thesis, Department of Geological Sciences and Geological Engineering, Queen's University, Kingston, Ontario, Canada, pp. 1-202. DOI: http://hdl.handle.net/1974/29466

Zhang, R., Frederick Hanselmann, F., Fochs, R., Lawrence, M., Hurley, K., and Prouty. M., 2022, Motion noise reduction in drone magnetometry using a dead-zone-free total-field magnetometer system magnetometry. The Leading Edge, July 2022, pp 481-485. https://doi.org/10.1190/ tle41070481.1

Zheng, Y.,Shiyan Li, S., Kang Xing, K. and Zhang, X., 2021, Unmanned Aerial Vehicles for Magnetic Surveys: A Review on Platform Selection and Interference Suppression. MDPI Drones 2021, 5, 93. https://doi.org/10.3390/drones5030093 (https://www.mdpi.com/2504-446X/5/3/93. Accessed 30 September, 2022).

15.2 Further Reading

Blakely, R. (1995). Potential Theory in Gravity and Magnetic Applications. Cambridge: Cambridge University Press. doi:10.1017/CBO9780511549816.

Dentith, M., & Mudge, S. (2014). Geophysics for the Mineral Exploration Geoscientist. Cambridge: Cambridge University Press. doi:10.1017/CBO9781139024358.

Hinze, W., Von Frese, R., & Saad, A. (2013). Gravity and Magnetic Exploration: Principles, Practices, and Applications. Cambridge: Cambridge University Press. doi:10.1017/CBO9780511843129.

Isles, D. & Rankin, L. (2013). Geological Interpretation of Aeromagnetic Data. ASEG. (https://www.aseg.org.au/publications/geological-interpretation-aeromagnetic-data. Accessed 30 September, 2022).

Milsom, J. & Eriksen, A. (2011). Field Geophysics, 4th Edition. Wiley. ISBN: 978-0-470-74984-5.

Reynolds, J.M. (2011). An Introduction to Applied and Environmental Geophysics, 2nd Edition. Wiley. ISBN: 978-0-471-48535-3.

15.3 Bibliography

The following bibliography is a selection from Zheng et al, 2021 reference section.

Álvarez Larrain, A.; Greco, C.; Tarragó, M. Participatory mapping and UAV photogrammetry as complementary techniques for landscape archaeology studies: An example from north-western Argentina. Archaeol. Prospect. 2021, 28, 47–61.

Anderson, D.; Pita, A. Geophysical Surveying with Georanger UAV; American Institute of Aeronautics and Astronautics Inc.: Reston, VA, USA, 2005; pp. 67–68.

Baji, M. Modeling and simulation of very high spatial resolution UXOs and landmines in a hyperspectral scene for UAV survey. Remote Sens. 2021, 13, 837.

Barnard, J. The use of unmanned aircraft in oil, gas and mineral exploration and production activities. In Proceedings of the 23rd Bristol International UAV Systems Conference 2008, Bristol, UK, 7–9 April 2008.

Baur, J.; Steinberg, G.; Nikulin, A.; Chiu, K.; Smet, T. Applying deep learning to automate UAV-based detection of scatterable landmines. Remote Sens. 2020, 12, 859.

Bickel, S.H. Small signal compensation of magnetic fields resulting from aircraft maneuvers. IEEE Trans. Aerosp. Electron. Syst. 1979, AES-15, 518–525.

Billings, S.; Wright, D. Optimal total-field magnetometer configuration for near-surface applications. Lead. Edge 2009, 28, 522–527.

Booysen, R.; Jackisch, R.; Lorenz, S.; Zimmermann, R.; Kirsch, M.; Nex, P.A.; Gloaguen, R. Detection of REEs with lightweight UAV-based hyperspectral imaging. Sci. Rep. 2020, 10, 17450.

Burkart, A.; Cogliati, S.; Schickling, A.; Rascher, U. A novel UAV-based ultra-light weight spectrometer for field spectroscopy.IEEE Sens. J. 2013, 14, 62–67.

Campana, S. Drones in archaeology. State-of-the-art and future perspectives. Archaeol. Prospect. 2017, 24, 275–296.

Caron, R.M.; Samson, C.; Straznicky, P.; Ferguson, S.; Sander, L. Aeromagnetic surveying using a simulated unmanned aircraft system. Geophys. Prospect. 2014, 62, 352–363.

Chen, L.; Wu, P.; Zhu, W.; Feng, Y.; Fang, G. A novel strategy for improving the aeromagnetic compensation performance of helicopters. Sensors 2018, 18, 1846.

Chen, Y.; Luo, G.; Mei, Y.; Yu, J.; Su, X. UAV path planning using artificial potential field method updated by optimal control theory. Int. J. Syst. Sci. 2016, 47, 1407–1420.

Cheng, L.; Tan, X.; Yao, D.; Xu, W.; Wu, H.; Chen, Y. A fishery water quality monitoring and prediction evaluation system for floating UAV based on time series. Sensors 2021, 21, 4451.

Cherkasov, S.; Kapshtan, D. Unmanned aerial systems for magnetic survey. In Drones: Applications; IntechOpen: London, UK, 2018; pp. 135–148.

China Aero Geophysical Survey and Remote Sensing Center for Land and Resources. Industry Standard: Criterion of Aeromagnetic Survey. 2010, DZ/T 0142-2010, released on 5 August 2010. Available online: https://www.chinesestandard.net/Related.aspx/DZT0142-2010 (accessed on accessed on 22 July 2021).

Cunningham, M.; Samson, C.; Laliberté, J.; Goldie, M.; Wood, A.; Birkett, D. Inversion of magnetic data acquired with a rotarywing unmanned aircraft system for gold exploration. Pure Appl. Geophys. 2021, 178, 501–516.

Cunningham, M.; Samson, C.; Wood, A.; Cook, I. Aeromagnetic surveying with a rotary-wing unmanned aircraft system: A case study from a zinc deposit in Nash Creek, New Brunswick, Canada. Pure Appl. Geophys. 2018, 175, 3145–3158.

De Melo, R.R.S.; Costa, D.B.; Álvares, J.S.; Irizarry, J. Applicability of unmanned aerial system (UAS) for safety inspection on construction sites. Saf. Sci. 2017, 98, 174–185.

De Smet, T.S.; Nikulin, A.; Romanzo, N.; Graber, N.; Dietrich, C.; Puliaiev, A. Successful application of drone-based aeromagnetic surveys to locate legacy oil and gas wells in Cattaraugus county, New York. J. Appl. Geophys. 2021, 186, 104250.

Doll, W.E.; Sheehan, J.R.; Gamey, T.J.; Beard, L.P.; Norton, J. Results of an airborne vertical magnetic gradient demonstration, New Mexico. J. Environ. Eng. Geophys. 2008, 13, 277–290.

Dou, Z.; Han, Q.; Niu, X.; Peng, X.; Guo, H. An adaptive filter for aeromagnetic compensation based on wavelet multiresolution analysis. IEEE Geosci. Remote Sens. Lett. 2016, 13, 1069–1073.

Dou, Z.; Han, Q.; Niu, X.; Peng, X.; Guo, H. An aeromagnetic compensation coefficient-estimating method robust to geomagnetic gradient. IEEE Geosci. Remote Sens. Lett. 2016, 13, 611–615.

Du, C.; Wang, H.; Wang, H.; Xia, M.; Peng, X.; Han, Q.; Zou, P.; Guo, H. Extended aeromagnetic compensation modelling including non-manoeuvring interferences. IET Sci. Meas. Technol. 2019, 13, 1033–1039.

Dual Mag System. Available online: http://www.mgt-geo.com/dual%20mag%20system.htm (accessed on 22 July 2021).

Eck, C.; Imbach, B. Aerial magnetic sensing with an UAV helicopter. Int. Arch. Photogramm. Remote Sens. Spat. Inf. Sci. 2011, 38, 81–85. Drones 2021, 5, 93 36 of 38

Emil, K.M.; Arne, D. Scalar magnetic difference inversion applied to UAV-based UXO detection. Geophys. J. Int. 2020, 224, 468–486.

Eschmann, C.; Kuo, C.; Kuo, C.; Boller, C. Unmanned Aircraft Systems for Remote Building. In Proceedings of the European Workshop on Structural Health Monitoring, Dresden, Germany, 3–6 July 2012; pp. 1–8.

Feng, Q.; Liu, J.; Gong, J. UAV remote sensing for urban vegetation mapping using random forest and texture analysis. Remote Sens. 2015, 7, 1074–1094.

Fernandez Romero, S.; Morata Barrado, P.; Rivero Rodriguez, M.A.; Vazquez Yañez, G.A.; De Diego Custodio, E.; Michelena, M.D. Vector magnetometry using remotely piloted aircraft systems: An example of application for planetary exploration. Remote Sens. 2021, 13, 390.

Fixed Wing Mag System. Available online: http://www.mgt-geo.com/fixed%20wing%20mag.htm (accessed on 21 July 2021).

Funaki, M.; Hirasawa, N. Outline of a small unmanned aerial vehicle (Ant-Plane) designed for Antarctic research. Polar Sci. 2008, 2, 129–142.

Gailler, L.; Labazuy, P.; Régis, E.; Bontemps, M.; Souriot, T.; Bacques, G.; Carton, B. Validation of a new UAV magnetic prospecting tool for volcano monitoring and geohazard assessment. Remote Sens. 2021, 13, 894.

Gavazzi, B.; Le Maire, P.; Munschy, M.; Dechamp, A. Fluxgate vector magnetometers: A multisensor device for ground, UAV, and airborne magnetic surveys. Lead. Edge 2016, 35, 795–797.

Gee, J.S.; Cande, S.C.; Kent, D.V.; Partner, R.; Heckman, K. Mapping geomagnetic field variations with unmanned airborne vehicles. Eos Trans. Am. Geophys. Union 2008, 89, 178–179.

Glen, J.M.; Egger, A.E.; Ippolito, C.; Athens, N. Correlation of geothermal springs with sub-surface fault terminations revealed by high-resolution, UAV-acquired magnetic data. In Proceedings of the 38th Workshop on Geothermal Reservoir Engineering: Stanford Geothermal Program Workshop Report SGP-TR-198, Stanford, CA, USA, 11–13 February 2013; pp. 1233–1242.

Ham, Y.; Han, K.K.; Lin, J.J.; Golparvar-Fard, M. Visual monitoring of civil infrastructure systems via camera-equipped Unmanned Aerial Vehicles (UAVs): A review of related works. Vis. Eng. 2016, 4, 1.

Hardwick, C. Important design considerations for inboard airborne magnetic gradiometers. Geophysics 1984, 49, 2004–2018.

Hashimoto, T.; Koyama, T.; Kaneko, T.; Ohminato, T.; Yanagisawa, T.; Yoshimoto, M.; Suzuki, E. Aeromagnetic survey using an unmanned autonomous helicopter over Tarumae Volcano, northern Japan. Explor. Geophys. 2014, 45, 37–42.

Irizarry, J.; Gheisari, M.; Walker, B.N. Usability assessment of drone technology as safety inspection tools. J. Inf. Technol. Constr. 2012, 17, 194–212.

Jackisch, R.; Lorenz, S.; Kirsch, M.; Zimmermann, R.; Tusa, L.; Pirttijärvi, M.; Saartenoja, A.; Ugalde, H.; Madriz, Y.; Savolainen, M. Integrated geological and geophysical mapping of a carbonatite-hosting outcrop in siilinjärvi, finland, using unmanned aerial systems. Remote Sens. 2020, 12, 2998.

Jackisch, R.; Madriz, Y.; Zimmermann, R.; Pirttijärvi, M.; Saartenoja, A.; Heincke, B.H.; Salmirinne, H.; Kujasalo, J.-P.; Andreani, L.; Gloaguen, R. Drone-borne hyperspectral and magnetic data integration: Otanmäki Fe-Ti-V deposit in Finland. Remote Sens. 2019, 11, 2084.

Jiang, D.; Zeng, Z.; Zhou, S.; Guan, Y.; Lin, T. Integration of an aeromagnetic measurement system based on an unmanned aerial vehicle platform and its application in the exploration of the Ma'anshan magnetite deposit. IEEE Access 2020, 8, 189576–189586.

Jirigalatu, J.; Krishna, V.; da Silva, E.L.S.; Døssing, A. Experiments on magnetic interference for a portable airborne magnetometry system using a hybrid unmanned aerial vehicle (UAV). Geosci. Instrum. Methods Data Syst. Discuss. 2020, 2020, 1–21.

Ju, X.; Niu, H.; Guo, H.; Han, S.; Wang, Y.; Lv, C.; Zheng, Q. Safety analysis and quality evaluation of the aeromagnetic measurement system of CH4 UAV. Prog. Geophys. 2020, 35, 1565–1571. (In Chinese)

Junfeng, L.; Yong, Y.; Weiwei, Z.; Suli, F.; Yijun, H.; Jiaqiang, W. Design of magnetic gradient tensor system for UAV. In Proceedings of the IOP Conference Series: Earth and Environmental Science, Zhangjiajie, China, 23–25 April 2021; p. 012142. Drones 2021, 5, 93 38 of 38

Junwei, Z.; Hongxiao, N.; Qiang, F.; Wuhai, Y.; Lijun, Z. Application of the UAV high resolution image and DEM data for geophysical prospecting in complex areas. Equip. Geophys. Prospect. 2014, 1, 55–60.

Kim, B.; Jeong, S.; Bang, E.; Shin, S.; Cho, S. Investigation of iron ore mineral distribution using aero-magnetic exploration techniques: Case study at Pocheon, Korea. Minerals 2021, 11, 665.

Kim, B.; Lee, S.; Park, G.; Cho, S.-J. Development of an unmanned airship for magnetic exploration. Explor. Geophys. 2020, 52, 462–467.

Kim, K.; Kim, S.; Shchur, D. A UAS-based work zone safety monitoring system by integrating internal traffic control plan (ITCP) and automated object detection in game engine environment. Autom. Constr. 2021, 128, 103736.

Kislik, C.; Dronova, I.; Kelly, M. UAVs in support of algal bloom research: A review of current applications and future opportunities. Drones 2018, 2, 35.

Koyama, T.; Kaneko, T.; Ohminato, T.; Yanagisawa, T.; Watanabe, A.; Takeo, M. An aeromagnetic survey of Shinmoe-dake volcano, Kirishima, Japan, after the 2011 eruption using an unmanned autonomous helicopter. Earth Planets Space 2013, 65, 657–666.

Kroll, A. Evaluation of an unmanned aircraft for geophysical survey. ASEG Ext. Abstr. 2013, 2013, 1–4.

Le Maire, P.; Bertrand, L.; Munschy, M.; Diraison, M.; Géraud, Y. Aerial magnetic mapping with an unmanned aerial vehicle and a fluxgate magnetometer: A new method for rapid mapping and upscaling from the field to regional scale. Geophys. Prospect. 2020, 68, 2307–2319.

Li, H.; Ge, J.; Dong, H.; Qiu, X.; Luo, W.; Liu, H.; Yuan, Z.; Zhu, J.; Zhang, H. Aeromagnetic compensation of rotor UAV based on least squares. In Proceedings of the 2018 37th Chinese Control Conference (CCC), Wuhan, China, 25–27 July 2018; pp. 10248–10253.

Li, W.; Qin, X.; Gan, X. The IGGE UAV aero magnetic and radiometric survey system. In Proceedings of the Near Surface Geoscience 2014—20th European Meeting of Environmental and Engineering Geophysics, Athens, Greece, 14–18 September 2014; pp. 1–5.

Li, Z.; Gao, S.; Wang, X. New method of aeromagnetic surveys with rotorcraft UAV in particular areas. Chin. J. Geophys. 2018, 61, 3825–3834. (In Chinese)

Lin, A.Y.-M.; Novo, A.; Har-Noy, S.; Ricklin, N.D.; Stamatiou, K. Combining GeoEye-1 satellite remote sensing, UAV aerial imaging, and geophysical surveys in anomaly detection applied to archaeology. IEEE J. Sel. Top. Appl. Earth Obs. Remote Sens. 2011, 4, 870–876. Drones 2021, 5, 93 34 of 38

Liu, F.-B.; Li, J.-T.; Liu, L.-H.; Geng, Z.; Zhang, Q.-M.; Huang, L.; Fang, G.-Y. Development and application of a new semi-airborne transient electromagnetic system with UAV platform. Prog. Geophys. 2017, 32, 2222–2229.

Lundberg, H. Results obtained by a helicopter borne magnetometer: Transactions. Can. Inst. Min. Metall. 1947, 50, 392–400. 37. Rogers, M.B.; Cassidy, J.R.; Dragila, M.I. Ground-based magnetic surveys as a new technique to locate subsurface drainage pipes: A case study. Appl. Eng. Agric. 2005, 21, 421–426.

Luoma, S.; Zhou, X. Construction of a fluxgate magnetic gradiometer for integration with an unmanned aircraft system. Remote Sens. 2020, 12, 2551.

Macharet, D.G.; Perez-Imaz, H.I.; Rezeck, P.A.; Potje, G.A.; Benyosef, L.C.; Wiermann, A.; Freitas, G.M.; Garcia, L.G.; Campos, M.F. Autonomous aeromagnetic surveys using a fluxgate magnetometer. Sensors 2016, 16, 2169.

Malehmir, A.; Dynesius, L.; Paulusson, K.; Paulusson, A.; Johansson, H.; Bastani, M.; Wedmark, M.; Marsden, P. The potential of rotary-wing UAV-based magnetic surveys for mineral exploration: A case study from central Sweden. Lead. Edge 2017, 36, 552–557.

Manfreda, S.; McCabe, M.F.; Miller, P.E.; Lucas, R.; Pajuelo Madrigal, V.; Mallinis, G.; Ben Dor, E.; Helman, D.; Estes, L.; Ciraolo, G. On the use of unmanned aerial systems for environmental monitoring. Remote Sens. 2018, 10, 641.

Matese, A.; Toscano, P.; Di Gennaro, S.F.; Genesio, L.; Vaccari, F.P.; Primicerio, J.; Belli, C.; Zaldei, A.; Bianconi, R.; Gioli, B. Intercomparison of UAV, aircraft and satellite remote sensing platforms for precision viticulture. Remote Sens. 2015, 7, 2971–2990.

McKay, M.D.; Anderson, M.O. Development of Autonomous Magnetometer Rotorcraft for Wide Area Assessment; Idaho National Laboratory (INL): Idaho Falls, ID, USA, 2011.

Metni, N.; Hamel, T. A UAV for bridge inspection: Visual servoing control law with orientation limits. Autom. Constr. 2007, 17, 3–10.

Mu, Y.; Xie, W.; Zhang, X. The joint UAV-borne magnetic detection system and cart-mounted time domain electromagneticsystem for UXO detection. Remote Sens. 2021, 13, 2343.

Mu, Y.; Zhang, X.; Xie, W.; Zheng, Y. Automatic detection of near-surface targets for unmanned aerial vehicle (UAV) magnetic survey. Remote Sens. 2020, 12, 452.

Naprstek, T.; Lee, M.D. Aeromagnetic compensation for UAVs. In Proceedings of the AGU Fall Meeting Abstracts, New Orleans, LA, USA, 11–15 December 2017; p. NS31A-0005.

Natesan, S.; Armenakis, C.; Benari, G.; Lee, R. Use of UAV-borne spectrometer for land cover classification. Drones 2018, 2, 16.

Niethammer, U.; James, M.; Rothmund, S.; Travelletti, J.; Joswig, M. UAV-based remote sensing of the Super-Sauze landslide: Evaluation and results. Eng. Geol. 2012, 128, 2–11.

Nikulin, A.; de Smet, T.S. A UAV-based magnetic survey method to detect and identify orphaned oil and gas wells. Lead. Edge 2019, 38, 447–452.

Noriega, G. Performance measures in aeromagnetic compensation. Lead. Edge 2011, 30, 1122–1127.

Noriega, G.; Marszalkowski, A. Adaptive techniques and other recent developments in aeromagnetic compensation. First Break. 2017, 35, doi:10.3997/1365-2397.2017018.

Pajares, G. Overview and current status of remote sensing applications based on unmanned aerial vehicles (UAVs). Photogramm. Eng. Remote Sens. 2015, 81, 281–330.

Parshin, A.; Bashkeev, A.; Davidenko, Y.; Persova, M.; Iakovlev, S.; Bukhalov, S.; Grebenkin, N.; Tokareva, M. Lightweight unmanned aerial system for time-domain electromagnetic prospecting—The next stage in applied UAV-Geophysics. Appl. Sci. 2021, 11, 2060.

Parshin, A.; Bydyak, A.; Blinov, A.; Kosterev, A.; Morozov, V.; Mikhalev, A. Low-altitude unmanned aeromagnetic survey in management of large-scale structural-geological mapping and prospecting for ore deposits in composite topography. Part 2. Geogr. Nat. Resour. 2016, 37, 144–149. (In Russian).

Parshin, A.; Morozov, V.; Snegirev, N.; Valkova, E.; Shikalenko, F. Advantages of gamma-radiometric and spectrometric low altitude geophysical surveys by unmanned aerial systems with small scintillation detectors. Appl. Sci. 2021, 11, 2247.

Parshin, A.V.; Morozov, V.A.; Blinov, A.V.; Kosterev, A.N.; Budyak, A.E. Low-altitude geophysical magnetic prospecting based on multirotor UAV as a promising replacement for traditional ground survey. Geo-Spat. Inf. Sci. 2018, 21, 67–74.

Parvar, K. Development and Evaluation of Unmanned Aerial Vehicle (UAV) Magnetometry Systems. Master's Thesis, Queen's University, Kingston, ON, Canada, 2016.

Pei, Y.; Liu, B.; Hua, Q.; Liu, C.; Ji, Y. An aeromagnetic survey system based on an unmanned autonomous helicopter: Development, experiment, and analysis. Int. J. Remote Sens. 2017, 38, 3068–3083.

Petzke, M.; Hofmeister, P.; Hördt, A.; Glaßmeier, K.; Auster, H. Aeromagnetics with an unmanned airship. In Proceedings of the Near Surface Geoscience 2013—19th EAGE European Meeting of Environmental and Engineering Geophysics, Bochum, Germany, 9–11 September 2013; p. cp-354-00005.

Pisciotta, A.; Vitale, G.; Scudero, S.; Martorana, R.; Capizzi, P.; D'Alessandro, A. A lightweight prototype of a magnetometric system for unmanned aerial vehicles. Sensors 2021, 21, 4691.

Qiao, Z.; Ma, G.; Zhou, W.; Yu, P.; Zhou, S.; Wang, T.; Tang, S.; Dai, W.; Meng, Z.; Zhang, Z. Research on the comprehensive compensation of aeromagnetic system error of multi-rotor UAV. Chin. J. Geophys. 2020, 63, 4604–4612. (In Chinese)

Reeves, C. Aeromagnetic Surveys: Principles, Practice and Interpretation; Geosoft: Toronto, Canada: 2005; pp. 38–43.

Rosser, J.C., Jr.; Vignesh, V.; Terwilliger, B.A.; Parker, B.C. Surgical and medical applications of drones: A comprehensive review. JSLS J. Soc. Laparoendosc. Surg. 2018, 22, e2018.00018.

Royo, P.; Pastor, E.; Barrado, C.; Cuadrado, R.; Barrao, F.; Garcia, A. Hardware design of a small UAS helicopter for remote sensing operations. Drones 2017, 1, 3.

Salamí, E.; Barrado, C.; Pastor, E. UAV flight experiments applied to the remote sensing of vegetated areas. Remote Sens. 2014, 6, 11051–11081.

Šálek, O.; Matolín, M.; Gryc, L. Mapping of radiation anomalies using UAV mini-airborne gamma-ray spectrometry. J. Environ. Radioact. 2018, 182, 101–107.

Schmidt, V.; Becken, M.; Schmalzl, J. A UAV-borne magnetic survey for archaeological prospection of a Celtic burial site. First Break 2020, 38, 61–66. Drones 2021, 5, 93 35 of 38

Schreiber, E.; Heinzel, A.; Peichl, M.; Engel, M.; Wiesbeck, W. Advanced buried object detection by multichannel, UAV/drone carried synthetic aperture radar. In Proceedings of the 2019 13th European Conference on Antennas and Propagation (EuCAP), Krakow, Poland, 31 March–5 April 2019.

Shahsavani, H. An aeromagnetic survey carried out using a rotary-wing UAV equipped with a low-cost magneto-inductive sensor. Int. J. Remote Sens. 2021, 1–14, doi:10.1080/01431161.2021.1930269. Drones 2021, 5, 93 37 of 38

Sheinker, A.; Moldwin, M.B. Adaptive interference cancelation using a pair of magnetometers. IEEE Trans. Aerosp. Electron. Syst. 2016, 52, 307–318.

Singhal, G.; Bansod, B.; Mathew, L. Unmanned aerial vehicle classification, applications and challenges: A review (preprint). Preprints 2018, doi:10.20944/preprints201811.0601.v1.

Single Mag System. Available online: http://www.mgt-geo.com/single%20mag%20system.htm (accessed on 22 July 2021).

Smith, N.G.; Passone, L.; Al-Said, S.; Al-Farhan, M.; Levy, T.E. Drones in archaeology: Integrated data capture, processing, and dissemination in the al-Ula Valley, Saudi Arabia. Near East. Archaeol. 2014, 77, 176–181.

Stöcker, C.; Bennett, R.; Nex, F.; Gerke, M.; Zevenbergen, J. Review of the current state of UAV regulations. Remote Sens. 2017, 9, 459.

Stoll, J.; Moritz, D. Unmanned aircraft systems for rapid near surface geophysical measurements. In Proceedings of the 75th EAGE Conference & Exhibition-Workshops, London, UK, 10–13 June 2013; p. cp-349-00062.

Tolles, W.; Lawson, J. Magnetic Compensation of MAD Equipped Aircraft; Airborne Instruments Lab. Inc.: Mineola, NY, USA, 1950; p. 201.

Tolles, W.E. Compensation of Aircraft Magnetic Fields. US Patent 2692970A, 26 October 1954.

Tsirel, V.; Parshin, A.; Ancev, V.; Kapshtan, D. Unmanned airborne magnetic survey technologies: Present and future. In Recent Advances in Rock Magnetism, Environmental Magnetism and Paleomagnetism; Springer: Cham, Switzerland, 2019; pp. 523–534.

Tsouros, D.C.; Bibi, S.; Sarigiannidis, P.G. A review on UAV-based applications for precision agriculture. Information 2019, 10, 349.

Tuck, L. Characterization and Compensation of Magnetic Interference Resulting from Unmanned Aircraft Systems. Ph.D. Thesis, Carleton University, Ottawa, ON, Canada, 2019.

Tuck, L.; Samson, C.; Polowick, C.; Laliberte, J. Real-time compensation of magnetic data acquired by a single-rotor unmanned aircraft system. Geophys. Prospect. 2019, 67, 1637–1651.

Tuck, L.E.; Samson, C.; Laliberté, J.; Cunningham, M. Magnetic interference mapping of four types of unmanned aircraft systems intended for aeromagnetic surveying. Geosci. Instrum. Methods Data Syst. 2021, 10, 101–112.

UAV Platforms—Gem Systems. Available online: https://www.gemsys.ca/uav-platforms/ (accessed on 21 July 2021).

UXO Magnetometer UAV—ISS Aerospace. Available online: https://www.issaerospace.com/portfolio/unexploded-ordinancemagnetometer-uxo-uav/ (accessed on 22 July 2021).

Walter, C.; Braun, A.; Fotopoulos, G. High-resolution unmanned aerial vehicle aeromagnetic surveys for mineral exploration targets. Geophys. Prospect. 2020, 68, 334–349.

Wang, B.; Jia, X.; Liu, J.; Zhao, G.; Sun, X.; Lu, D. The trial and application of the aeromagnetic system based on unmanned blimp platform. Geophys. Geochem. Explor. 2016, 40, 1138–1143. (In Chinese)

Wang, J.; Guo, Z.; Qiao, Y. Magnetic compensation of the fixed-wing UAV aeromagneic detection system. Prog. Geophys. 2015, 30, 2931–2937. (In Chinese)

Watts, A.C.; Ambrosia, V.G.; Hinkley, E.A. Unmanned aircraft systems in remote sensing and scientific research: Classification and considerations of use. Remote Sens. 2012, 4, 1671–1692.

Wells, M. Attenuating Magnetic Interference in a UAV System. Master's Thesis, Carleton University, Ottawa, ON, Canada, 2008.

Wierzbicki, D. Multi-camera imaging system for UAV photogrammetry. Sensors 2018, 18, 2433.

Wood, A.; Cook, I.; Doyle, B.; Cunningham, M.; Samson, C. Experimental aeromagnetic survey using an unmanned air system. Lead. Edge 2016, 35, 270–273.

Xi, Y.; Lu, N.; Zhang, L.; Li, J.; Zhang, F.; Wu, S.; Liao, G.; Ben, F.; Huang, W. Integration and application of an aeromagnetic survey system based on unmanned helicopter platform. Geophys. Geochem. Explor. 2019, 125–131. (In Chinese)

Xu, Q.; Liu, L.; Huang, S.; Wu, F. Research and test of compensation method for cesium optical pump aeromagnetic system of domestic UAV helicopter. J. Nav. Inst. Aeronaut. Eng. 2020, 35, 141–148. (In Chinese)

Yao, H.; Qin, R.; Chen, X. Unmanned aerial vehicle for remote sensing applications—A review. Remote Sens. 2019, 11, 1443. 20. Villa, T.F.; Gonzalez, F.; Miljievic, B.; Ristovski, Z.D.; Morawska, L. An overview of small unmanned aerial vehicles for air quality measurements: Present applications and future prospectives. Sensors 2016, 16, 1072.

Yoo, L.-S.; Lee, J.-H.; Lee, Y.-K.; Jung, S.-K.; Choi, Y. Application of a drone magnetometer system to military mine detection in the demilitarized zone. Sensors 2021, 21, 3175.

Yu, P.; Zhao, X.; Jia, J.; Zhou, S. An improved neural network method for aeromagnetic compensation. Meas. Sci. Technol. 2021, 32, 045106.

Zabulonov, Y.L.; Burtnyak, V.; Zolkin, I. Airborne gamma spectrometric survey in the Chernobyl exclusion zone based onoktokopter UAV type. Prob. At. Sci. Technol. 2015, 5, 163–167.

Zeng, C.; King, D.J.; Richardson, M.; Shan, B. Fusion of multispectral imagery and spectrometer data in UAV remote sensing.Remote Sens. 2017, 9, 696.

Zhang, B.; Guo, Z.; Qiao, Y. A simplified aeromagnetic compensation model for low magnetism UAV platform. In Proceedings of the 2011 IEEE International Geoscience and Remote Sensing Symposium, Vancouver, BC, Canada, 24–29 July 2011; pp. 3401–3404.

Zhang, F.; Wen, J.; Zhao, X.; Fang, W. Development and application of aeromagnetic measurement system for unmanned helicopter. Prog. Geophys. 2019, 34, 1694–1699. (In Chinese)

Zhao, G.; Han, Q.; Peng, X.; Zou, P.; Wang, H.; Du, C.; Wang, H.; Tong, X.; Li, Q.; Guo, H. An aeromagnetic compensation method based on a multimodel for mitigating multicollinearity. Sensors 2019, 19, 2931.

Zhou, J.; Lin, C.; Chen, H. A method for aircraft magnetic interference compensation based on small signal model and LMS algorithm. Chin. J. Aeronaut. 2014, 27, 1578–1585.

THIS PAGE LEFT INTENTIONALLY BLANK

END OF DOCUMENT